Effects of Increasing the Allowable Compressive Stress at Release on the Shear Strength of Prestressed Concrete Girders

by

Christopher Peter Heckmann, B.S.C.E.

Thesis

Presented to the Faculty of the Graduate School of

The University of Texas at Austin

in Partial Fulfillment

of the Requirements

for the Degree of

Master's of Science in Engineering

The University of Texas at Austin

August 2008

Effects of Increasing the Allowable Compressive Stress at Release on Shear Strength of Prestressed Concrete Girders

APPROVED BY
SUPERVISING COMMITTEE:

Oguzhan Bayrak, Supervisor

Sharon Wood

Acknowledgements

The research conducted in this study was funded entirely through the Texas Department of Transportation. I would like to thank the project director, Jeff Cotham, for his dedication to the research, as well as all the TxDOT inspectors who were involved in the quality control of the project. I would also like to thank the individual precasters who fabricated the beams we used for making this study possible.

I owe a great amount of appreciation to Dr. Bayrak, my supervising professor, for his guidance and encouragement, as well as for awarding me the honor of working on this project.

I would like to acknowledge a handful of individuals at the Ferguson Structural Engineering Laboratory who aided in this research. First, my research partner Brian Schnittker, your hard work and dedication is greatly valued. Without you, this study would not have been possible. I am also thankful for other graduate students who have assisted me with my research or writing, primarily Alejandro Avendaño and David Birrcher, as well as my hard-working undergraduate assistant, Stacy Holland. Last but not least, the assistance of the technical and administrative staff at the FSEL including Blake Stassney, Dennis Fillip, Andrew Valentine, Eric Schell, Mike Wason, Barbara Howard, Cari Billingsly Goudeau, and Jessica Hantan is greatly appreciated.

Effects of Increasing the Allowable Compressive Stress at Release on the Shear Strength of Prestressed Concrete Girders

Christopher Peter Heckmann, M.S.E.
The University of Texas at Austin, 2008
SUPERVISOR: Oguzhan Bayrak

In recent years, several research projects have been conducted to study the feasibility of increasing the allowable compressive stress in concrete at prestress transfer, currently defined as $0.60f'_{ci}$ in the AASHTO LRFD Bridge Design Specifications. Increasing the limit would result in many economical and design benefits for the precast concrete industry, such as increased span lengths and faster turnover of beams in stressing beds. This research study focuses on the effects of increasing the allowable compressive stress at release on the shear strength of prestressed concrete members, a topic which has not yet been explored by past research projects. The current experimental work is funded under TxDOT Project 5197, which initiated in 2004 at the University of Texas at Austin.

In the shear performance evaluation, 18 shear tests were performed. In the shear tests, the beams were loaded to fail in web-shear, with a shear span to depth

ratio of 2.22. The diagonal cracking shears and shear capacities were experimentally measured for all specimens tested. All test specimens were TxDOT Type-C highway bridge girders (40-inch deep pretensioned I-beams) and were fabricated by three different precast plants in Texas. The compressive stress at release for the test specimens ranged from $0.57f'_{ci}$ to $0.77f'_{ci}$. The measured cracking shears and shear capacities were compared to the estimated cracking shears and shear capcities, as calculated using ACI 318-08 and AASHTO LRFD (2007), and the effects of higher release stresses on shear strength were evaluated by examining the conservativeness and accuracy of the predictions. Based on the experimental results reported in this thesis, an increase in the allowable maximum compressive stress in concrete in the end regions of prestressed concrete beams at prestress transfer to $0.65f'_{ci}$ or $0.70f'_{ci}$ can be justified.

Table of Contents

List of Tables

List of Figures

CHAPTER 1
Introduction

1.1 ALLOWABLE COMPRESSIVE STRESS AT PRESTRESS TRANSFER

The allowable compressive stress in a prestressed concrete member at the time of the release of tension in the prestressing steel is a concept that was first introduced by the American Association of State Highway and Transportation Officials (AASHTO) in 1961 and the American Concrete Institute (ACI) in 1963. The 1961 edition of the AASHTO Bridge Design Specifications and the 1963 edition of the ACI 318 Building Design Specifications included a clause limiting the allowable compressive stress in the concrete at release to a percentage of the compressive strength of the concrete at release. The allowable compressive stress in the concrete at prestress transfer adopted by these specifications remained unchanged until 2008, when a change was introduced in ACI 318-08. In ACI 318-63, the compressive stress limit was worded as follows:

> *Temporary stresses immediately after transfer, before losses due to creep and shrinkage, shall not exceed the following: 1. Compression… $0.60f'_{ci}$…* (ACI 318, 1963).

Currently, in ACI 318-08, the general compressive limit remains the same, but a clause was added to address the compressive stresses in the ends of simply supported beams. The compressive stress limit in ACI 318-08 is worded as the following:

> *Stresses in concrete immediately after prestress transfer (before time-dependent prestress losses): (a) Extreme fiber stress in compression except as permitted in (b) shall not exceed $0.60f'_{ci}$. (b) Extreme fiber stress in compression at ends of simply supported members shall not exceed $0.70f'_{ci}$…* (ACI 318, 2008).

In AASHTO LRFD (2007), the compressive stress limit, which has not changed since its inception, reads:

> *The compressive stress limit for pretensioned and post-tensioned concrete components, including segmentally constructed bridges, shall be* $0.60f'_{ci}$ (AASHTO LRFD 2007).

In these provisions, f'_{ci} is the compressive strength of the concrete at the time of prestress transfer.

In the last ten to fifteen years, considerable attention has been given to the idea of increasing the allowable compressive stress limit at prestress transfer from $0.60f'_{ci}$ to $0.65f'_{ci}$ or $0.70f'_{ci}$ which could lead to production and design improvements of prestressed concrete girders (Birrcher and Bayrak, 2007). Some primary benefits of increasing the allowable compressive stress at release include:

- The reduction in cycle time of precast facilities
- The reduction of the overall cement content
- The increase in span capabilities due to an increase in the number of prestressing strands in a given section
- The removal of "unnecessary" conservatism in current practice

To evaluate the feasibility of raising the extreme fiber stress in compression at prestress transfer, several research studies have been conducted in recent years. In these studies, numerous effects of increasing the allowable stresses were studied, such as the live load performance, creep, camber, and prestress loss of beams subjected to release stresses in excess of the current allowable limit. One of these studies, conducted by Birrcher and Bayrak at the University of Texas at Austin in 2006 establishes the foundation of the research presented in this thesis.

A research project, funded by the Texas Department of Transportation, was initiated at the Ferguson Structural Engineering Laboratory at the University of Texas at Austin. This research project (TxDOT Project 5197) has been ongoing for approximately four years and has consisted of two separate phases. In Phase I, completed in 2006, Birrcher and Bayrak focused on the live load performance of prestressed concrete members subjected to compressive stresses at prestress transfer in excess of the current

allowable limit as well as the impact of the compressive stresses on initial camber. In the study, 36 pretensioned beams were tested statically to experimentally evaluate their cracking load under live loads. Of these, 24 of the beams were scaled rectangular, tee, and inverted-tee beams and 12 were TxDOT Type-A beams (28-inch deep I-beam). In addition, four of the scaled specimens were tested under fatigue loads and an initial camber database was compiled from the results of 223 tests on pretensioned girders. (Birrcher and Bayrak, 2007)

After the completion of Phase I of this research study, a recommendation was made to study the effects of different section types and concrete mixture designs with different coarse aggregates on the live load performance of pretensioned beams subjected to compressive stresses at prestress transfer in excess of the current allowable limit, as well as potential adverse effects at the ends of pretensioned members, such as shear capacity and excessive bursting crack formation at release. From these recommendations, Phase II of the research project was initiated in 2007. This phase (Phase II) was divided into two distinctly different components: The focus of Part 1 was on the live load performance of pretensioned beams subjected to compressive stresses at prestress transfer in excess of the current allowable limit and the focus of Part 2 was on the shear performance. As recommended by Birrcher and Bayrak (2007), section properties and coarse aggregate type were the additional variables of the Phase II study. In Part 1, 45 TxDOT Type-C beams (40-inch deep I-beam) were tested in flexure to study premature flexural cracking due to compressive stress in excess of the current allowable limit at release. 10 TxDOT 4B28 box beams (4-foot wide, 28-inch deep box beam) are scheduled to be tested as well. In Part 2, 18 of the Type-C beams were tested in shear until failure. This thesis is dedicated to Part 2 of Phase II of the current research study.

1.2 SCOPE OF RESEARCH

Within the current project, a literature review and experimental research on the shear performance of prestressed concrete girders were performed. In the literature review (Chapter 2), a brief history of code provisions on shear strength is presented. In

addition, pertinent historical and recent studies dedicated to the shear performance of prestressed concrete members are discussed. In the experimental program, 18 prestressed concrete beams were tested in a test setup designed to create a web-shear failure in the beams. All 18 specimens were TxDOT Type-C bridge girders. The design of the specimens is discussed in Chapter 3. The C-beam specimens were fabricated by three different fabricators in the state of Texas, referred to in this thesis as Fabricator B, Fabricator C, and Fabricator D. Fabricator A constructed 12 Type-C beams that were only used in Part 1 of the current experimental research. The 10 box beams are being fabricated in August and September of 2008. The main variable in the test specimens was the maximum compressive stress at release. Eight specimens were released to achieve a target maximum stress of $0.70f'_{ci}$, four were targeted to achieve $0.65f'_{ci}$, and six were targeted to achieve $0.60f'_{ci}$. The aforementioned maximum compressive stresses occurred at the transfer length ($60d_b$ from the end of the beam) and at the locations of the strand hold down points. ACI 318-08 limits the maximum stresses at these points to $0.70f'_{ci}$ and $0.60f'_{ci}$, respectively. AASHTO LRFD 2007 limits the maximum stress to $0.60f'_{ci}$ across the length of the beam. The research presented in this thesis evaluates the feasibility of a stress limit of $0.70f'_{ci}$ in the end regions of prestressed concrete beams.

1.3 CHAPTER OUTLINE

In Chapter 2, a brief literature review is presented. First, the history of the shear design provisions in the ACI 318 and AASHTO LRFD specifications are presented and discussed. Relevant past research projects directly related to the shear strength of prestressed concrete members are discussed. From these research projects, data are presented using the University of Texas Prestressed Concrete Shear Database to evaluate the effectiveness of the code provisions in estimating the web cracking strength and ultimate shear capacity of prestressed concrete beams.

In Chapter 3, the 45 TxDOT Type-C specimens that were fabricated for Phase II of the research project are described. For Part 2 of the study, 18 of the C-beams were tested to failure in shear, with a maximum compressive stress at prestress transfer ranging

from $0.57f'_{ci}$ to $0.77f'_{ci}$. The flexural design and shear reinforcement design are discussed, as well as the fabrication process and the process of storing and shipping the beams to the Ferguson Structural Engineering Laboratory.

In Chapter 4, the experimental program is described. In the shear performance evaluation, 18 beams were tested by using a shear span to depth ratio of 2.22, ensuring a web-shear failure of the beams. For each test, the diagonal cracking shears and shear capacities were experimentally measured.

In Chapter 5, the behavior of the test specimens under shear loads is presented and analyzed. The measured first diagonal cracking shear of each specimen is compared to the diagonal cracking shear estimated by using ACI 318-08 and AASHTO LRFD 2007 (simplified procedure) provisions for web-shear cracking. In addition, the experimentally obtained shear strengths of the test specimens are compared to the estimates obtained through the use of the ACI 318-08 and AASHTO LRFD 2007 provisions for nominal shear capacity. Recommendations for the feasibility of increasing the allowable compressive stress at release were based on the analysis of this test data.

In Chapter 6, the conclusions and recommendations of the current study are summarized. In addition, recommendations for future work are provided. Lastly, four appendices are provided. Appendix A summarizes the bursting crack formation in the end regions, Appendix B provides important sample calculations for prestressed concrete shear capacity, Appendix C provides shop drawings of the test specimens, and Appendix D provides strength gain versus time plots for all concrete casting operations used in the fabrication of the 45 C-beams.

CHAPTER 2
Literature Review

2.1 OVERVIEW

In this chapter, a brief history of the ACI 318 and AASHTO LRFD shear design provisions are summarized. This summary is provided because an understanding of current code equations is paramount to the analysis of the test data presented in this thesis. In addition, an overview of previous research conducted on the shear strength of prestressed concrete members is presented.

The main topics discussed in the following sections are: 1) the history of the ACI 318 and AASHTO LRFD shear design provisions and 2) the literature on shear strength of prestressed concrete beams with particular emphasis on the effects of increasing the allowable compressive stress at release. Previous research projects have focused on various effects of increasing the allowable compressive stress at release, such as live load performance and camber. Part 1 of the current research study is devoted to the live load performance of prestressed concrete beams, which is not discussed in this thesis. Research related to other effects of increasing the allowable compressive stress at release as well as a complete overview of the history of allowable release stresses is presented in TxDOT Report 0-5197-1 (Birrcher and Bayrak, 2007).

2.2 EVALUATION OF CURRENT DESIGN SPECIFICATIONS

The equations for nominal shear capacity found in the ACI 318 and AASHTO LRFD specifications were empirically derived from the findings of past research projects. Knowledge of these equations is important for an understanding of the data presented in this thesis. The history of the ACI 318 and AASHTO LRFD shear design provisions are discussed in this section.

2.2.1 History of the ACI 318 Shear Design Provisions

2.2.1.1 ACI 318-63

Design provisions for prestressed concrete members first appeared in the ACI 318 specifications in 1963. The original expression for the shear strength of concrete at diagonal cracking was given as the lesser of the shear needed to transform a flexural crack into a diagonal crack, V_{ci}, and the shear needed to form a diagonal web crack, V_{cw}, as seen in Equation 2-1 and Equation 2-3, respectively, but not less than $1.7b'd\sqrt{f_c'}$.

$$V_{ci} = 0.6b'd\sqrt{f_c'} + \frac{M_{CR}}{\frac{M}{V} - \frac{d}{2}} + V_d \qquad \textbf{Equation 2-1}$$

where:

$$M_{CR} = \frac{1}{y}\left(6\sqrt{f_c'} + f_{pe} - f_d\right) \qquad \textbf{Equation 2-2}$$

$$V_{cw} = b'd(3.5\sqrt{f_c'} + 0.3f_{pc}) + V_p \qquad \textbf{Equation 2-3}$$

where:

V_{ci} = shear at diagonal cracking due to all loads, when such cracking is a result of combined shear and moment

V_{cw} = shear force at diagonal cracking due to all loads, when such cracking is the result of excessive principal tension stresses in the web

b' = minimum width of the web of a flanged member

d = distance from extreme compression fiber to centroid of the prestressing force

f_c' = Compressive strength of concrete (units of psi)

M = bending moment due to externally applied loads

V = shear due to externally applied loads

V_d = shear due to dead load only

f_{pc} = compressive strength of concrete at the centroid of the cross section resisting the applied loads after all prestressing losses have occurred

V_p = vertical component of the effective prestressing force at the section being considered

y = distance from the centroidal axis of the section resisting the applied loads to the extreme fiber in tension

f_{pe} = compressive stress in concrete due to prestress only at the extreme tension fiber after all losses

f_d = stress due to dead load at the extreme fiber of a section at which tension stresses are caused by applied loads

The shear strength carried by transverse reinforcement was included in the 1963 ACI 318 code, in terms of the total area of web reinforcement, as:

$$A_v = \frac{V's}{f_v d} \qquad \textbf{\textit{Equation 2-4}}$$

where:

A_v = total area of web reinforcement

s = spacing of perpendicular stirrups

V' = shear carried by web reinforcement

f_v = tensile stress in web reinforcement

d = distance from extreme compression fiber to centroid of tension reinforcement

The contribution of the transverse reinforcement to the shear capacity could be calculated from Equation 2-4 by rearranging the terms to solve for *V'*.

The equations given in ACI 318-63 for shear strength of prestressed concrete members were calibrated by using the results of tests conducted on "*244 bonded prestressed beams which failed in shear"* (ACI 318-63 Commentary). Though empirically derived, the equations proved to be adequate predictors of the shear strength of prestressed concrete members.

2.2.1.2 ACI 318-71

In the next edition of the ACI 318 Specifications, published in 1971, a conservative simplified equation proposed by MacGregor and Hanson (1969) was given to calculate the shear strength of concrete members which had an effective prestress force of at least 40 percent of the tensile strength of the flexural reinforcement. The equation as seen in ACI 318-71 is as follows:

$$v_c = 0.6\sqrt{f_c'} + 700\frac{V_u d}{M_u} \qquad \textbf{Equation 2-5}$$

where V_u and M_u are factored shear force and bending moment due to factored loads. In 1971 a minor change in the V_{ci} equation was made. The minus *d/2* term in Equation 2-1 was dropped from the denominator to allow the equation to represent the strength of the section being investigated, and not a section just at *d/2* inches from the support reaction. The modification added extra conservatism to the equation for V_{ci}. The equation as seen in ACI 318-71 is given in Equation 2-6.

$$v_{ci} = 0.6\sqrt{f_c'} + \frac{V_d + V_l M_{cr}}{b_w d} \qquad \textbf{Equation 2-6}$$

In Equation 2-6, V_l is the shear force at the section occurring simultaneously with M_{max}. M_{cr} was expressed in the same way as in ACI 318-63 but the width of the web was changed symbolically from *b'* to b_w. Unlike V_{ci}, the expression for V_{cw} did not change in ACI 318-71. Expressed as a shear stress, V_{cw} in ACI 318-71 was given as:

$$v_{cw} = (3.5\sqrt{f_c'} + 0.3f_{pc}) + \frac{V_p}{b_w d} \qquad \textbf{Equation 2-7}$$

When both sides of equations 2-5 through 2-7 are multiplied by $b_w d$, the shear is calculated and this format corresponds to the provisions in the current version of the ACI 318 Specifications.

2.2.1.3 ACI 318-08

The current ACI 318 equations for shear strength of concrete in prestressed concrete members have not changed since 1971 other than a few minor notation changes and definitions. MacGregor and Hanson's (1969) simplified expression for computing v_c, the shear stress in concrete, is currently expressed as a shear force as:

$$V_c = (0.6\sqrt{f_c'} + 700\frac{V_u d_p}{M_u})b_w d \qquad \textbf{Equation 2-8}$$

where V_c need not be taken greater than $5\sqrt{f_c'}b_w d$ but not less than $2\sqrt{f_c'}b_w d$ and d is defined as the distance from the extreme compression fiber to the centroid of tension reinforcement. For a member with only prestressed reinforcement, d is equal to d_p. The simplified expression is only to be used if the V_{ci} and V_{cw} approach is not. If a more detailed calculation is needed, the shear strength of concrete is said to be the lesser of V_{ci} and V_{cw}, defined in ACI 318-08 as:

$$V_{ci} = 0.6\sqrt{f_c'}b_w d_p + V_d + \frac{V_i M_{cre}}{M_{\max}} \qquad \textbf{Equation 2-9}$$

where:

$$M_{cre} = \frac{1}{y_t}\left(6\sqrt{f_c'} + f_{pe} - f_d\right) \qquad \textbf{Equation 2-10}$$

$$V_{cw} = (3.5\sqrt{f_c'} + 0.3f_{pc})b_w d_p + V_p \qquad \textit{Equation 2-11}$$

The definitions of the individual terms remain the same as defined in ACI 318-71, but the notation of M_{cr} has been changed to M_{cre} and V_l has been changed to V_i. There is no numerical difference in M_{cr} and M_{cre} and the difference between V_l and V_i is that V_i is currently defined as the factored shear force whereas V_l was not defined as factored. V_{ci} and V_{cw} represent the two types of inclined shear cracking: flexure-shear cracking and web-shear cracking, respectively. Flexure-shear cracking is premeditated by flexural cracking, whereas web-shear cracking begins in the web of a member. In this research project, the shear strength of the concrete in the beams was calculated by using these equations.

The current ACI 318 equation for the shear strength carried by transverse reinforcement has not changed since 1963, other than minor notation changes and the terms were rearranged to what is seen in Equation 2-12.

$$V_s = \frac{A_v f_{yt} d}{s} \qquad \textit{Equation 2-12}$$

2.2.2 History of the AASHTO LRFD Shear Design Provisions

AASHTO began publishing bridge design specifications in 1931 (AASHTO Standard Specifications). The document was known as the AASHTO Standard Specifications for Bridge Design. Currently, the shear design provisions of the AASHTO Standard Specifications for Highway Bridges (17th Edition) are identical to the corresponding provisions found in ACI 318-08. Since the two specifications give the same equations for prestressed concrete shear design, the AASHTO Standard Specifications for Highway Bridges will not be discussed for sake of brevity.

2.2.2.1 AASHTO LRFD (1994) Interim

The first AASHTO LRFD Bridge Design Specification was published in 1994. The sectional design model for shear introduced in the document was a hand-based shear

design procedure derived from Modified Compression Field Theory (MFCT) (Avendaño and Bayrak, 2008). The nominal shear capacity was given as the sum of the concrete component, the reinforcement component, and the vertical component of the effective prestressing force. The concrete contribution was given as:

$$V_c = 0.0316\beta\sqrt{f'_c}\,b_v d_v \qquad \textbf{Equation 2-13}$$

where f'_c is the compressive strength of concrete in units of ksi, b_v is the effective web width, d_v is the effective shear depth, and β is a factor indicating the ability of diagonally cracked concrete to transmit tension and shear. β is taken from a table that lists the ratio of shear stress in concrete to concrete strength, v_u/f'_c, as rows and the longitudinal strain at middepth of the member, ε_c, as columns. The longitudinal strain at middepth is dependent upon another factor, θ, which represents the theoretical angle of diagonal cracking. Both θ and β are presented in Table 2.1 and Table 2.2. θ is the number on top in each cell and β is the number on bottom. The two different tables represent tables for members with transform reinforcement and for members without transverse reinforcement. The process of solving for θ is a complicated iterative process with ε_c. It is not the intention of this literature review to instruct the reader in the use of this procedure. (In recent versions of the AASHTO LRFD specifications, a detailed flowchart, shown in Figure 2.1, to facilitate the use of this method has been provided.)

The reinforcement component of the nominal shear capacity was given as (for stirrups perpendicular to the longitudinal axis of a beam):

$$V_s = \frac{A_v f_y d_v \cot\theta}{s} \qquad \textbf{Equation 2-14}$$

The equation is similar to the one found in the ACI 318 specifications but differs in the definition of d_v and the angle of diagonal cracking. In Equation 2-14, d_v is taken as the distance from the centroid of the longitudinal reinforcement to the centroid of the compressive zone in flexure and θ is the same angle of diagonal cracking as described above. Once again, solving for θ becomes an iterative process with ε_c.

Table 2.1 Values of θ and β for Sections with Transverse Reinforcement, AASHTO LRFD (1994)

$\frac{v}{f'_c}$	ϵ_x x 1,000										
	-0.2	-0.15	-0.1	0	0.125	0.25	0.5	0.75	1	1.5	2
<= 0.05	27.0 6.78	27.0 6.17	27.0 5.63	27.0 4.88	27.0 3.99	28.5 3.49	29.0 2.51	33.0 2.37	36.0 2.23	41.0 1.95	43.0 1.72
0.075	27.0 6.78	27.0 6.17	27.0 5.63	27.0 4.88	27.0 3.65	27.5 3.01	30.0 2.47	33.5 2.33	36.0 2.16	40.0 1.90	42.0 1.65
0.1	23.5 6.50	23.5 5.87	23.5 5.31	23.5 3.26	24.0 2.61	26.5 2.54	30.5 2.41	34.0 2.28	36.0 2.09	38.0 1.72	39.0 1.45
0.125	20.0 2.71	21.0 2.71	22.0 2.71	23.5 2.60	26.0 2.57	28.0 2.5	31.5 2.37	34.0 2.18	36.0 2.01	37.0 1.60	38.0 1.35
0.15	22.0 2.66	22.5 2.61	23.5 2.61	25.0 2.55	27.0 2.50	29.0 2.45	32.0 2.28	34.0 2.06	36.0 1.93	36.5 1.50	37.0 1.24
0.175	23.5 2.59	24.0 2.58	25.0 2.54	26.5 2.50	28.0 2.41	30.0 2.39	32.5 2.20	34.0 1.95	35.0 1.74	35.5 1.35	36.0 1.11
0.2	25.0 2.55	25.50 2.49	26.5 2.48	27.5 2.45	29.0 2.37	31.0 2.33	33.0 2.10	34.0 1.82	34.5 1.58	35.0 1.21	36.0 1.00
0.225	26.5 2.45	27.0 2.38	27.5 2.43	29.0 2.37	30.5 2.33	32.0 2.27	33.0 1.92	34.0 1.67	34.5 1.43	36.5 1.18	39.0 1.14
0.25	28.0 2.36	28.5 2.32	29.0 2.36	30.0 2.30	31.0 2.28	32.0 2.01	33.0 1.64	34.0 1.52	35.5 1.40	38.5 1.30	41.5 1.25

Table 2.2 Values of θ and β for Sections without Transverse Reinforcement, AASHTO LRFD (1994)

s_x	ϵ_x x 1,000								
	-0.2	-0.1	0	0.25	0.5	0.75	1	1.5	2
<= 5	26.0 6.90	26.0 5.70	27.0 4.94	29.0 3.78	31.0 3.19	33.0 2.82	34.0 2.56	36.0 2.19	38.0 1.93
10	27.0 6.77	28.0 5.53	30.0 4.65	34.0 3.45	37.0 2.83	39.0 2.46	40.0 2.19	43.0 1.87	45 1.65
15	27.0 6.57	30.0 5.42	32.0 4.47	37.0 3.21	40.0 2.59	43.0 2.23	45.0 1.98	48.0 1.65	50.0 1.45
25	28.0 6.24	31.0 5.36	35.0 4.19	41.0 2.85	45.0 2.26	48.0 1.92	51.0 1.69	54.0 1.40	57.0 1.18
50	31.0 5.62	33.0 5.24	38.0 3.83	48.0 2.39	53.0 1.82	57.0 1.50	59.0 1.27	63.0 1.00	66.0 0.83
100	35.0 4.78	35.0 4.78	42.0 3.47	55.0 1.88	62.0 1.35	66.0 1.06	69.0 0.87	72.0 0.65	75.0 0.52
200	42.0 3.83	42.0 3.83	47.0 3.11	64.0 1.39	71.0 0.90	74.0 0.66	77.0 0.53	80.0 0.37	82.0 0.28

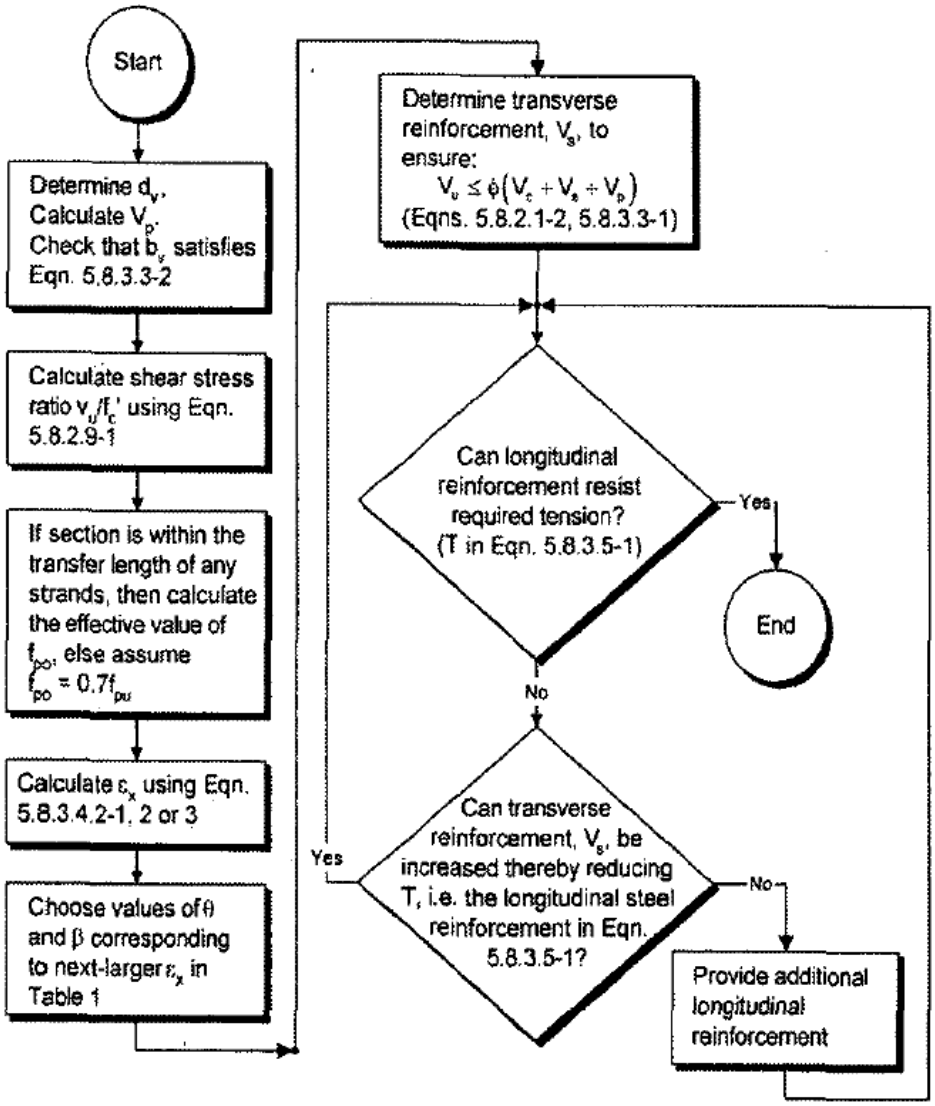

Figure 2.1 Flow Chart for use of MCFT Method, AASHTO LRFD (2007)

2.2.2.2 AASHTO LRFD 2007 Interim

In the AASHTO LRFD (2007) Bridge Design Specifications, two methods are given for calculating the concrete component of the shear capacity. The iterative procedure from the 1994 specification remains the same, though slightly modified, but a simplified procedure, based on the results of *NCHRP Report 549*: *Simplified Shear Design of Structural Concrete Members,* for prestressed and nonprestressed sections was introduced. In the simplified procedure, similar to the shear design provisions of ACI 318-08, the shear resisted by concrete is said to be the lesser of V_{ci} and V_{cw}, as seen in Equation 2-15 and Equation 2-17, respectively.

$$V_{ci} = 0.02\sqrt{f_c'}b_v d_v + V_d + \frac{V_i M_{cre}}{M_{\max}} \geq 0.06\sqrt{f_c'}b_v d_v \qquad \textbf{Equation 2-15}$$

$$M_{cre} = S_c(fr + f_{cpe} - \frac{M_{dmc}}{S_{nc}}) \qquad \textbf{Equation 2-16}$$

$$V_{cw} = (0.06\sqrt{f_c'} + 0.30 f_{pc})b_v d_v + V_p \qquad \textbf{Equation 2-17}$$

The AASHTO LRFD (2007) equations for V_{ci} and V_{cw} only differ from the ACI 318-08 equations in the constants in front of the square roots term, the definition of the shear depth, d_v, the definition of M_{cre}, and the units of f'_c (ksi in AASHTO LRFD, psi in ACI 318)

The equation for the shear capacity of transverse reinforcement was identical to the equation from the 1994 specification but a clause was added to allow $\cot\theta$ to be taken as:

$$\cot\theta = 1.0 + 3(\frac{f_{pc}}{\sqrt{f'_c}}) \leq 1.8 \qquad \textbf{Equation 2-18}$$

Equation 2-18 provided a shortcut around the iterative procedure originally needed to solve for θ.

2.2.3 Comparison between ACI 318 and AASHTO LRFD Shear Design Provisions

The equations for nominal shear capacity found in the ACI 318 and AASHTO LRFD specifications (simplified procedure) are similar in nature but differ by nomenclature and empirically based constants. In the ACI 318 equation for flexural-shear cracking strength, V_{ci}, the term $0.6\sqrt{f_c'}$ needs to be divided by 1000 to convert to units of kips per square inch. In the AASHTO LRFD counterpart equation, the conversion is already made by taking the square root of 1000 out of the first term. If the ACI 318 equation is converted to the same units as the AASHTO LRFD equation, it yields a term of $0.019\sqrt{f_c'}$ as compared to $0.02\sqrt{f_c'}$, showing that the two codes are almost identical for flexure-shear cracking. The equation for M_{cre} in AASHTO LRFD appears different on paper but the terms are all identical to the terms in the ACI 318 equation with the exception of the modulus of rupture being defined in ACI 318 as $6\sqrt{f_c'}$ and in AASHTO LRFD as $6.32\sqrt{f_c'}$.

The equation for V_{cw} is defined the same in ACI 318 as in AASHTO LRFD with the only difference being the $3.5\sqrt{f_c'}$ term in ACI 318-08, which converts to $0.11\sqrt{f_c'}$ when the units are made to match AASHTO LRFD (2007). The constant term in AASHTO LRFD (2007) is given as $0.06\sqrt{f_c'}$, leading to a large difference in the web-cracking shear strengths as defined by the two different codes. The reason for this difference lies in the lack of distinction made for prestressed and nonprestressed members in AASHTO LRFD (2007). Equations 2-15 and 2-17 are applicable to both types of members, whereas in ACI 318, the V_{ci} and V_{cw} equations are only applicable to prestressed members. When evaluated for a nonprestressed member, Equation 2-17 reduces to $0.06\sqrt{f_c'}b_w d_v$, which closely relates to the lower bound of reinforced concrete shear strength found in ACI 318-08 of $0.063\sqrt{f_c'}b_w d$ (in units made to match AASHTO LRFD). The AASHTO LRFD (2007) V_{ci} and V_{cw} expressions serve to estimate the

diagonal cracking load while also serving as a lower bound estimate of the concrete contribution to nominal shear capacity. An identical V_{cw} equation to the one in ACI 318-08 is found in the AASHTO Standard Specifications.

The ACI 318 and AASHTO LRFD code provisions for the shear strength provided by transverse reinforcement are similar but differ mainly in the definition of the angle of diagonal cracking. ACI 318 assumes a diagonal crack angle of 45 degrees which all V_s calculations are based on instead of the actual angle of diagonal cracking. AASHTO LRFD provides a method for getting a better estimate of the diagonal cracking angle, as described in Section 2.2.2.2

The V_{ci} and V_{cw} equations used by AASHTO LRFD (2007) are based on the recommendations of Hawkins and Kuchma (*NCHRP Report 549*, 2005) and the concepts in ACI 318-05. However, the concepts were modified to be applicable to both prestressed and nonprestressed members. The shear strength estimates from AASHTO LRFD (2007) are typically more conservative than the estimates obtained by using ACI 318-08 due to the difference in web cracking equations. It is also useful to note that the ACI 318-08 equations for concrete contribution to shear capacity are representative of the cracking loads whereas the AASHTO LRFD (2007) equations are representative of the nominal shear capacity minus the contribution from the transverse steel, which allows for the concrete to carry additional capacity after initial cracking. Even with the allowance for additional concrete contribution to load carrying capacity, the AASHTO LRFD (2007) provisions (simplified procedure) still prove to give lower estimates of the shear strength of prestressed concrete members than the ACI 318-08 provisions because of the fact that they are applicable to reinforced concrete members as well.

2.3 TECHNICAL LITERATURE: PRESTRESSED CONCRETE SHEAR

The shear strength of prestressed concrete members is a topic that has been extensively researched. Since 1954, 30 studies have been dedicated to various aspects of prestressed concrete shear design (References 6 – 7, 9 – 10, 12, 14 – 23, 25 – 29, 31 – 36, and 38 - 41). The 30 studies are summarized by research category in Table 2.3. It is important to note that the research projects listed under one category typically address more issues than what is implied by the simplified title of the category in Table 2.3. While this fact was recognized, it was found useful to organize the research projects into the different categories indicated in Table 2.1. The primary objectives and main conclusions from these research projects are presented in the following sections.

Table 2.3 Summary of Research on Prestressed Concrete Shear Strength

Research Category	Researchers	Year	Reference No.
Early US Research	Zwoyer and Siess	1954	41
	Hernandez	1958	18
	Sozen, Zwoyer, and Siess	1959	34
	MacGregor	1960	24
	Bruce	1962	12
Research To Examine Code Provisions	Bennett and Balasooriya	1971	10
	Lyngberg	1976	22
	Rangan	1991	32
	Alshegeri and Ramirez	1992	6
	Shahawy and Batchelor	1996	35
	Raymond, Bruce, and Roller	2005	33
	Laskar, Wang, Hsu, and Mo	2007	20
	Avendaño and Bayrak	2008	9
Effects of Continuous Spans	Morice and Lewis	1955	29
	Zekaria	1958	39
	Mattock and Kaar	1961	28
	Hawkins, Sozen, and Siess	1961	17
	Magnel	1954	26
	Lin	1955	21
Effects of Welded Wire Fabric as Shear Reinforcement	Durrani and Robertson	1987	14
	Xuan, Rizkalla, and Maruyama	1988	38
Effects of High Strength Concrete	Elzanaty, Nilson, and Slate	1986	15
	Hartman, Breen, and Kreger	1988	16
	Kaufman and Ramirez	1988	19
	Ma, Tadros, and Baishya	2000	23
	NCHRP Report 579	2005	31
Effects of Strand Slippage	Maruyama and Rizkalla	1988	27
Effects of Distributed Loading	Arthur, Bhatt, and Duncan	1973	7
Effects of Draped Reinforcement	MacGregor, Sozen, and Siess	1960	25
Minimum Required Shear Reinforcement	Teoh, Mansur, and Wee	2002	36

2.3.1 Early Research in United States

The shear strength of prestressed concrete members is a topic that was first researched in the 1950s. Early investigations on prestressed concrete shear capacity established the foundation for the empirical provisions in the codes today. The majority of the research projects from the 1950s and 1960s on prestressed concrete shear were dedicated to general knowledge of shear behavior. The early research projects are discussed in this section.

The first known study on prestressed concrete shear capacity in the United States was conducted by Zwoyer and Siess in 1954 at the University of Illinois. The goal of the study was to determine a method of computing the shear strength of prestressed concrete beams. To accomplish their goal, the researchers tested 34 twelve-inch deep simply supported rectangular prestressed concrete beams without shear reinforcement. Thirty-two of the beams were post-tensioned and two were pretensioned. Variables in the experimental program included the area of longitudinal steel, the concrete strength, and the shear span to depth ratio. Of the 34 beams, 29 failed in shear. All 29 beams that failed in shear experienced flexural cracks which transformed into flexure-shear cracks. Failure resulted from the concrete crushing between diagonal cracks. From the results of the tests and prior knowledge of reinforced concrete shear strength and flexural strength, the researchers derived expressions for the shear strength of prestressed concrete members without shear reinforcement.

In 1958, another study on the shear strength of prestressed concrete members was conducted at the University of Illinois by Hernandez. The objective of the study was to investigate how longitudinal reinforcement, web thickness, amount of web reinforcement, stirrup spacing, yield stress of stirrups, concrete strength, and shear span affected the overall shear carrying capacity of prestressed concrete members. Thirty-eight twelve-inch deep I-beams were tested under a concentrated load with the factors listed above varied between beams. Eleven of the beams failed in shear along diagonal cracks. The main conclusion Hernandez drew from his research was that shear failures could be

prevented by using adequate amounts of vertical stirrups. He also derived an empirical equation for the shear strength carried by vertical stirrups.

A study by Sozen, Zwoyer, and Siess in 1959 was aimed at obtaining a better understanding of the shear behavior of reinforced and prestressed concrete beams without web reinforcement. Forty-three rectangular beams and 56 I-beams were tested in the study, none of which had web reinforcement. All beams were 12 inches deep. The primary variables in the study were shape of cross section, prestress level, shear span, amount of longitudinal reinforcement, and concrete strength. Ninety of the 99 beams failed in shear. The research showed that prestressed concrete beams without web reinforcement were vulnerable to shear failures and that the shear failure load may be significantly less than the load corresponding to the flexural capacity of the beam. The study also led the researchers to propose an empirical expression for the diagonal cracking load of a prestressed concrete beam.

Adding to the work of Hernandez (1958), two more studies took place at the University of Illinois in the early 1960s. MacGregor (1960) studied the behavior of prestressed concrete beams with web reinforcement by testing 36 twelve-inch deep prestressed I-beams and rectangular beams, 13 of which failed in shear. Bruce (1962) studied the effects that web reinforcement had on the shear strength of prestressed concrete members by testing 24 simply supported I-beams with depths of 12 or 14 inches. Sixteen shear failures were reported from the 24 tests. The primary variable in these research projects was the type of web reinforcement. The data taken from the studies led to the development of a method for calculating the shear stress in transverse reinforcement. Similarly to the conclusions of Sozen et al. (1959), the main conclusion drawn from the studies was that the shear failures could be prevented by providing adequate amounts of vertical stirrups.

From the results of the numerous studies at the University of Illinois, MacGregor, Sozen, and Siess (1960) empirically derived expressions for diagonal cracking load and shear capacity of prestressed concrete members. These expressions formed the basis of the prestressed concrete shear provisions in the ACI 318 specifications.

2.3.2 Research to Examine Code Provisions

Many research projects have been dedicated to a general evaluation of code provisions or evaluating code provisions for a specific type of beam. This section summarizes the research projects that fall into the category of general research on code provisions.

A study of the shear strength of prestressed concrete beams with thin webs was conducted by Bennett and Balasooriya in 1971. Twenty-six prestressed concrete beams of 10 or 18 inch depth were tested in shear to investigate the upper limit of shear strength associated with crushing of the web. The researchers were concerned that there was no accurate estimate of the maximum shear stress a prestressed concrete beam could endure before web crushing. The results showed that the behavior at failure could be represented by a truss formed by the stirrups and the concrete struts. Based on the truss model, design formulas were suggested for the upper limit of shear strength associated with web crushing.

In 1976, Lyngberg studied the effect of prestress force on the shear strength of prestressed concrete members failing in web crushing. Nine prestressed concrete I-beams were tested with variable prestress forces. All beams were 24 inches deep. Web reinforcement, cross-sectional area, flexural capacity, and shear span were all held constant. Eight of the beams failed along diagonal shear cracks (V_{cw} failure) and the other failed from crushing of the top flange. Lyngberg found that higher prestress forces led to more explosive shear failures. However, he concluded that the failure load was not influenced significantly by the prestress force.

In 1991, Rangan studied the web crushing strength of prestressed and reinforced concrete beams. The goal of the research was to evaluate the upper limit on shear strength given by the ACI 318 specifications and other international codes. Sixteen prestressed and reinforced concrete I-beams with depths of 24 inches were tested. The primary variables in the experiments were the amount of transverse reinforcement and amount of longitudinal reinforcement. All beams failed due to crushing of the concrete

in the web. To analyze the data, the test measurements for shear capacity were compared to the maximum allowable shear strength. The maximum allowable shear strength in the ACI 318 specification is currently defined as

$$V_{\max} \le V_c + 8\sqrt{f_c'} b_w d \qquad \textbf{\textit{Equation 2-19}}$$

Rangan (1991) found that the ACI 318 code provision for maximum allowable shear strength was the most conservative of all the codes analyzed (ACI 318, Australian Standard, and Canadian Standard).

The strut and tie method is an alternative way recognized by the ACI 318 specification of calculating shear capacities. Alshegeir and Ramirez conducted a study in 1992 that was aimed at evaluating the strength and behavior of deep prestressed concrete beams in shear using the strut and tie method. Three I-beams (two 28-inches deep and one 36-inches deep) were tested in shear, all of which failed by crushing of the web concrete. In all tests, the strut and tie method was able to accurately model the shear behavior of the prestressed concrete beams.

In 1996, Shahawy and Batchelor conducted an extensive study of prestressed concrete shear behavior aimed at comparing the 1989 edition of the AASHTO Standard Specification and the 1994 edition of the AASHTO LRFD specification. Forty I-beams were tested with varying cross sections and amounts of transverse and longitudinal reinforcement. All beams were 44-inches deep. The results of the tests showed that the AASHTO Standard shear provisions were better predictors of shear strength than the ASHTO LRFD shear provisions.

In 2005, Raymond, Bruce, and Roller studied the shear strength of deep bulb-tee prestressed concrete girders. The 3 girders tested were each 96-feet long and 72-inches deep. Shear tests were performed on each end of the girders, giving a total of six tests. The study was conducted because of a growing interest in 72-inch deep bulb-tee girders in Louisiana. Two of the beams were designed in accordance with the AASHTO LRFD specifications and the other was designed in accordance with the ACI 318 specification. The researchers concluded that both the ACI 318 and AASHTO LRFD provisions for

shear strength of prestressed concrete were conservative for 72-inch deep bulb-tee girders.

Another investigation on the effectiveness of the AASHTO LRFD prestressed concrete shear provisions was conducted by Laskar, Wang, Hsu, and Mo in 2007. Five 28-inch deep prestressed concrete I-beams (TxDOT A-Beams) were tested in shear to evaluate the ACI 318 and AASHTO LRFD equations for the shear strength of prestressed concrete members and propose a new simplified equation. The new proposed equation reduced the ultimate shear capacity of a prestressed concrete member to a single equation.

In 2008, Avendaño and Bayrak studied the shear strength of a new TxDOT girder (Tx28) that was designed to optimize flexural performance. Four shear tests on two 28-inch deep prestressed concrete I-beams were performed to evaluate the applicability of current shear design provisions when applied to the new type of girder. The results showed that the current code provisions for shear strength were acceptable and conservative for the new girders.

2.3.3 Research on Effects of Continuous Spans

Six research studies of the late 1950s and early 1960s were dedicated to evaluating the shear strength of prestressed concrete members used to create continuous spans. Continuous spans are fairly common in construction, but are rarely investigated experimentally. Most bridges are constructed with concrete beams as simply supported members but some are made continuous by placing longitudinal reinforcement in the deck slab above the supports (Mattock and Kaar, 1961).

An early investigation into the effects of continuous spans on the behavior of prestressed concrete members was conducted by Morice and Lewis in 1955. Twenty-eight six-inch deep two-span continuous girders were tested, all but one of which failed in flexure. The one shear failure occurred from a diagonal crack forming out of a flexural crack. Because the vast majority of the failure modes were flexural, conclusions about

the shear strength of continuous spans were not given. However, the research proved useful for the study of flexural performance of continuous spans.

In 1958, Zekaria studied the shear strength of continuous prestressed beams without web reinforcement. At the time, no code provisions existed for calculating the shear strength of prestressed concrete members. The research study was thought to be the first dedicated solely to the shear strength of continuous prestressed beams. The primary goal of the study was to determine the modes of shear failures. To accomplish the goals, 12 tests were conducted on two-span continuous prestressed concrete rectangular beams. The beams, all of which were post-tensioned, were only eight inches deep, and featured no web reinforcement. Of the beams tested, only six failed in shear and those that failed in shear all experienced diagonal cracks forming from flexural cracks (V_{ci} failure). The main conclusion found from the tests was that continuous beams without web reinforcement could fail in shear before full flexural capacity was developed.

An extensive research project conducted by Mattock and Kaar at the University of Illinois in 1961 studied the effects that a special type of continuous highway bridge construction method had on the shear strength of the prestressed concrete T-beams used in the bridge. The bridge consisted of prestressed girders with an in-situ-cast deck slab which created continuous spans due to longitudinal reinforcement in the deck. The bridge was simulated in the laboratory by fabricating a single span girder with a cantilever overhang of nine feet. Loads were then placed on each side of the support creating a negative moment region above the support. In addition to different loading positions, the researchers also tested different spacings of shear reinforcement provided by No. 2 stirrups. The experiments showed that flexural cracking in the negative moment region had no negative effect on the shear strength of the continuous members and that continuous spans performed similarly to simplee spans under shear loads.

In 1961 at the University of Illinois, Hawkins, Sozen, and Siess investigated the shear strength and behavior of continuous prestressed concrete beams. Twenty-four two-span continuous rectangular and I-beams were tested with depths of 12-inches each. The

main variables in the experimental program were cross-sectional shape, concrete strength, effective depth, and amount of web reinforcement. Nine of the 24 specimens failed in shear due to diagonal tension cracks. From the data, the authors concluded that the shear strength of continuous prestressed girders could be calculated to an acceptable level of accuracy from basic strength and deformation characteristics of two-span continuous beams. (At the time of this research project, ACI 318 and AASHTO Standard specifications did not include shear provisions for prestressed concrete beams).

Two similar studies on effects of continuous spans were conducted in the mid 1950s for use in text books. Magnel tested a three-span continuous post-tensioned concrete beam for his 1954 textbook "Prestressed Concrete" (Magnel 1954). The object of the test was to determine the factors of safety against flexural cracking and ultimate failure for a three-span beam. Final failure occurred by crushing of the web above a diagonal flexure-shear crack. Lin tested four two-span continuous post-tensioned concrete beams for his 1955 book "Design of Prestressed Concrete Structures" (Lin, 1955). Similar to Magnel's beam, the beams failed due to crushing of the concrete above a diagonal crack.

2.3.4 Research on Effects of Welded Wire Fabric as Shear Reinforcement

Two studies in the late 1980s explored the feasibility of using welded wire fabric (WWF) as shear reinforcement for prestressed concrete beams. WWF is useful for beams with thin webs, such as double-tees, and provides an economical alternative to conventional stirrups in prestressed and reinforced concrete members.

In 1987, Durrani and Robertson studied the effects of using WWF as shear reinforcement by testing 13 prestressed concrete T-beams. Each beam was 20-inches deep and was tested over a span of 11-feet designed to create a web-shear failure. The primary variable studied was the type of shear reinforcement. Nine beams were reinforced with WWF, one with conventional stirrups, and three had no shear reinforcement. The results of the experimental program led the researchers to conclude

that WWF performed just as good as individual stirrups for use as shear reinforcement (Durrani et. al. 1987).

Building on the research of Durrani et. al. (1987), Xuan, Rizkalla, and Maruyama (1987) also evaluated the effectiveness of using WWF as shear reinforcement in prestressed concrete beams. They tested six 19-inch deep prestressed concrete T-beams; one had no shear reinforcement, one had conventional double-legged stirrups, one had single-legged stirrups, and the other three featured different types of commercially available WWF. All six tests produced shear failures resulting from web crushing. The data showed that the effectiveness of WWF as shear reinforcement was the same as that of conventional stirrups under static loading, confirming the conclusions of Durrani et. al (1987).

2.3.5 Research on Effects of High Strength Concrete

Five research studies have focused on the effects of high strength concrete (HSC) on the shear strength of prestressed concrete members. With the increasing popularity of HSC in recent years, researchers have begun to question the applicability of current code equations to concretes with high compressive strengths.

In 1986, Elzanaty, Nilson, and Slate studied the effects of using HSC on the shear strength of prestressed concrete beams. The researchers were concerned that the ACI 318 code equations might not have been safe when applied to high strength concrete beams. To study their concerns, they tested 34 beams, half of which were designed for flexure-shear cracking and the other half of which were designed for web-shear cracking. The beams had depths of either 14 or 18 inches. After the tests were complete, they found that the ACI 318 equations for V_{ci} and V_{cw} were conservative in estimating the shear strength of HSC prestressed concrete beams and that the equations became more conservative with increasing concrete compressive strength.

In 1988, Hartman, Breen, and Kreger also conducted an investigation into code effectiveness for prestressed concrete members fabricated with HSC. Ten beams were tested with concrete compressive strengths ranging from 10,800 to 13,160 psi. Each

beam had a deck cast on top using normal strength concrete (3,300 to 5,350 psi). The primary variable in the testing was the amount of shear reinforcement, which varied from no reinforcement to reinforcement in excess of the maximum allowable transverse steel limits. All beams experienced diagonal web-shear cracking (V_{cw}) and failed along diagonal struts. Similar to the conclusions of Elzanaty et. al. (1986), Hartman et. al. concluded that ACI 318 and AASHTO Standard shear provisions were acceptable for concrete strengths up to 12,000 psi.

Also in 1988, Kaufman and Ramirez studied the effectiveness of using truss models (strut and tie method) to predict the ultimate shear behavior of high strength prestressed concrete I-beams. They claimed that truss models could better explain the behavior of HSC members and sought to evaluate their hypothesis by testing six prestressed concrete I-beams. Four of the beams had depths of 25.5 inches and two had depths of 33.3 inches. The primary variables in the experimental program were beam length, span length, shear span, and web reinforcement. The results of the tests indicated that the truss model was more effective than ACI 318 provisions in estimating shear strength of high strength prestressed concrete members due to the increased load carrying capacity of the diagonal struts.

Similar to the studies by Elzanaty et. al. (1986) and Hartman et. al. (1988), Ma, Tadros, and Baishya (2000) initiated a research project that was intended to evaluate the applicability of the AASHTO LRFD shear provisions to HSC. The researchers tested two 43-inch deep girders spanning over 70 feet each with concrete compressive strengths of 8,490 to 11,990 psi (Ma et al. 2000). Primary variables in the experimental program included draped versus shielded strands and type of shear reinforcement (conventional bars versus vertical and inclined orthogonal welded wire fabric). Each end of the beam was tested, resulting in four shear failures. The researchers found that the maximum shear carried by the test specimens exceeded the estimates obtained by the AASHTO LRFD and Standard shear provisions and concluded that the use of both AASHTO design specifications resulted in conservative strength estimates.

Building on the efforts of the other studies on effects of HSC on prestressed concrete shear strength., *NCHRP Report 579* (2005), entitled "*Application of LRFD Bridge Design Specifications to High-Strength Structural Concrete: Shear Provisions"*, addressed the issue of whether or not the AASHTO LRFD code provisions for shear strength were applicable to concrete with compressive strengths greater than 10 ksi. Section 5.4.2.1 of AASHTO LRFD (2004) states that "design concrete strengths above 10.0 ksi shall be used only when allowed by specific Articles or when physical tests are made to establish the relationships between the concrete strength and other properties" (AASHTO LRFD 2004). The intent of *Report 579* was to establish whether or not the shear provisions could be applied to HSC. The researchers performed 20 tests on 63-inch deep bulb-tee bridge girders with concrete compressive strengths between 8 and 18 ksi. The predictions for the ultimate shear capacity of the prestressed concrete sections were calculated using AASHTO LRFD 2004, ignoring the limitation of 10 ksi for maximum concrete strength, and a simplified procedure proposed by the authors *NCHRP Report 549* (V_{ci} and V_{cw} method in AASHTO LRFD 2007). The research showed that the V_{ci} and V_{cw} method was applicable to HSC and predicted the cracking loads and ultimate loads to an acceptable level of accuracy.

2.3.6 Research on Effects on Strand Slippage

In 1988, Maruyama and Rizkalla studied the influence of stand slippage on the shear behavior of prestressed concrete beams. For beams with low shear span to depth ratios, diagonal web-shear cracks can cause premature failure due to slippage of the prestressing strands. To investigate the issue of strand slippage, nine 19.3-inch deep prestressed concrete beams were tested in shear, as well as two non-prestressed beams. Strains were measured on each tendon in order to monitor strand slippage. The non-prestressed beams failed in shear before any slippage of the reinforcing bars. However, in the prestressed beams, slippage of the strands occurred prematurely and led to significant increases in diagonal crack widths and premature failures. From the results, the researchers concluded that premature strand slippage was a serious concern in the

design of prestressed concrete members and that it could be addressed by providing proper development lengths.

2.3.7 Research on Effects of Distributed Loading

A 1973 study by Arthur, Bhatt, and Duncan explored the effects of distributed loads on the shear performance of prestressed concrete members. The vast majority of research on shear strength is conducted using single-point loading since such loading is easier to create in a laboratory. However, many loading patterns in the field are distributed. Nineteen 12-inch deep I-beams with varying cross sections were tested, none of which had shear reinforcement. Shear failures were produced in all 19 beams and the researchers concluded that distributed loading did not affect the shear strength of the beams when it came to estimating the shear capacity.

2.3.8 Research on Effects of Draped Reinforcement

MacGregor, Sozen, and Siess (1960) studied the effects of draped strands versus straight strands on the shear strength of prestressed concrete beams. Nineteen 12-inch deep simply supported pretensioned concrete beams were tested (18 I-beams and one rectangular beam). The main variable in the experiment was the angle of draped reinforcement. Other varied parameters included concrete compressive strength, amount of shear reinforcement, and length of shear span. From the data, the researchers concluded that draping the longitudinal reinforcement had no detrimental effect on the diagonal cracking load or the ultimate shear strength of the beams tested.

2.3.9 Research on Mimimum Required Transverse Reinforcement

In 2002, Teoh, Mansur, and Wee studied the adequacy of the minimum shear reinforcement requirements of various codes. Six 27.6-inch deep prestressed and four 27.6-inch deep reinforced concrete simply supported I-beams were tested with low amounts of shear reinforcement. Based on the 1999 edition of the ACI 318 specifications, the researchers found that the code equations for minimum required shear

reinforcement were inadequate for providing an acceptable margin of safety for prestressed concrete members. Based on their research, an equation for minimum shear reinforcement in prestressed and reinforced concrete members was proposed. The proposed equation is nearly identical to the minimum shear requirement in ACI 318-08.

2.4 UNIVERSITY OF TEXAS PRESTRESSED CONCRETE SHEAR DATABASE (AVENDAÑO AND BAYRAK, 2008)

A prestressed concrete shear database (PCSD) was assembled by University of Texas at Austin researchers (Avendaño and Bayrak, 2008). The database comprises the results of 506 shear tests from 30 research projects (References 6 – 7, 9 – 10, 12, 14 – 23, 25 – 29, 31 – 36, and 38 - 41). The database was assembled to provide future researchers with an accurate portrayal of how prestressed concrete beams fail in shear. The database allows researchers to find historical data on similar beams and formulate more accurate predictions of failure loads. For example, for the 40-inch deep I-beams tested in the shear performance evaluation of this research study, the data in the database showed that similar beams experienced shear failures at loads approximately 40 to 60 percent greater than ACI 318-08 estimated.

Of the 506 tests in the database, a total of 367 shear failures were reported. Of the 367 shear failures, 214 failed in shear along a diagonal web crack (V_{cw}). Of the 214 beams that experienced a web-shear failure, 130 included shear reinforcement and had an overall depth greater than 12 inches. Lastly, the web-shear cracking load was only reported for 65 of the 130 beams. Only beams which experienced diagonal cracking in the web first (V_{cw}) are comparable to the prestressed concrete beams tested in the shear performance evaluation of the current study. Of relevance to the current study is the ratio of actual diagonal cracking shear to estimated diagonal cracking shear, the ratio of actual shear strength to estimated shear strength, and maximum compressive stress in concrete at prestress transfer from these 65 tests. Graphical representations of all 65 ratios of actual cracking shear to calculated cracking shear and actual shear strength to calculated

shear strength as estimated by ACI 318-08 and AASHTO LRFD (2007) are shown in Figure 2.2 through Figure 2.5.

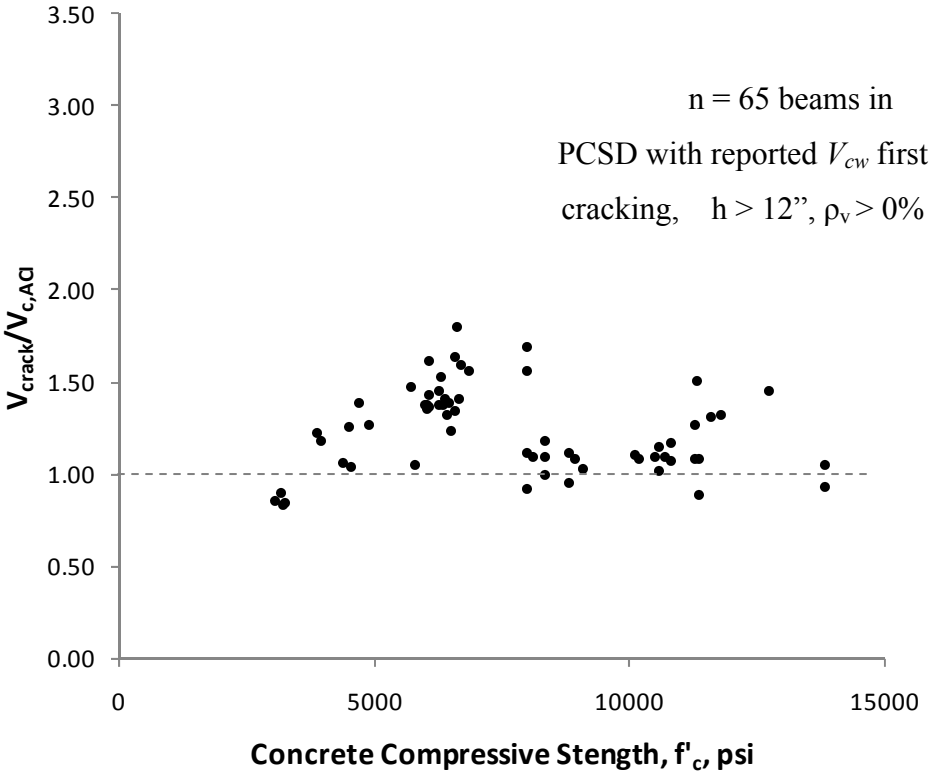

Figure 2.2 Ratio of Measured to Estimated Diagonal Cracking Shear, ACI 318-08 (Avendaño and Bayrak, 2008)

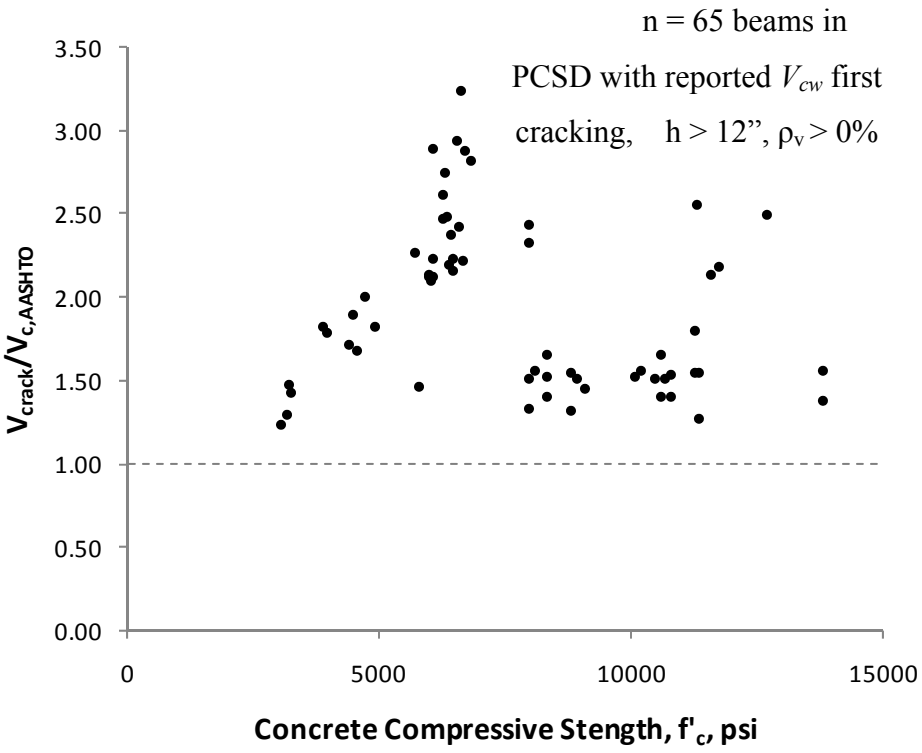

Figure 2.3 Ratio of Measured to Estimated Diagonal Cracking Shear, AASHTO LRFD (2007) (Avendaño and Bayrak, 2008)

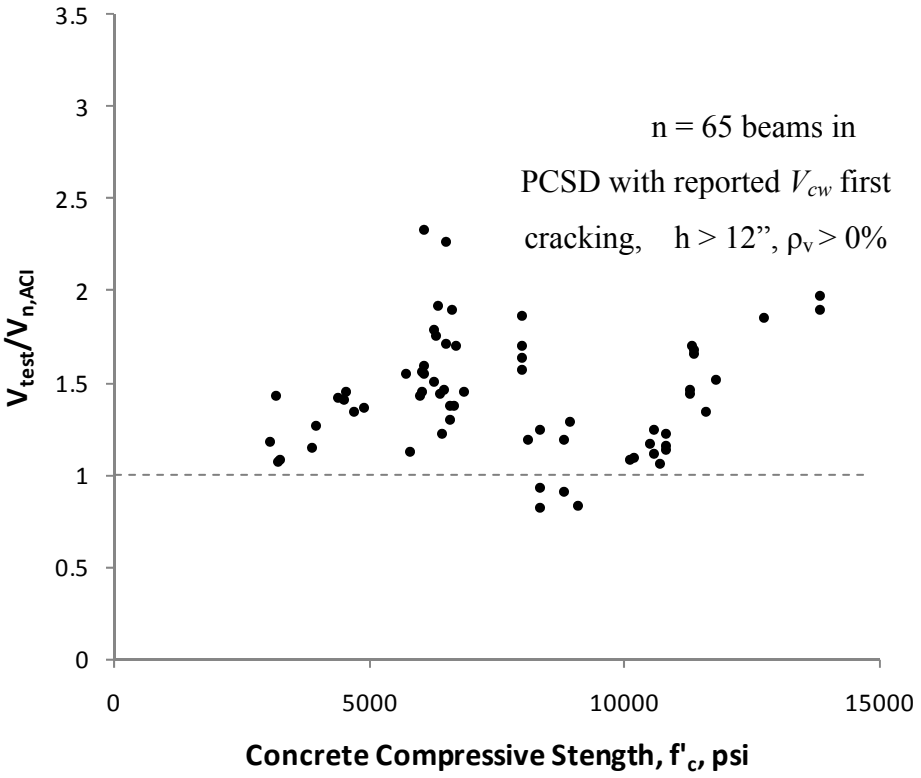

Figure 2.4 Ratio of Measured to Estimated Shear Strength, ACI 318-08 (Avendaño and Bayrak, 2008)

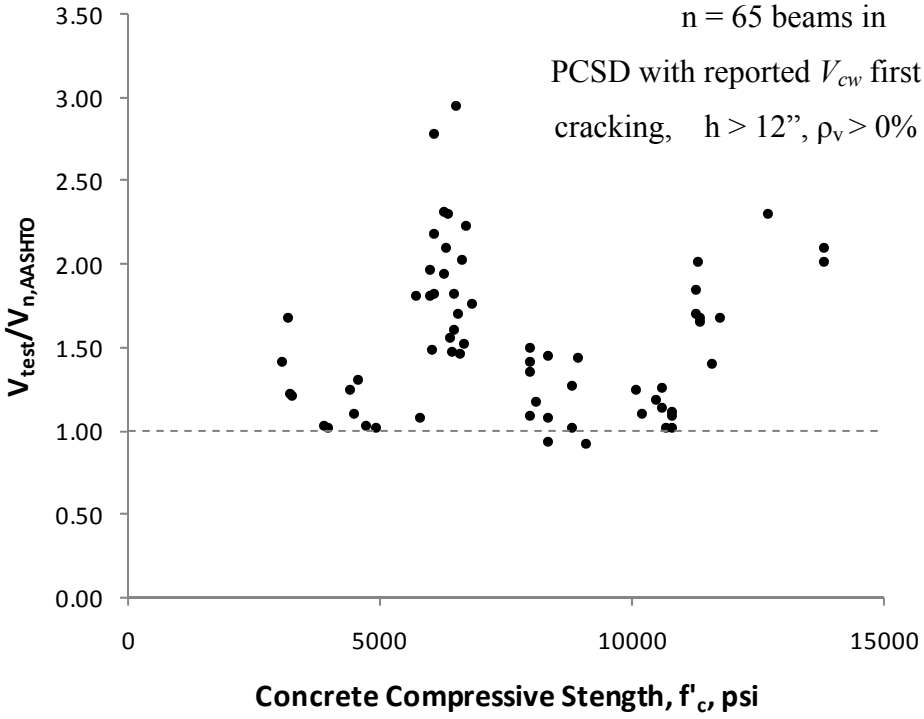

Figure 2.5 Ratio of Measured to Estimated Shear Strength, AASHTO LRFD(2007) (Avendaño and Bayrak, 2008)

Figure 2.2 through Figure 2.5 show that the ACI 318-08 and AASHTO LRFD (2007) code provisions for V_{cw} were conservative for the beams analyzed. It is important to observe that the compressive strength of concrete at prestress transfer was not typically reported by previous researchers. A plot of $V_{test}/V_{estimated}$ versus ratio of concrete compressive stress to compressive strength at release would have been ideal, but of the 65 tests analyzed, only four tests (Avendaño and Bayrak) reported enough information to calculate compressive stresses at release. Every effort was made in this literature review to find data on release stresses, but the data encountered on release stresses were found to be virtually non-existent, thus showing the need for the current research study. For the reasons explained above, the current research project is deemed the first study dedicated solely to the relationship between the shear strength of prestressed concrete members and the allowable compressive stress in concrete at prestress transfer.

2.5 SUMMARY

The shear performance of prestressed concrete members is a subject that has been extensively researched since the 1950s. Early research laid a foundation for the empirical code provisions found in the current editions of the ACI 318 and AASHTO LRFD specifications. From the results of 506 tests from 30 individual research projects, the University of Texas Prestressed Concrete Shear Database was created by Avendaño and Bayrak (2008). Of the 506 tests in the database, only 130 were conducted on specimens with shear reinforcement and depths 12 inches or greater that failed in shear after forming diagonal web cracks (V_{cw} failure). Of the 130 similar tests, the first diagonal cracking load was only reported on 65 of the beams. From the results of the 65 tests, the ACI 318-08 and AASHTO LRFD (2007) code provisions for web-shear failures were found to be conservative.

The majority of researchers of the past did not report concrete compressive strengths at prestress transfer, making the data from their experiments not directly applicable to the primary focus of this thesis. As explained in this chapter, no previous research has been conducted on the effects of increasing the allowable compressive

release strength on the shear strength of prestressed concrete members. For the reasons explained above, the experimental research summarized in the subsequent chapters is deemed necessary for the study of release stresses on shear capacity of prestressed concrete beams.

CHAPTER 3
Test Specimens

3.1 OVERVIEW

During the course of this research study (Phase II of TxDOT Project 5197), a total of 45 TxDOT Type-C highway bridge girders were fabricated. The C-beams were fabricated by four different precast plants in Texas. The plants will be referred to in this thesis as fabricators A, B, C, and D. Twelve beams prepared by fabricators A, C, and D and nine beams prepared by Fabricator B were used in this research study. In the shear performance evaluation part of the study, 18 of the C-beams were tested in shear. Actual compressive stresses at release ranged from $0.57f'_{ci}$ to $0.77f'_{ci}$. The target release stresses were $0.60f'_{ci}$, $0.65f'_{ci}$, and $0.70f'_{ci}$. Six beams were tested from Fabricator B, six were tested from Fabricator C, and six were tested from Fabricator D, with the goal of having two beams from each fabricator at each target release stress. Beams produced by Fabricator A were not designed to be shear-critical and as such were not tested in shear (Section 3.2.1). The design of the specimens is discussed in Section 3.2

3.2 DESIGN OF TXDOT C-BEAM SPECIMENS

As explained earlier, for Phase II of this research study, a total of 45 C-beams and 10 box beams were fabricated and 18 C-beams were tested in shear. Of the 45 C-beams, 21 were designated as "Series 1" and 24 were designated as "Series 2." (Three Series 1 beams were rejected from Fabricator B lowering the total number of beams from that plant to nine: 4 x 12 – 3 = 45 beams.) There were three primary differences in the two types of beams. First, Series 1 beams were designed for a nominal release strength of 4,000 psi, whereas Series 2 beams were designed for 6,500 psi. Second, the strand pattern (Figure 3.1 through Figure 3.3) was different in each series. Series 1 beams contained 26 strands and the beams in Series 2 contained 36 strands. The strand patterns

also led to different centerline and end eccentricities, as seen in Figure 3.1, which controlled the variation in compressive release stresses. Third, the hold down force for each series was different. Series 1 featured a hold down force of 8.8 kips while Series 2 featured a hold down force of 9.3 kips. Another key variable that did not vary between beam series but varied between fabricators was the type of coarse aggregate used in the concrete mixture design. Section properties for Series 1 and Series 2 beams are provided in Table 3.1 and a list of the key variables for each fabricator is provided in Table 3.2.

Table 3.1 Section Properties of TxDOT Type-C Beams

Beam Series	A_g (in^2)	I_g (in^4)	y_t (in)	y_b (in)	e_{cen} (in)	e_{end} (in)	w (lb/ft)
1	494.9	82602	22.91	17.09	11.86	8.78	516
2					11.09	8.76	

Table 3.2 Key Variables: TxDOT Type-C Beams

Variable	Fabricator			
	A	**B**	**C**	**D**
Series	1		2	
Nominal Release Strength, psi	4000		6500	
Coarse Aggregate	crushed limestone	hard river gravel	crushed limestone	hard river gravel
# of Strands	26	26	36	36
Hold Down Force, kips	8.8	8.8	9.3	9.3

The test specimens were designed so that bottom fiber compressive stresses at release were reasonably uniform at the hold down points and the transfer length ($60d_b$ from beam ends). Figure 3.1 shows the locations where the bottom fiber compressive stresses were calculated as well as the locations of the maximum compressive stress at release. Figure 3.1 also serves to show an elevation of the test specimen with dimensions and tendon eccentricities at beam ends and hold down points.

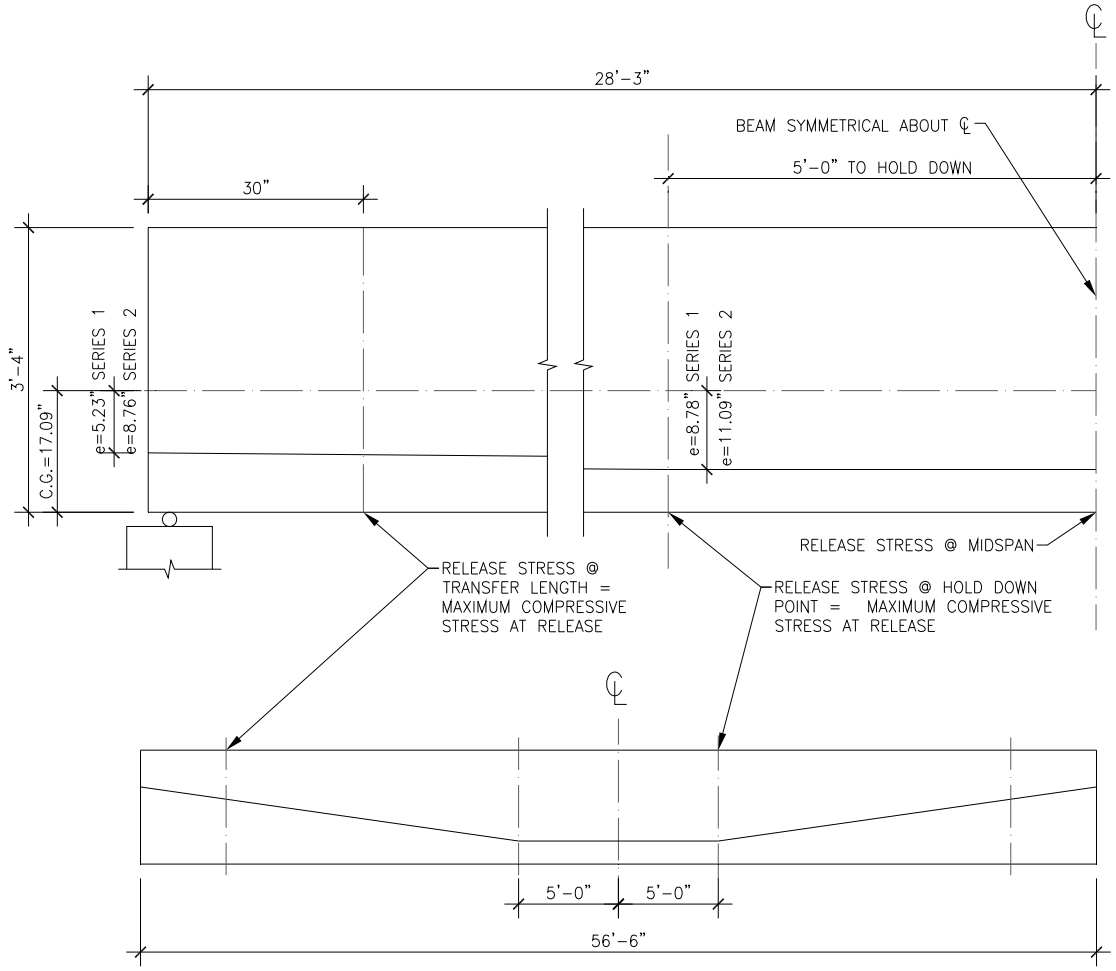

Figure 3.1 Elevation of Beam Specimens

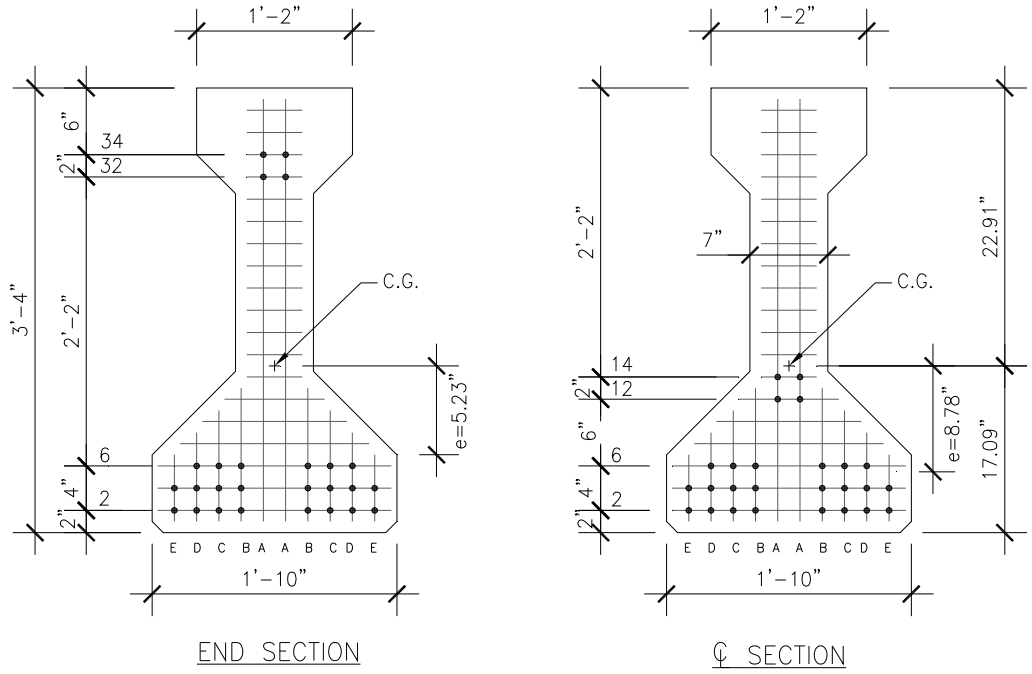

Figure 3.2 Series 1 Beam Dimensions and Strand Pattern

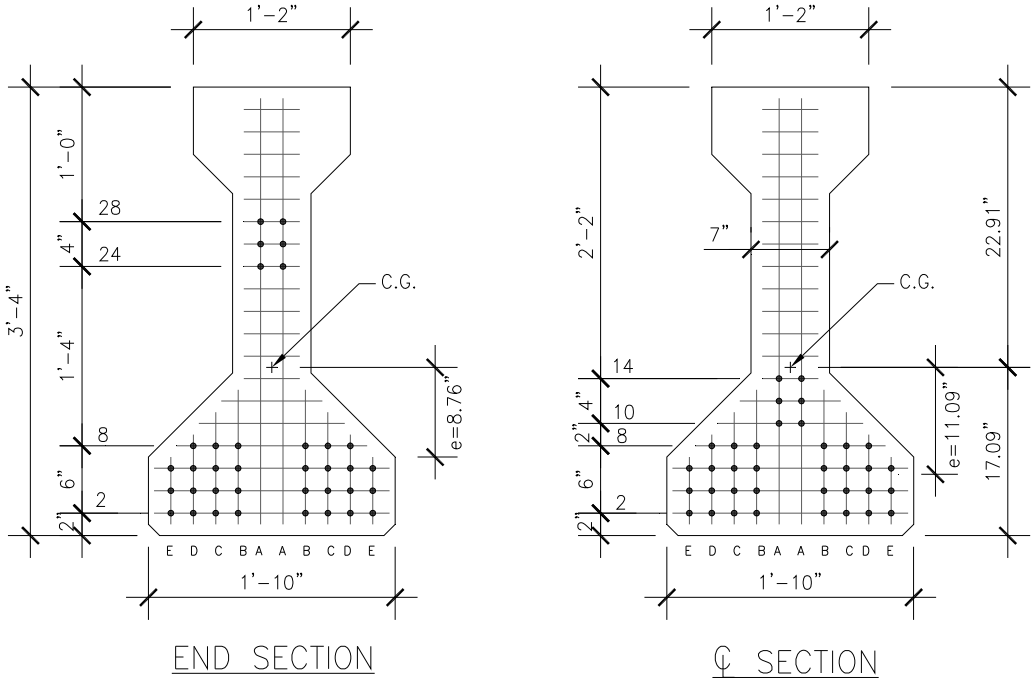

Figure 3.3 Series 2 Beam Dimensions and Strand Pattern

Typical of TxDOT beam fabrication practice, the strands used in each beam were low-relaxation strands with a tensile strength of 270 ksi. For the Series 1 beams, four of the 26 strands were deflected (Figure 3.2) to minimize tensile stresses in the end regions and match compressive stresses in the end regions to compressive stresses at the hold down points. For the Series 2 beams, six of the 36 strands were deflected (Figure 3.3). The deflected strands were held down at sections approximately five feet away from the midspan of the beam for both cases, as shown in Figure 3.1. Within each beam series, the primary experimental variables were the type of coarse aggregate and the maximum compressive stress in concrete at prestress transfer. For the Series 1 beam specimens, the target release strength ranged from 4,000 psi to 4,700 psi. For the Series 2 beam specimens, it ranged from 5,400 psi to 6,400 psi. The target release strengths are summarized in Table 3.3. Also included in the table are the corresponding maximum compressive release stresses, expressed as percentages of the release strength. At precast plants A, C, and D, three beams were fabricated for a target release stress of $0.70f'_{ci}$ (70 percent), six were fabricated for $0.65f'_{ci}$ (65 percent), and three were fabricated for $0.60f'_{ci}$ (60 percent). For the shear testing, two beams were taken from each group of target release stresses from fabricators C and D. Fabricator B produced six beams targeted at $0.70f'_{ci}$ and three targeted at $0.60f'_{ci}$, of which four were tested from the $0.70f'_{ci}$ group and two from the $0.60f'_{ci}$ group. All beams were cast in groups of three or six at a time and had a length of 56.5 feet.

Table 3.3 Target Design Values for TxDOT C-Beam Specimens

Beam Series	Compressive Strength at Release f'_{ci}, (psi)	Compressive Stress at Transfer Length (% of f'_{ci})	Compressive Stress at Hold Down Points (% of f'_{ci})
1	4000	69.3	69.3
	4300	64.7	64.8
	4700	59.5	59.6
2	5400	70.1	70.4
	5850	65.1	65.3
	6400	59.8	60.1

Shear reinforcement (R-bars in Figure 3.4 and Figure 3.5) was provided by double legged #4 stirrups that were spaced at 4 inches in the end regions and at 24 inches across the rest of the beam. (Dimensions of all transverse reinforcement are shown in Appendix C.) The shear reinforcement design is discussed in Section 3.2.1. Although bursting reinforcement was provided, the shear reinforcement also served to control the widths of the bursting cracks in the end regions. An analysis of the bursting cracks for the 45 C-beams is presented in Appendix A. Confining steel was provided in the bottom flange with #4 bars. Lifting loops were provided at sections 5.75 feet away from each end of the beam and consisted of two ½" strands. The tensile stress limit at release of $7.5\sqrt{f_{ci}'}$ was satisfied along the length of the member. All other aspects of the C-beam specimens follow the standard TxDOT Type-C Beam design and are in accordance with the AASHTO LRFD (2007) Bridge Design Specifications.

3.2.1 Shear Reinforcement Design

The first set of 12 beams (Fabricator A), were designed for shear according to standard TxDOT details, with a stirrup spacing of 8 or 15 inches in the low-shear region of the beam and 4 inches in the end regions (Figure 3.4). The TxDOT design, however, was modified after the first fabricator since the first beam tested failed in flexure under the applied load due to top flange crushing during shear testing. At that point, it was decided that the stirrup spacing needed to be increased substantially, thus decreasing the shear carrying capacity of the transverse steel and subsequently decreasing the overall shear capacity of the beam. The shear reinforcement design was changed to feature a stirrup spacing of 24 inches, ensuring a shear failure for the shear tests (Figure 3.5). The spacing of 24 inches was chosen because it was the maximum transverse reinforcement spacing allowed by the AASHTO LRFD (2007) Bridge Design Specifications. The shear reinforcement spacing in the end regions was kept at four inches in order to properly study the bursting stresses in the beams from fabricators B, C, and D. The stirrup spacing outside the end regions was increased to 24 inches to effectively study: 1) if a change in

release factor from 0.6 to a higher value would result in early diagonal cracking and 2) the concrete contribution to shear strength in a case where the stirrup contribution was minimized. The differences between the original (TxDOT C-Beams) and modified shear reinforcement designs are shown in Figure 3.4 and Figure 3.5.

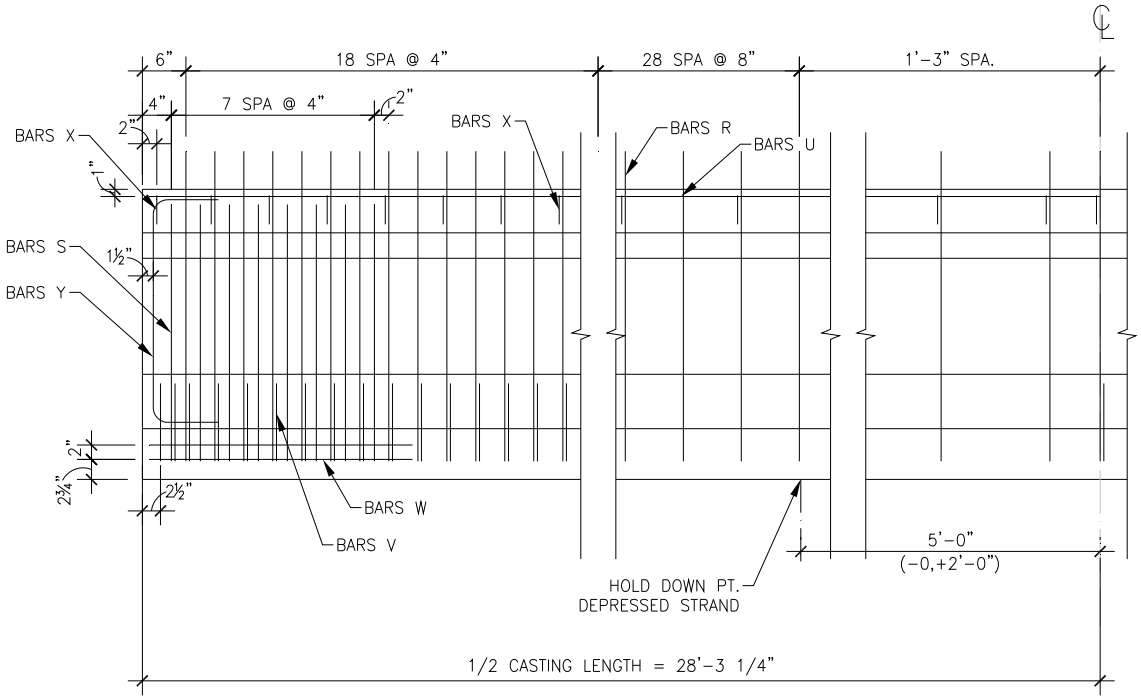

Figure 3.4 Shear Reinforcement Design: TxDOT C-Beam Specimens

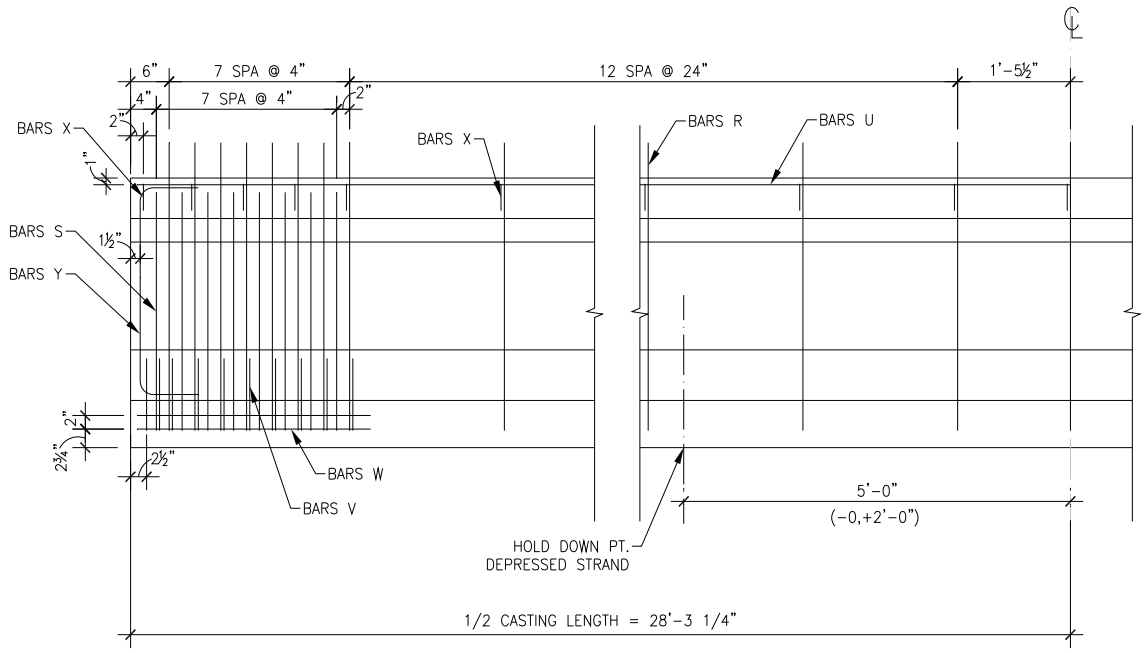

Figure 3.5 Modified Shear Reinforcement Design: Project 5197 C-Beam Specimens

3.2.2 Concrete Mixture Design

Concrete mixture designs used in Texas' precast concrete plants can vary greatly. One of the primary goals of the current research was to study the differences in concrete mixture designs and fabrication processes. Four similar concrete mixture designs were used in the fabrication of the 45 C-beams. The amount of cement, water, aggregates, and admixtures used varied depending upon the preferences of each fabricator. Within each series of beam, 12 beams were fabricated with hard river gravel as the coarse aggregate and the other 12 were fabricated with crushed limestone, as shown in Table 3.2. The main difference between the two coarse aggregates is that concrete made with river gravel is generally stiffer than concrete made with crushed limestone (Birrcher and Bayrak, 2007). Evaluating beams of similar concrete mixtures with different aggregates was crucial in determining the aggregates' effect on the shear strength of prestressed

concrete beams. The differences in the concrete mixture designs from each fabricator are shown in Table 3.4.

Table 3.4 Concrete Mixture Design Properties per Fabricator

Components	A	B	C	D
Coarse Aggregate Type	CL*	HRG*	CL*	HRG*
Water/Cement Ratio	0.37	0.27	0.37	0.33
Water (lbs/CY)	207	233	242	196
Type III Cement (lbs/CY)	564	658	658	611
Fine Aggregate (lbs/CY)	1486	1191	1326	1285
Coarse Aggregate (lbs/CY)	1796	1789	1789	1990
Retarding Admixture (oz/CY)	17	4	19	18
Water Reducing Admixture (oz/CY)	40	57	43	165
Theoretical unit Weight (lbs/ft^3)	150	149	149	151

*CL = crushed limestone, HRG = hard river gravel

The concrete mixtures used for fabrication of the beams were designed and batched by each individual fabricator at their plant, with each fabricator having a unique mixture design. For example, Fabricator D used much more water reducing admixture in their design than fabricators A, B, and C. Since early strength gain was vital for the beams, as is typical in conventional prestressed concrete beam fabrication, Type III Cement was used by all the fabricators. The rate of strength gain for each concrete depended upon the concrete mixtures, as well as the ambient conditions such as air temperature and concrete temperature. Plots of strength gain as a function of time for each concrete placement at each plant are presented in Appendix D. The main differences in the concrete mixture designs were in the cement and water contents, as seen in Table 3.4, but in general the mixtures were similar for all four fabricators. The ambient temperature conditions varied for each fabricator. Table 3.5 presents the morning low and afternoon high temperatures for each concrete casting operation at each precast plant. The table shows that Fabricator D experienced the coldest weather, casting in late winter, while Fabricator A experienced the warmest weather, casting in early fall.

Table 3.5 Ambient Temperatures for each Concrete Casting Operation

Fabricator	Target Compressive Release Stress	Date of Casting	Ambient Temperature (°F)		Casting Time
			Morning Low	Afternoon High	
A	$0.70f'_{ci}$	9/26/2007	63	92	8:00 AM
A	$0.65f'_{ci}$	10/9/2007	70	86	5:50 PM
A	$0.60f'_{ci}$	10/3/2007	72	90	1:15 PM
B	$0.70f'_{ci}$	5/6/2008	63	80	7:50 AM
B	$0.60f'_{ci}$	4/23/2008	71	88	6:50 AM
C	$0.70f'_{ci}$	3/14/2008	57	82	6:20 PM
C	$0.65f'_{ci}$	3/26/2008	57	80	6:00 PM
C	$0.60f'_{ci}$	4/1/2008	58	84	6:05 PM
D	$0.70f'_{ci}$	3/4/2008	37	74	5:00 PM
D	$0.65f'_{ci}$	3/7/2008	39	70	1:20 PM
D	$0.65f'_{ci}$	3/14/2008	63	77	4:15 PM
D	$0.60f'_{ci}$	3/12/2008	46	71	10:20 AM

3.3 FABRICATION OF TXDOT C-BEAM SPECIMENS

The four precast plants in Texas used to fabricate the 45 C-beams used for Phase II of the research study are located in San Marcos, Eagle Lake, Victoria, and San Antonio. Figure 3.6 shows the locations of the plants (the four black stars in the figure) on a map of Texas. The beams were cast in a series of three or six at a time, depending upon the desired release strength. The beams were labeled according to the type of specimen, fabricator, target compressive release strength, and beam number. For example, Specimen CA-70-1 indicates a TxDOT Type-C Beam fabricated at Precast Plant A with a target release strength of $0.70f'_{ci}$. The "1" indicates that it was the first beam cast from the $0.70f'_{ci}$ group. The Project 5197 Beam Fabrication Specifications are provided in Appendix C. Each beam was released as close as possible to the specified compressive release strength shown in Table 3.3. A summary of the actual release

strengths for each beam can be found in Table 3.6 through Table 3.9. The process of determining the actual release strengths is described in Section 3.3.2. Each release was monitored by TxDOT inspectors and University of Texas graduate research assistants. It should be noted that due to varying ambient conditions, a reduction in cycle time for earlier releases was not observed in all cases. Once the beams were released and the forms removed, they were stored at the fabrication plant and shipped to the Ferguson Structural Engineering Laboratory as needed. The stressing and casting operations, release operations, and storage and shipment operations are discussed in the following sections.

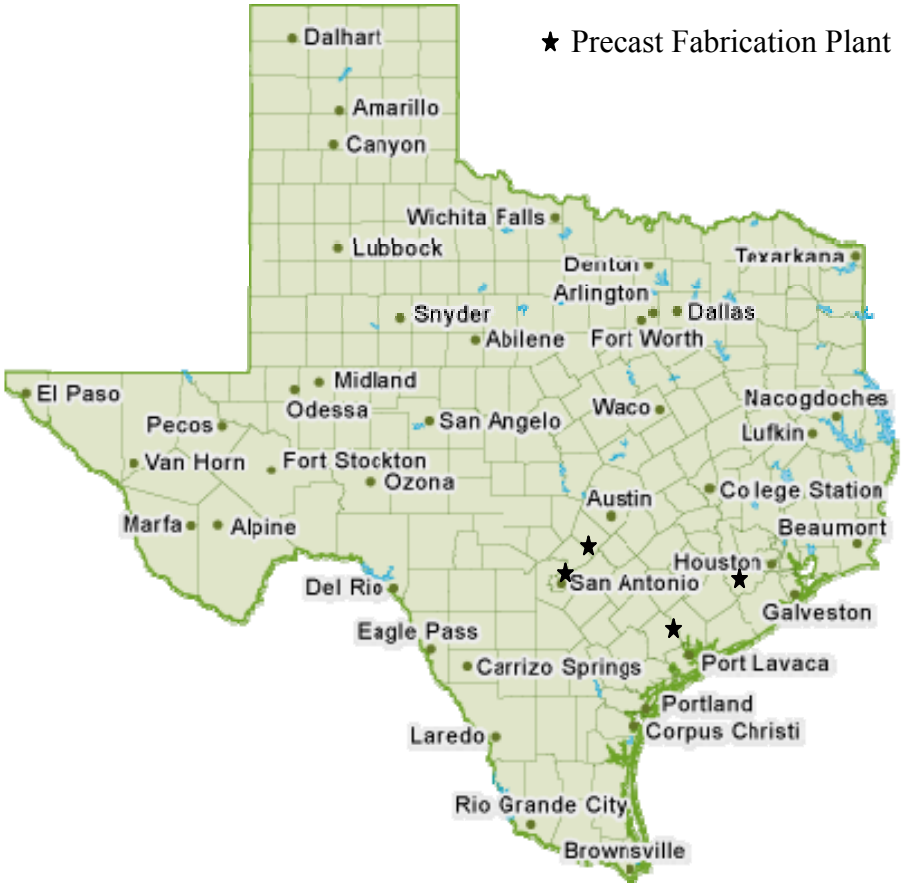

Figure 3.6 Location of Precast Plants in Texas (Reference 42)

Table 3.6 Fabricator A Casting Details

Specimen Designation	Maximum Compressive Release Stress*, σ_{bottom}		f'_{ci} (psi)	Age at Release (hr)**	Date of Casting
	Target	Actual			
CA-70-1	$0.70f'_{ci}$	$0.72f'_{ci}$	3930	12	9/26/2007
CA-70-2		$0.72f'_{ci}$	3930		
CA-70-3		$0.71f'_{ci}$	3940		
CA-65-1	$0.65f'_{ci}$	$0.65f'_{ci}$	4370	12.5	10/9/2007
CA-65-2		$0.65f'_{ci}$	4380		
CA-65-3		$0.66f'_{ci}$	4310		
CA-65-4		$0.65f'_{ci}$	4340		
CA-65-5		$0.65f'_{ci}$	4330		
CA-65-6		$0.66f'_{ci}$	4300		
CA-60-1	$0.60f'_{ci}$	$0.62f'_{ci}$	4540	10	10/3/2007
CA-60-2		$0.62f'_{ci}$	4540		
CA-60-3		$0.62f'_{ci}$	4540		

*Maximum compressive release stresses calculated at transfer length

**Age at Release represents the length of time from when the cylinders were cast until when the prestress force was released

Table 3.7 Fabricator B Casting Details

Specimen Designation	Maximum Compressive Release Stress*, σ_{bottom}		f'_{ci} (psi)	Age at Release (hr)**	Date of Casting
	Target	Actual			
CB-70-1	$0.70f'_{ci}$	$0.63f'_{ci}$	4540	8	5/6/2008
CB-70-2		$0.65f'_{ci}$	4360		
CB-70-3		$0.68f'_{ci}$	4180		
CB-70-4		$0.70f'_{ci}$	4030		
CB-70-5		$0.73f'_{ci}$	3880		
CB-70-6		$0.77f'_{ci}$	3680		
CB-60-1	$0.60f'_{ci}$	$0.59f'_{ci}$	4820	7.5	4/23/2008
CB-60-2		$0.57f'_{ci}$	5010		
CB-60-3		$0.62f'_{ci}$	4620		

*Maximum compressive release stresses calculated at transfer length

**Age at Release represents the length of time from when the cylinders were cast until when the prestress force was released

Table 3.8 Fabricator C Casting Details

Specimen Designation	Maximum Compressive Release Stress*, σ_{bottom}		f'_{ci} (psi)	Age at Release (hr)**	Date of Casting
	Target	Actual			
CC-70-1	$0.70f'_{ci}$	$0.72f'_{ci}$	5380	13.5	3/14/2008
CC-70-2		$0.72f'_{ci}$	5360		
CC-70-3		$0.72f'_{ci}$	5330		
CC-65-1	$0.65f'_{ci}$	$0.65f'_{ci}$	5970	13	3/26/2008
CC-65-2		$0.65f'_{ci}$	6000		
CC-65-3		$0.63f'_{ci}$	6130		
CC-65-4		$0.64f'_{ci}$	6070		
CC-65-5		$0.61f'_{ci}$	6350		
CC-65-6		$0.62f'_{ci}$	6250		
CC-60-1	$0.60f'_{ci}$	$0.61f'_{ci}$	6350	21	4/1/2008
CC-60-2		$0.61f'_{ci}$	6370		
CC-60-3		$0.61f'_{ci}$	6370		

*Maximum compressive release stresses calculated at transfer length

**Age at Release represents the length of time from when the cylinders were cast until when the prestress force was released

Table 3.9 Fabricator D Casting Details

Specimen Designation	Maximum Compressive Release Stress*, σ_{bottom}		f'_{ci} (psi)	Age at Release (hr)**	Date of Casting
	Target	Actual			
CD-70-1	$0.70f'_{ci}$	$0.69f'_{ci}$	5580	12	3/4/2008
CD-70-2		$0.70f'_{ci}$	5500		
CD-70-3		$0.71f'_{ci}$	5420		
CD-65-1	$0.65f'_{ci}$	$0.68f'_{ci}$	5670	28	3/7/2008
CD-65-2		$0.68f'_{ci}$	5670		
CD-65-3		$0.68f'_{ci}$	5670		
CD-65-4		$0.65f'_{ci}$	5940	14.5	3/14/2008
CD-65-5		$0.65f'_{ci}$	5940		
CD-65-6		$0.65f'_{ci}$	5940		
CD-60-1	$0.60f'_{ci}$	$0.62f'_{ci}$	6320	19.5	3/12/2008
CD-60-2		$0.62f'_{ci}$	6310		
CD-60-3		$0.62f'_{ci}$	6300		

*Maximum compressive release stresses calculated at transfer length

**Age at Release represents the length of time from when the cylinders were cast until when the prestress force was released

3.3.1 Stressing and Casting Operations

The stressing and casting work consisted of several steps. First, the prestressing strands were stressed to their appropriate jacking stress at the live end of the bed, as seen in Figure 3.7. The elongation of each strand was then checked to confirm the reading from the pressure gauge at the live end of the beam. The allowable range for the jacking stress was within plus or minus two percent of the required gauge reading. The method used by each fabricator to deflect the harped strands was somewhat different, though fabricators A and B used similar processes. They deflected the strands by pulling on them from the bottom of the stressing bed (Figure 3.8). Fabricator C deflected the strands by running them through rollers (Figure 3.9). Fabricator D's method consisted of pushing the deflected strands down with hollow cylindrical rods (Figure 3.10). In their method, the concrete was cast around the hollow cylindrical rods, leaving a vertical hole (about two inch diameter) in the beam at the location of the hold down points. As such, the beams from Fabricator D each had two vertical holes approximately five feet from midpan whereas the beams from the other fabricators had no such holes. The photographs in Figure 3.8 through Figure 3.10 serve to illustrate the difference in the "pulling" (fabricators A and B), "rolling" (Fabricator C), and "pushing" (Fabricator D) methods of strand harping.

Once the strands were set and stressed, the non-prestressed reinforcement was placed and tied. The steel C-beam forms were then placed and secured. The concrete for each cast was mixed at a batching plant on site and then transported to the beams with 4-cubic-yard concrete transporting trucks. During the cast, slump and air content tests were performed on the concrete to ensure quality control. A typical casting operation for one beam usually lasted about 15 minutes and required two trucks making one trip each. The casting operations were similar for all four fabricators. Once the beams were cast, a wet tarp (Figure 3.11) was placed on the forms and 24 cylinders were made.

Figure 3.7 Typical Live End of Stressing Bed

Figure 3.8 Typical Deflected Strands at Precast Plant A (Photographs courtesy of David Birrcher)

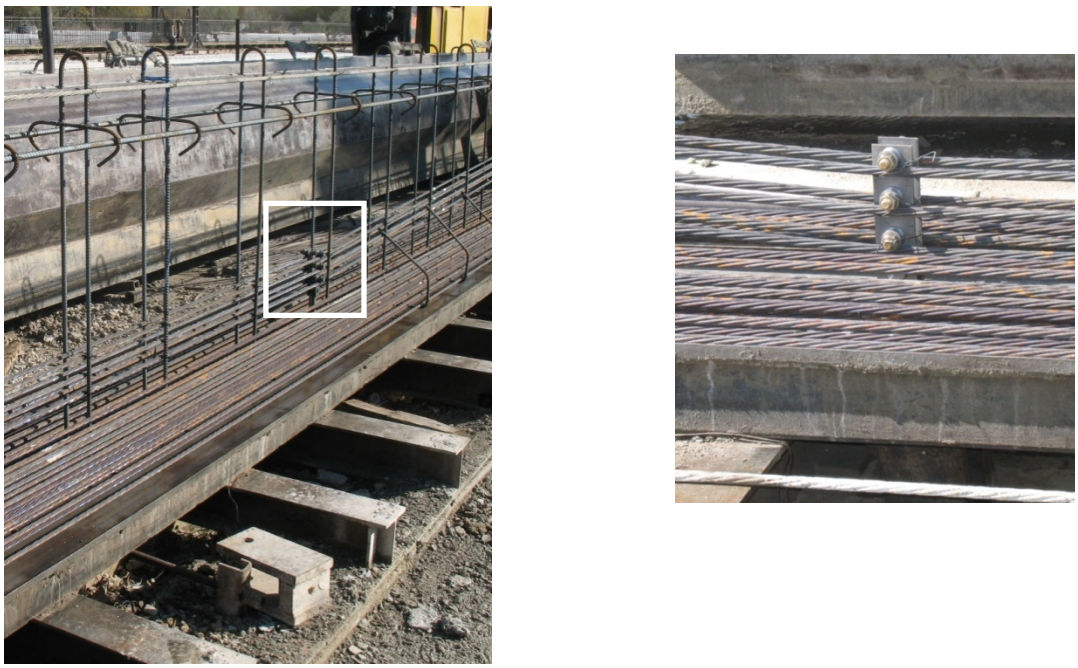

Figure 3.9 Typical Deflected Strands at Precast Plant C

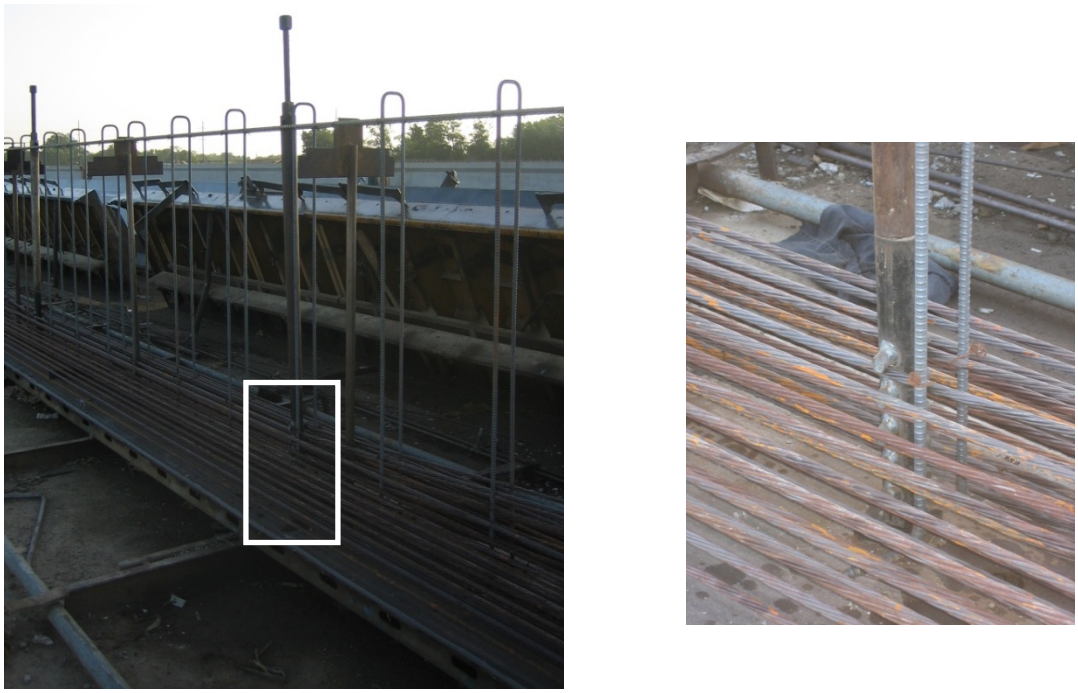

Figure 3.10 Typical Deflected Strands at Precast Plant D (Photographs courtesy of David Birrcher)

Figure 3.11 Typical Tarp on Beam during Curing Process

3.3.2 Prestress Transfer Operation

Prestress transfer operations vary between precast concrete plants. Of the four plants used in Phase II in the current research study, fabricators A and B had similar operations and fabricators C and D each had unique operations. At fabrication plants A, B, and D, 18 of the cylinders were temperature match-cured (Sure-Cure) to track the strength gain of the concrete (the other six were sent to the Ferguson Structural Engineering Laboratory). Temperature match-curing consisted of monitoring the temperature of the beams on the stressing bed and controlling the temperature of the match-cured cylinders to match the monitored temperature. The temperature match-curing process ensured that the strength gain of the cylinders being tested was very similar to the strength gain of the precast beams. Fabricator C did not have a temperature match-curing system but instead chose to let their cylinders cure on top of the steel forms under a heavy tarp which trapped the heat from the hydration process.

The Project 5197 Beam Fabrication Specifications (Appendix C) called for the first two cylinders to be tested at approximately six hours after casting of the beams, then for two cylinders to be broken every hour until the compressive strength of the concrete reached within 1000 psi of the targeted release strength. At that point, two cylinders were to be tested every 30 minutes until the targeted release strength was reached. The actual cylinder testing operation was slightly different, with cylinders being tested at an increased or decreased rate depending upon the strength gain of the concrete and the discretion of the quality control managers and the University of Texas research team. The first cylinders at fabricators A and B were tested approximately at the six hour mark. On the other hand, the first cylinders at fabricators C and D were tested approximately 12 hours after casting. The decision on when to test the first cylinders was usually made by the quality control manager at the precast plant. When the strength of the concrete began to approach the target release strength, the side forms of the beams were loosened by removing the top and bottom ties. Once the strength of the concrete cylinders reached

within approximately 50 - 100 psi of the target release strength, the prestress force was released.

When the required compressive strength was reached and the prestress force was released, two cylinders were immediately tested. The cylinder breaks from after the transfer were averaged with the cylinder breaks recorded immediately prior to the transfer and reported as the actual release strength for the beams. (Afterward, more precise release strengths were calculated, as seen in Table 3.6 through Table 3.9, based on the start and stop times for the casting operations of each beam.) Once the prestress force was released, the forms were moved away and the strands were flame-cut with an oxy-acetylene torch. It is important to note here that the strands did not need to be cut to completely release the prestress force in them. After the beams were approved, they were moved by a crane (or forklift in the case of Fabricator D) to the storage yard to await shipment to the Ferguson Structural Engineering Laboratory.

3.3.3 Storage and Shipment

The beams were stored in the yards of the fabrication plants for at least 28 days after they were cast. At that point, they were shipped by trucks to the Ferguson Structural Engineering Laboratory one beam or two beams at a time as needed. Using a spreader beam, the C-beam specimens were lifted off of the trucks with a 25-ton crane and transported to the testing setup. Fabricators A and D shipped one beam at time and fabricators B and C shipped two beams at a time. In the case of two beams being received on the same truck, one was placed in the testing setup and the other was placed on the laboratory floor. Once a beam was tested, it was set to the side or moved out of the laboratory using a similar process. A crane lifting a specimen off of a truck is depicted in Figure 3.12 and a crane lifting a sheared specimen out of the testing setup is shown in Figure 3.13.

Figure 3.12 Unloading a C-Beam Specimen off of Truck

Figure 3.13 Removal of Failed C-Beam Specimen out of Test Setup

After lifting difficulties with the beams from Fabricator A, special lifting loops were included on the drawings for the next three fabricators. The loops were not intended to replace the ones used by the fabricators at their plants but only to allow the beams to be handled easily at the Ferguson Structural Engineering Laboratory. The special lifting loops were specified as being no greater than five inches from the top of the beam and to be parallel to the R-bars, as shown in Figure 3.14. The large loops at three feet nine inches from the end of the beam in Figure 3.14 represent a typical fabricator's lifting loop. The special loops proved to be adequate for safely getting the beams across the laboratory floor and into the testing setup. A beam being moved across the laboratory floor with the special lifting loops is shown in Figure 3.15.

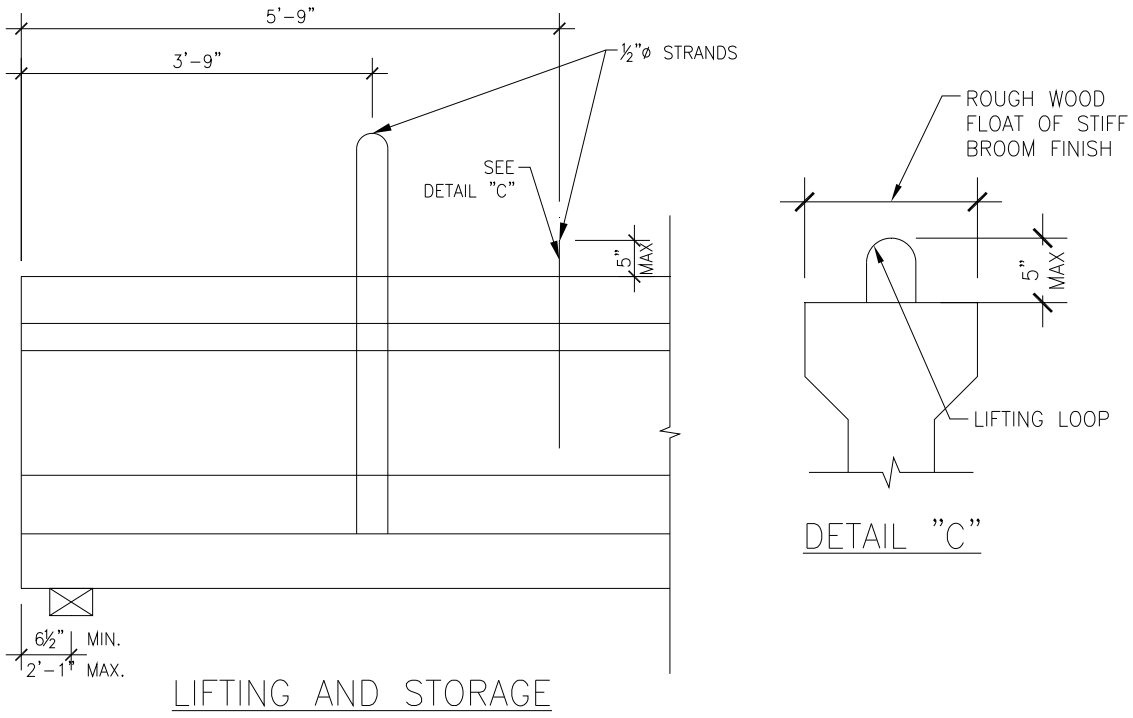

Figure 3.14 Special Lifting Loop for Specimen Handling at the Ferguson Structural Engineering Laboratory

Figure 3.15 C-Beam Being Moved Across Laboratory

3.4 SUMMARY

Forty-five C-beams were fabricated and 18 were tested in shear. All beams were fabricated by four different precast plants in Texas. The beams were designed according to standard TxDOT details, except for a modified shear reinforcement design, with a target maximum compressive strength at release of $0.60f'_{ci}$, $0.65f'_{ci}$, or $0.70f'_{ci}$. The primary variables of the experimental program were the maximum compressive stress at prestress transfer and the coarse aggregate type used in the concrete mixture. Two longitudinal prestresssing reinforcement patterns were used and all test specimens featured shear reinforcement spaced at 24 inches in the shear span tested. The experimental program is summarized in Chapter 4.

CHAPTER 4
Experimental Program

4.1 OVERVIEW

The experimental program for Phase II of TxDOT Project 5197 consisted of two parts:

- Part 1: Live load testing of C-beams and box beams (55 tests)
- Part 2: Shear testing of C-beams (18 tests)

For Part 1, the beams were tested in flexure at midspan until flexural cracks extended into the web (the beams were not loaded until flexural failure). As mentioned earlier, the focus of this thesis is on Part 2 of Phase II of the testing program. For the shear tests, a point load was applied near the end of the beam at a shear span of six feet (a/d = 2.22) until a shear failure in the web was created. During the testing, a linear potentiometer was used to measure deflection at midspan and a load cell was used to record applied load. The load was increased continuously just prior to the occurrence of diagonal cracking and then the load was increased incrementally while crack widths were measured and cracks were mapped on the beam. Once failure occurred, photographs were taken and the load was released.

4.2 SHEAR TESTING OF TXDOT TYPE-C BEAMS

Shear tests were performed on 18 of the C-beams used for Phase II of the research project. The test setup, instrumentation and data acquisition, and load protocol for the testing of the C-beams are discussed in the following sections.

4.2.1 Test Setup

The 18 beams tested in shear were subjected to a single point load at a shear span of six feet, resulting in a shear span to depth ratio of 2.22 in the test region (Figure 4.1).

The bearing support on the tested end was designed to produce a beam overhang distance of 4'-3" beyond the centerline of the support. The overhang allowed for the beam to have an adequate shear span to depth ratio while still having the stirrups spaced at 24 inches across the entire shear span. In this way, the end of the beam, reinforced heavily (as per TxDOT standards) against bursting and spalling effects, was located in the overhang and not tested under shear loads. The overhang also served to avoid any possible strand anchorage issues. The key dimensions of the test setup and test specimens are illustrated in Figure 4.1.

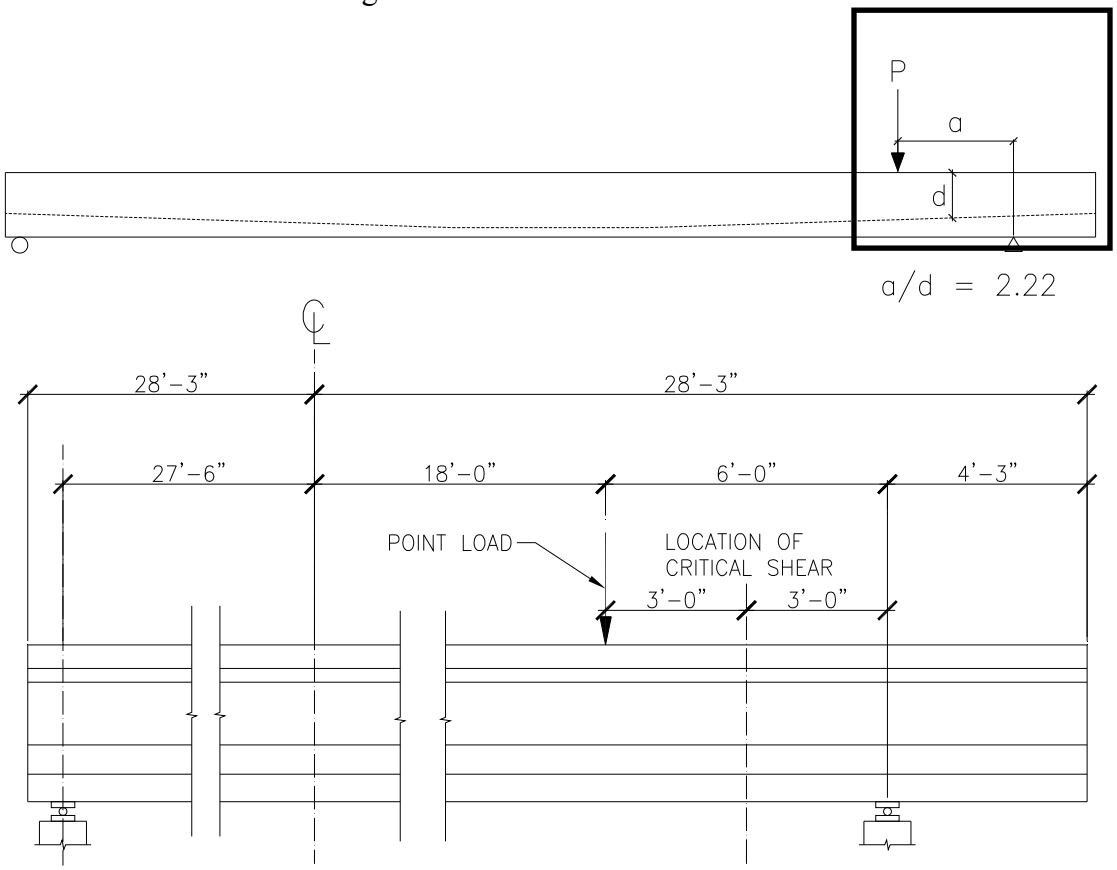

Figure 4.1 End Region Dimensions for Shear Test

The entire test setup is depicted in Figure 4.2. The reaction frame of the setup consisted of a wide flange beam that spanned between two steel wide flange beams that each spanned between two wide flange columns that were bolted to the strong floor of the

laboratory. The testing frame was centered at the location of the loading point (Figure 4.2). An 800-kip hydraulic ram used to apply load was bolted directly into the bottom of the wide flange beam. A neoprene bearing pad (14”x9”x2½”) was placed on the beam at the location of the point load. On top of the pad, a large steel rectangular prism (22”x22”x2½”) was placed in order to provide support for the 1000-kip load cell that was bolted on top of the prism (Figure 4.3). Also bolted to the load cell were steel shackles that provided a loop so that chains could run through and connect the load cell to the handles of the ram to keep it from being damaged by falling down after failure (Figure 4.4). In between the load cell and the hydraulic ram, a spherical head was placed in order to simulate a true point load and to ensure even distribution of the applied load. Additional steel blocks were placed as needed in order to limit the stroke of the ram. For safety concerns, lateral braces were bolted to a column on each side of the beam in order to stabilize the specimen if it laterally buckled or rotated. The lateral bracing consisted of two steel 5x5x5/16 angles that were bolted into the columns and cantilevered out to a distance of about one half of an inch from the web of the prestressed concrete beam. An enlarged diagram of the test setup can be seen in Figure 4.3 and a photograph of the various loading components described above can be seen in Figure 4.4.

The test specimens were simply supported with a pinned connection at the tested end and a roller connection at the other end. To simulate the simply supported conditions, two steel plates (22”x6”x2”) which sandwiched a cylindrical steel bar (2 inch diameter) were used as the supports beneath each end of the beam. Each steel plate – round bar assembly rested on concrete blocks that were placed on the strong floor of the laboratory. At the pinned connection end, the round bar was welded to the bottom plate so that the beam was not free to move horizontally. At the other end of the beam, however, the round bar was not attached to the plates in any way, thus allowing the beam to move horizontally. The support conditions replicated a theoretical “fixed – pinned” condition. The details of each support can be seen in Figure 4.5.

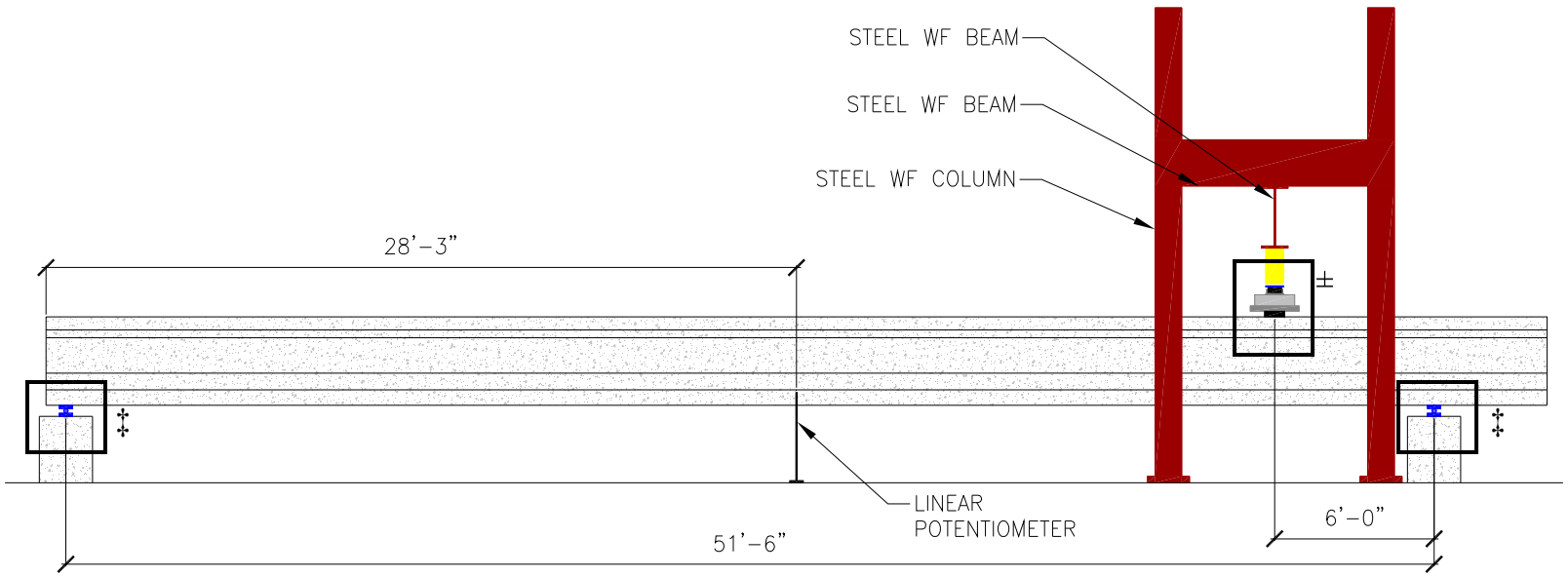

± = Figure 4.4

‡ = Figure 4.5

Figure 4.2 Test Setup

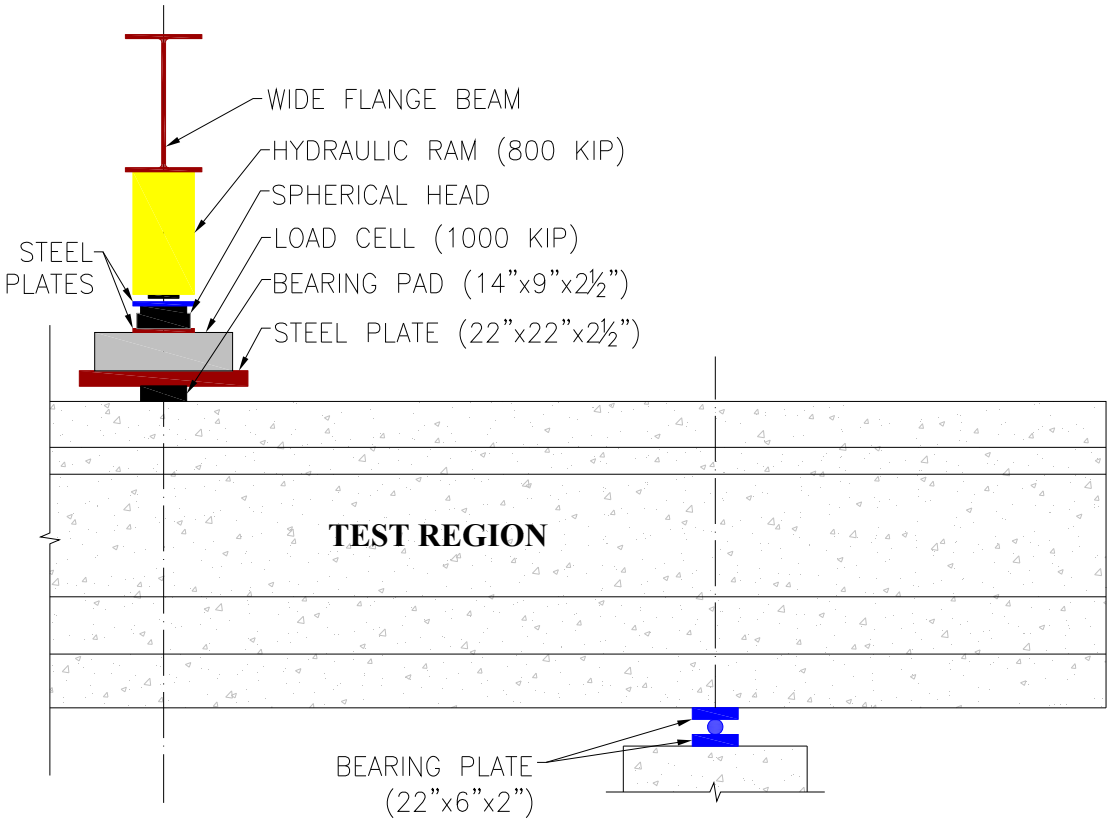

Figure 4.3 Test Setup Diagram for Shear Test

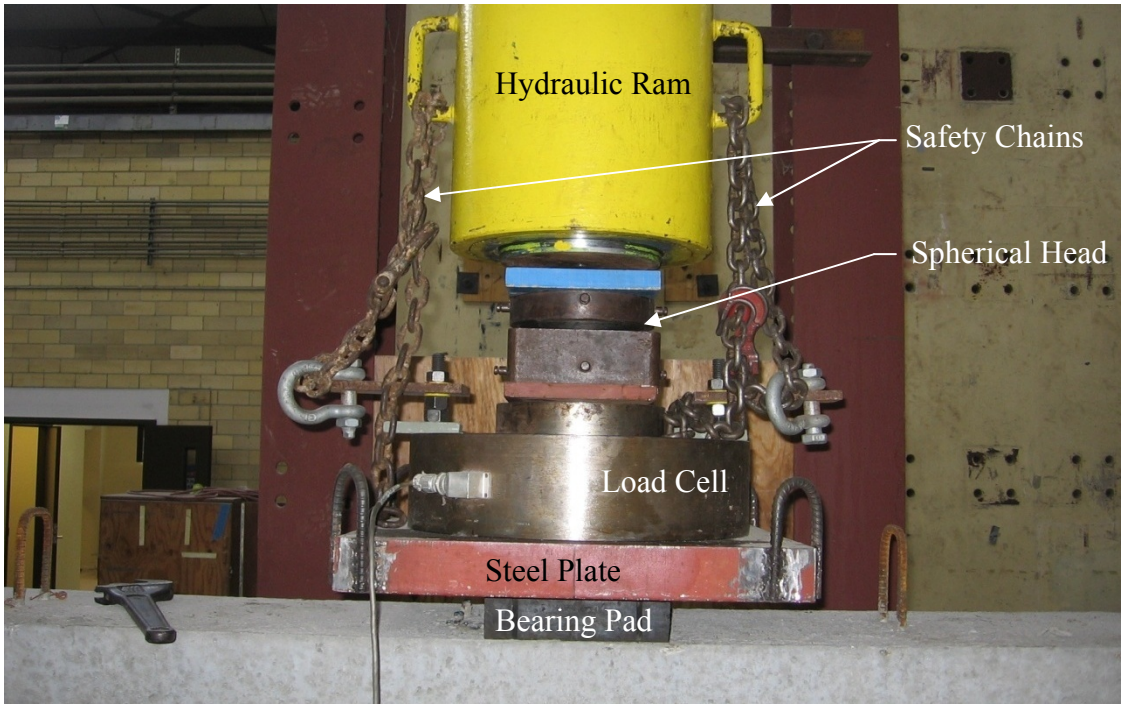

Figure 4.4 Photograph of Loading Assembly

Figure 4.5 Pinned and Roller Support Conditions

4.2.2 Instrumentation and Data Acquisition

All of the instrumentation used in the data collection process measured changes in voltage. The voltage readings were scanned into a computer (Figure 4.6) where they were converted to the correct engineering quantity by preprogrammed calibration equations. For the shear tests, applied load and midspan deflection were recorded. A 1000-kip load cell was used to measure the applied load and a 6-inch linear potentiometer was used to measure midspan deflection.

The load was applied by using an 800-kip ram (Figure 4.4) and measured using a 1000-kip load cell (Figure 4.4) that was calibrated before testing to ensure its accuracy. The applied load was measured in each shear test to determine the shear in the beam at first diagonal cracking and at failure. The load was applied using a pneumatic hydraulic pump (Figure 4.7) that was attached through a hydraulic line to the ram. When the pressure on the pump was increased the ram pressed downward creating the applied load on the beam. The hydraulic pressure gage on the pump also measured the pressure on the hydraulic supply line. By converting the hydraulic pressure into load, the load cell measurements were verified. The same load cell was used in all 18 shear tests.

One 6-inch linear potentiometer (shown in Figure 4.2) was used to measure midspan deflections. The deflections were needed to create load-deflection plots for each test. The load-deflection plots were not used to make judgments about the effects of release stresses on shear strength, but solely to illustrate the brittle nature of the failures. The linear potentiometer was placed at midspan because the most deflection was experienced at that location and the instrument was also safe from damage.

Figure 4.6 Data Acquisition System

Figure 4.7 Load Being Applied by Pump

4.2.3 Load Protocol

The load from the hydraulic ram was applied at two constant rates throughout the testing of the beam. In the linear-elastic range, the load was increased at a rate of approximately 50 kips per minute until it reached roughly 90 percent of the anticipated diagonal cracking load. The first diagonal web-shear crack formation created a loud splitting sound, "pop," in all beams which made determining the cracking load very easy. The load was held constant for about thirty to sixty seconds and if no "pop" was heard or if no crack was visually noticed it was increased at a rate of approximately 10 kips per minute at 5 kip increments until the diagonal crack formed. Once the diagonal crack appeared it was marked and photographed. After the first diagonal crack formed, the load was increased and loading was stopped at 20 kip intervals in order to thoroughly record all cracks in the beam specimens. At each stage of loading, the load was maintained and diagonal web-shear cracks and their respective widths were marked on the beam (cracks shown in blue in Figure 4.8). If flexural cracking occurred, cracks were marked on the beam in a different color (cracks shown in red in Figure 4.8). A crack comparator card was used to measure the widths of the widest diagonal cracks and the measurements were recorded on data sheets (Appendix B) along with the corresponding load. The crack width measuring process is depicted in Figure 4.9. In addition to the measurements, photographs were also taken of both sides of the beam at each load stage.

Incremental loading of the beams was stopped at approximately 75 percent of the anticipated failure load. At that point, a video camera was set up to record the failure (Figure 4.10). The beam was then loaded at a constant rate until failure, which occurred in the form of diagonal tension or crushing of the web of the beam (the differences in the two modes of web-shear failure are discussed in Chapter 5). A slight drop in the applied load usually gave warning that the beam was about to fail. Some concrete usually spalled off from the web, then the failure occurred suddenly, creating a very loud explosion. Once the beam failed, it was immediately unloaded. More details of the shear failures are provided in Chapter 5.

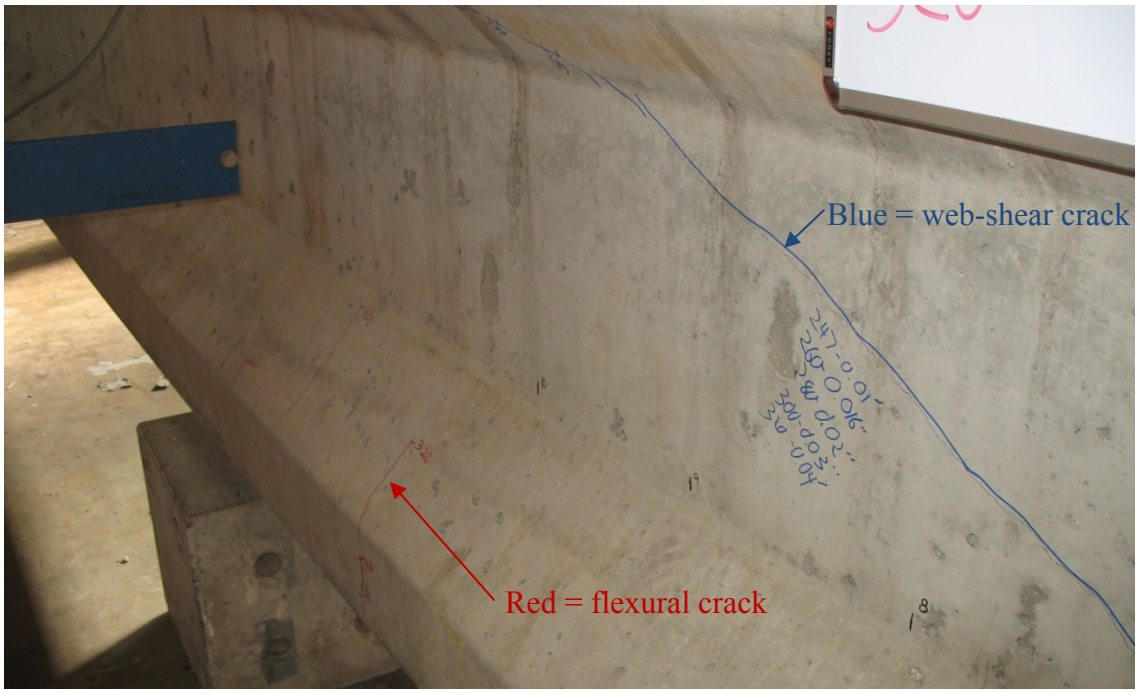

Figure 4.8 Web-Shear and Flexural Crack Marks

Figure 4.9 Measurement of Diagonal Crack Width

Figure 4.10 Video Camera Setup behind Protective Shield

4.3 SUMMARY

In shear performance evaluation, 18 TxDOT C-Beam specimens were tested in shear at a shear span to depth ratio of 2.22. The test setup was designed to induce a web-shear failure in the beams. A 1000-kip load cell was used to record the applied load which was produced by a pneumatic hydraulic pump connected to an 800-kip ram. During the test, vertical deflection was measured at the midspan of the beam using a linear potentiometer. The load was applied until the first diagonal web-shear crack appeared. At that point, cracks were marked and measured at predetermined increments until the load reached approximately 75 percent of the anticipated failure load to thoroughly record crack propagation. The measurements of primary importance in each test were the applied load and diagonal crack widths. Each test was photographed thoroughly and recorded on video. The results of the shear tests are summarized in Chapter 5.

CHAPTER 5
Analysis of Test Results

5.1 OVERVIEW

In this chapter, the results of 18 shear tests conducted during Phase II of TxDOT Project 5197 are presented. Two important parameters are used to analyze the results from each test: the ratio of the measured diagonal cracking shear to the estimated diagonal cracking shear and the ratio of the measured shear capacity to the estimated shear capacity. All estimates were calculated using equations from ACI 318-08 and AASHTO LRFD (2007). All applied loads were measured using the data acquisition equipment, instruments, and processes described in Chapter 4 and all measured shears were calculated from these applied loads and the self weight of the test specimens. The calculated first diagonal cracking shears and shear capacities are analyzed to identify trends with increasing maximum compressive stress in concrete at prestress transfer. In this way, the impact of increasing the allowable compressive release stress limit on strength and serviceability behavior of prestressed concrete members in shear is evaluated.

5.2 RESULTS OF SHEAR TESTS

Diagonal web-shear cracks form in a prestressed concrete beam when the shear stress induced tensile stresses in the concrete exceed the tensile strength of concrete. The concrete contribution to shear strength is typically defined as the shear at which the first diagonal crack forms. For a beam without transverse reinforcement, this shear also corresponds to the shear capacity. For beams with transverse reinforcement, the shear capacity is greater than the first diagonal cracking shear. Once diagonal cracking occurs, the mechanism through which shear is resisted changes. However, the nominal strength of the concrete is generally assumed to remain the same in diagonally cracked concrete, allowing the total shear resistance to be taken as the sum of the concrete contribution and

the transverse reinforcement contribution. In this research study, the prestressed concrete beam specimens were designed and loaded such that web-shear cracking and web-shear failures were more significant.

The critical section for shear in the beam specimens tested was assumed to be at the middle of the shear span at a location halfway between the point of the applied load and the point of the support. The total shear at the critical section was considered to be the sum of the shear from the applied point load and the shear from the self weight of the beam. The beam weighed 29.15 kips, making its self weight an important factor in determining shear strength. Figure 5.1 shows the loading and shear force diagrams for the applied load and self weight separately. The shear at the critical section is 0.88P for the applied load, where P is the measured applied load in kips, and the shear at the critical section is 11.8 kips for the self weight of the beam (sample calculations shown in Appendix B). Hence, the total shear at the critical section at any time is

$$V = 0.88P + 11.8 \qquad \textbf{\textit{Equation 5-1}}$$

The procedures used to calculate and measure the actual first diagonal cracking and failure shears are discussed next.

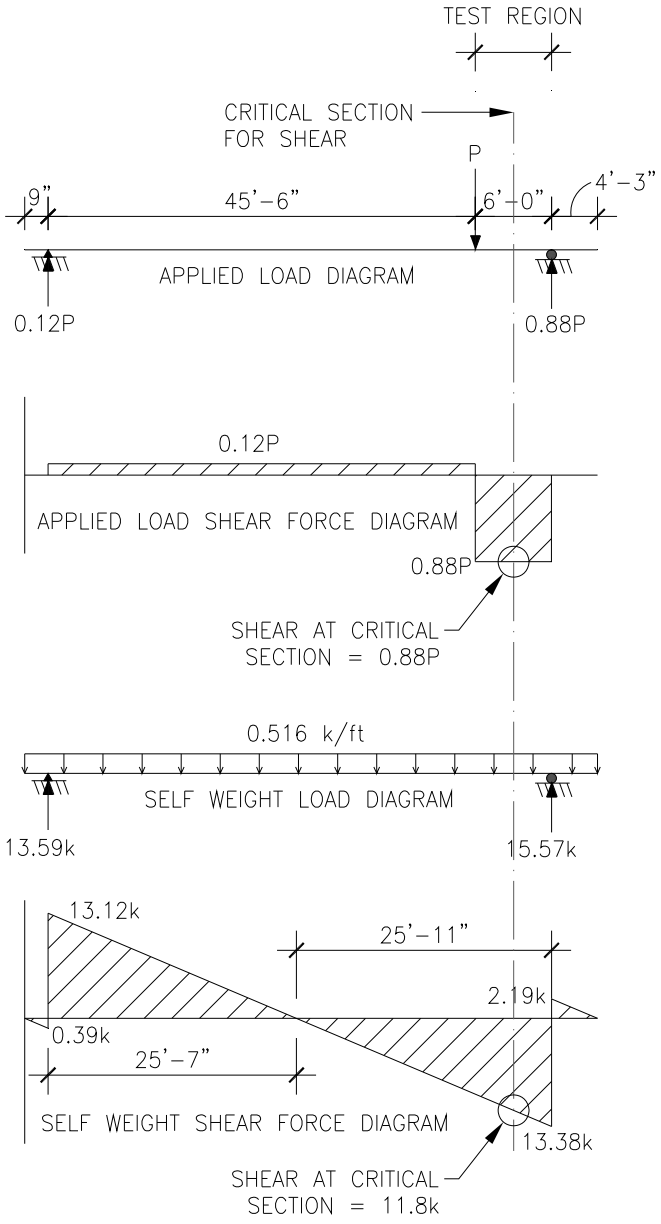

Figure 5.1 Shear Diagrams

5.2.1 Determination of Measured Diagonal Cracking Shear

Determining the contribution of concrete to total shear strength for a prestressed concrete member loaded in shear is a simple process. Web-shear cracks occur suddenly and with little warning, almost always creating an audible "pop" sound denoting splitting of the concrete web along the diagonal crack. When members with relatively small shear span to depth ratios are loaded to failure, a diagonal crack opens up spanning across the web on a relatively straight line approximately from the point of the load to the point of the support.

In order to properly record the applied load at web-shear cracking, the applied load on the beam was increased to approximately 90 percent of the expected diagonal cracking load. When this load level was reached, the loading was paused while the test specimen was thoroughly inspected for cracking. If no crack was seen, the applied load was increased. In a typical test, when the first web-shear crack formed, the loading was stopped, the diagonal crack was marked, and the crack width was measured. The typical maximum diagonal crack width at first cracking was about 0.01 inches. The crack width was measured with a crack comparator card as shown in Figure 5.2. (For picture clarity, Figure 5.2 shows the measurement of a diagonal crack well after its original formation.) The angle of the crack was also measured by creating a triangle with the crack as the hypotenuse and measuring the opposite and adjacent sides. The angle measuring process is depicted in Figure 5.3. Subsequently, the crack was photographed. A typical first diagonal crack is depicted in Figure 5.4. The diagonal cracking shear was then calculated from Equation 5-1. Table 5.1 summarizes the diagonal cracking shears for all 18 specimens.

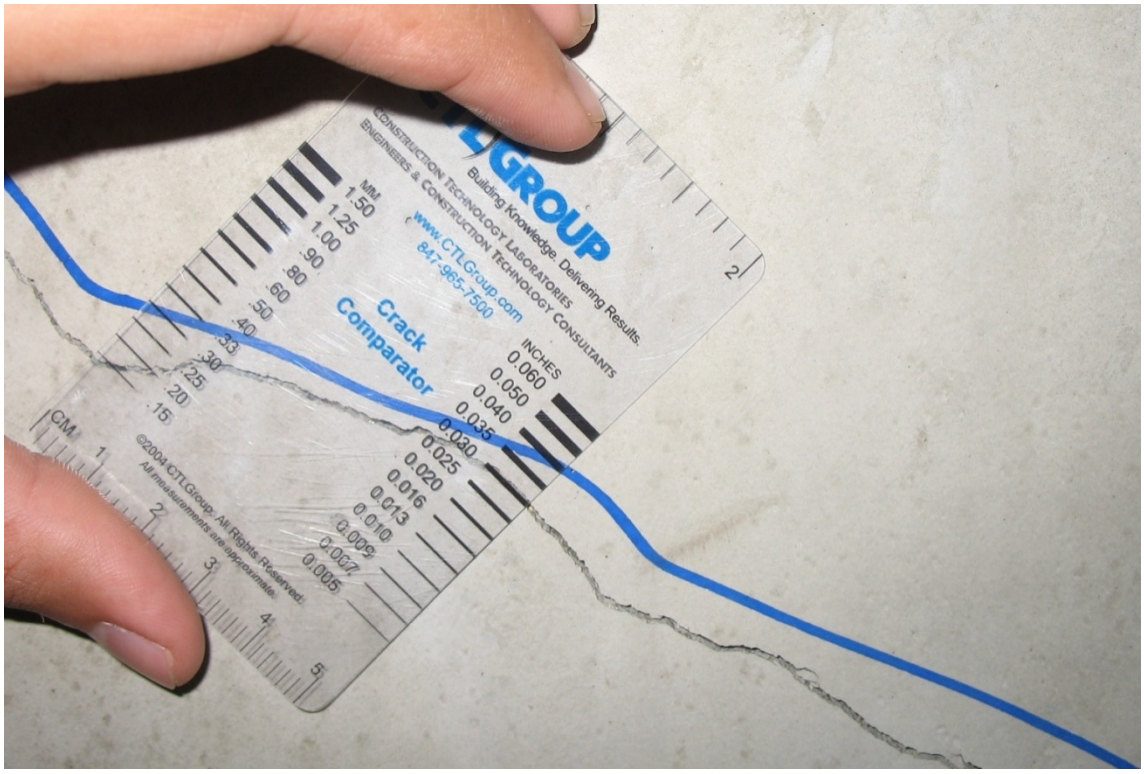

Figure 5.2 Crack Width Measurement with Crack Comparator

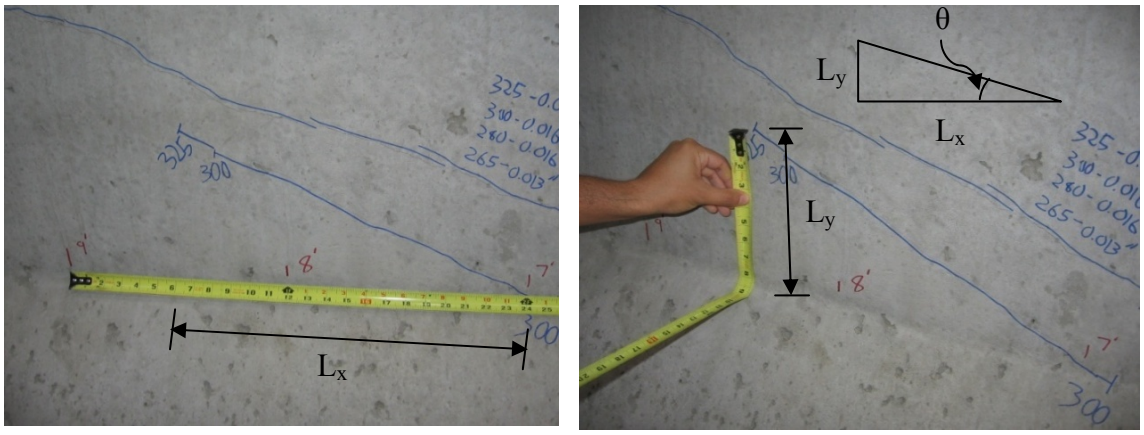

Figure 5.3 Crack Angle Measurement

Figure 5.4 First Web-Shear Crack on Beam CD-60-2

Table 5.1 Measured Diagonal Cracking Shears

Fabricator	Specimen Designation	Measured Diagonal Cracking Shear, V_{crack} (kips)
Fabricator B (Series 1)	CB-60-1	228
	CB-60-2	219
	CB-70-1	219
	CB-70-4	232
	CB-70-5	219
	CB-70-6	229
Fabricator C (Series 2)	CC-70-1	224
	CC-70-2	228
	CC-65-3	232
	CC-65-4	237
	CC-60-1	215
	CC-60-2	210
Fabricator D (Series 2)	CD-70-1	241
	CD-70-2	246
	CD-65-3	250
	CD-65-4	246
	CD-60-1	241
	CD-60-2	246

Once the first crack was properly recorded, documented, and photographed, the load was increased gradually and the maximum crack width was measured and recorded at preselected load stages. At a given load stage, if the first diagonal crack propagated further, it was marked and maximum diagonal crack widths and corresponding loads were marked on the beam. If a flexural crack appeared, it was marked on the beam with a different color. The preselected load stages were 260, 280, 300 and 320 kips for the Series 1 beams and 270, 290, 310, and 330 kips for the Series 2 beams. The load stages were chosen to keep a consistent standard of comparison between the beams in each series. The last load stage (320/330 kips) was chosen to be approximately 75 percent of the expected failure load to ensure the safety of the research team. The expected failure

load was based on statistics from the University of Texas Prestressed Concrete Database and was thought to be approximately 40 to 60 percent greater than the load corresponding to the shear capacity calculated by ACI 318-08. Among the various load stages, the initial web-shear crack usually increased in width by about 0.005 to 0.01 inches. Typically, no other web shear cracks occurred at the intermediate load stages and the first crack propagated slowly into the bottom flange near the location of the support. The beam was photographed at each load stage. The camera used was mounted to a tripod and setup so that each photograph would capture the exact same section of the beam. A depiction of a typical beam at the last load stage is shown in Figure 5.5.

In some cases, a second diagonal crack would form in the web during the intermediate load stages (Specimens CB-60-2, CB-70-4, CC-60-1, and CD-70-2). Figure 5.6 shows a Series 1 beam at the second to last load interval with two clear diagonal cracks. In the case of a second crack forming, the crack widths would not increase as much as a beam with only one diagonal crack. Once the final load stage was reached, a protective Plexiglas sheet was placed between the specimen and the camera (Figure 4.12). At the final load stage, the digital camera was replaced with the video camera to the record the failure on video. Subsequently, the beam was gradually loaded to failure.

Figure 5.5 Last Load Stage on Beam CD-60-2

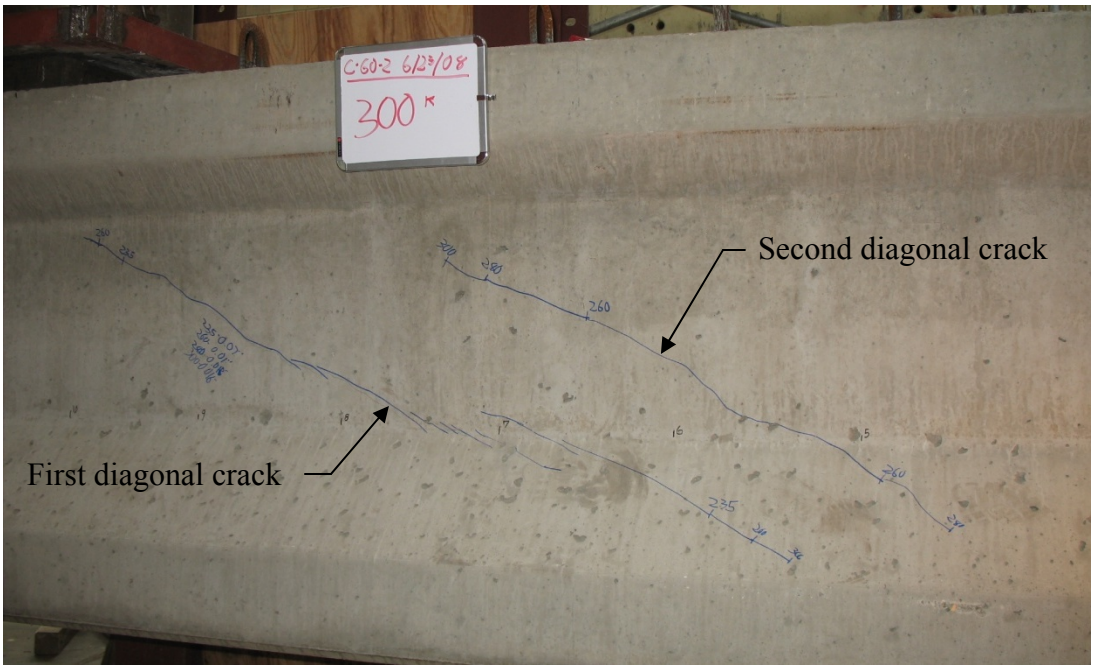

Figure 5.6 Second Diagonal Crack on Beam CB-60-2

5.2.2 Determination of Measured Shears Capacity

After the last load stage when the crack widths were measured, safety precautions were put in place, the video camera was set to record, and the beam was gradually loaded to failure. While the beam was being loaded, the immediate area surrounding the test region was taped off to ensure the safety of observers and the students operating the testing equipment were protected behind plywood and Plexiglas shields. While one student operated the pump, the other took close-in pictures of the web-shear crack widening with a digital camera. As the beam approached its capacity, the width of the first diagonal crack began to increase rapidly. For safety reasons, the width of the crack was not measured during the loading stages close to failure. As the first crack began to open up, a second diagonal crack formed, usually about three to four inches above and parallel to the first crack, as seen in Figure 5.7. In cases where a second crack already existed, a third crack opened up, similar to the second crack in the aforementioned cases. Warning of impending failure was given when the load measurements obtained from the load cell started to stall.

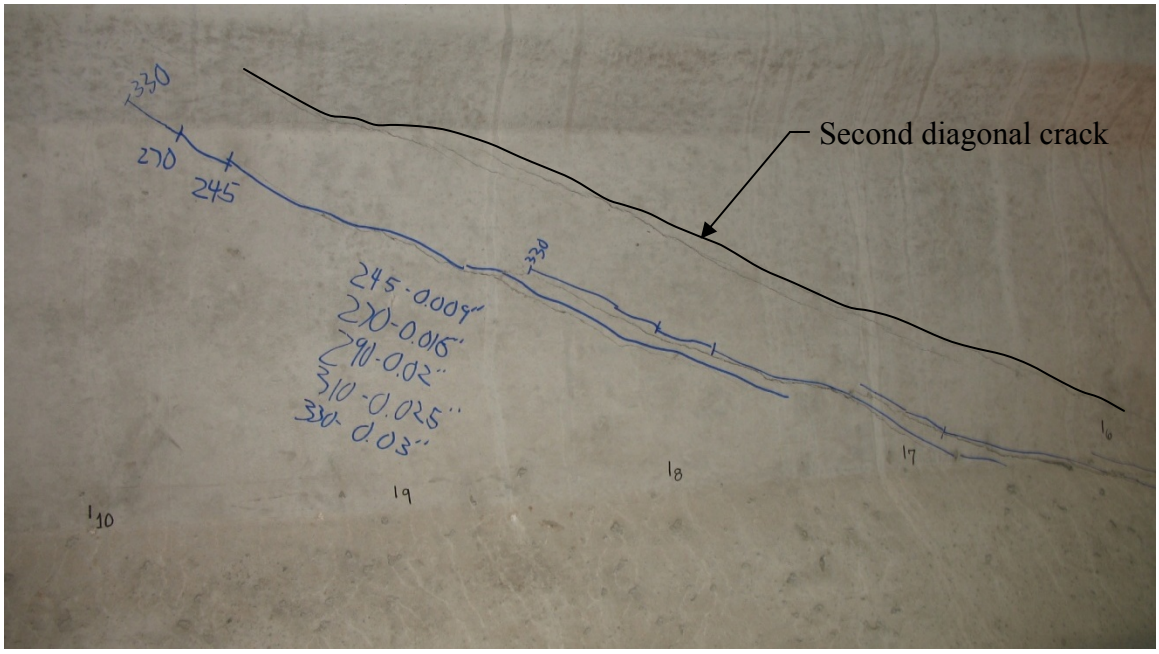

Figure 5.7 Typical Second Diagonal Crack Formation

Failure of the prestressed concrete beams in shear consisted of either diagonal tension or web crushing. Diagonal tension failures occurred when the stirrups ruptured, causing the beam to split smoothly along a diagonal crack. On the other hand, web crushing failures occurred when the concrete in the web crushed without rupturing the stirrups. The difference in the two modes of failure is illustrated in Figure 5.8 and a depiction of each is shown in Figure 5.9 and Figure 5.10.

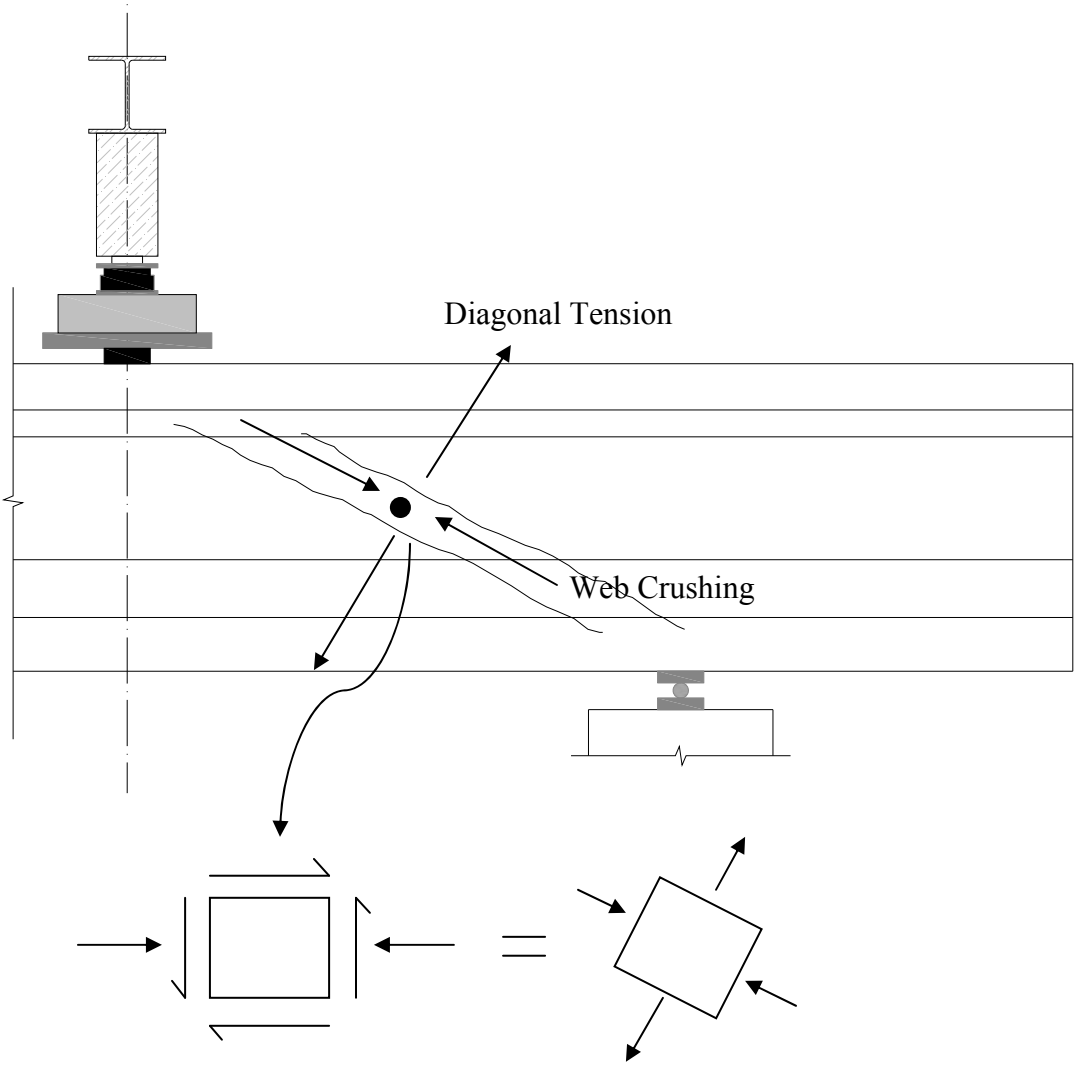

Figure 5.8 Diagonal Tension and Web Crushing Failures

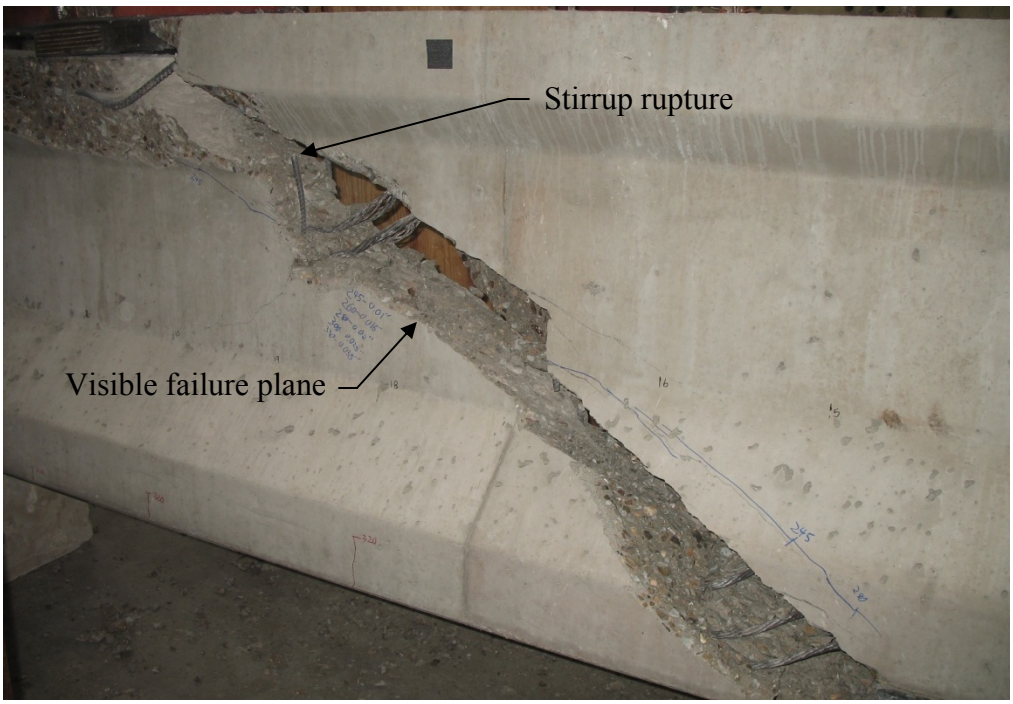

Figure 5.9 Diagonal Tension Failure

Figure 5.10 Web Crushing Failure

Both modes of failure were brittle. In the shear tension failures, the beam split into two entirely separate pieces being held together only by the longitudinal steel. The longer part of the beam fell down and the stopper block shown in Figure 5.11 was used to stop the beam from falling to the laboratory floor. In the web crushing failures, the longer part of the beam did not drop directly on the stopper block below. As seen in Table 5.2, all beams from Fabricator B (Series 1 with hard river gravel) failed in diagonal tension. All beams from Fabricator C (Series 2 with crushed limestone) failed in web crushing. Half of the beams from Fabricator D (Series 2 with hard river gravel) failed in each mode. The modes of failure seem to suggest that that maximum compressive stress at release had no discernable effect on whether a beam failed in diagonal tension or web crushing but that the coarse aggregate type had an effect. More specifically, it is important to note that all beams made with concrete containing crushed limestone coarse aggregate failed by displaying a web crushing failure mode. In contrast, most of the beams made with concrete containing hard river gravel coarse aggregate failed in diagonal tension.

Figure 5.11 Stopper Block used to Catch Beam after Failure

Table 5.2 Measured Shear Capacities and Modes of Failure

Fabricator	Specimen Designation	Measured Shear Capacity, (kips)	Failure Mode*
Fabricator B (Series 1)	CB-60-1	365	DT
	CB-60-2	359	DT
	CB-70-1	359	DT
	CB-70-4	356	DT
	CB-70-5	340	DT
	CB-70-6	374	DT
Fabricator C (Series 2)	CC-70-1	372	WC
	CC-70-2	408	WC
	CC-65-3	382	WC
	CC-65-4	395	WC
	CC-60-1	379	WC
	CC-60-2	378	WC
Fabricator D (Series 2)	CD-70-1	398	DT
	CD-70-2	409	DT
	CD-65-3	389	WC
	CD-65-4	403	WC
	CD-60-1	401	DT
	CD-60-2	413	WC

*DT = Diagonal Tension, WC = Web Crushing

Figure 5.12 shows the progression of a diagonal tension failure. Figure 5.13 shows a similar progression for a web crushing failure. The pictures were captured from screenshots of the videos that were recorded to document the failure of specimens CB-60-1 and CD-60-2. Since the video camera was behind a Plexiglas shield, a slight reflection that can be seen in the screenshots was unavoidable. The interval of time from Screenshot A to Screenshot D in Figure 5.12 and Figure 5.13 is less than two seconds. As documented in the screenshots, both failure modes were explosive and very brittle. For the diagonal tension failure, as seen in Screenshot A of Figure 5.12, not much spalling of concrete occurred, then the beam split suddenly about a diagonal crack (Screenshot B). A minimal amount of concrete debris fell from the beam. When the dust settled, a clear failure plane was seen.

Contrary to the diagonal tension failure, in the web crushing failure, the concrete from the web began to flake off, as seen in Screenshot A of Figure 5.13, giving a sign of impending failure. From there, crushing of the concrete in an explosive manner occurred, as seen in Screenshot B. Screenshot C was taken 0.04 seconds after Screenshot B, showing how fast the concrete crushes at failure. Screenshot D was taken after the concrete debris from the web had hit the floor. Both modes of failure are shear failures controlled by web-shear (V_{cw} failure).

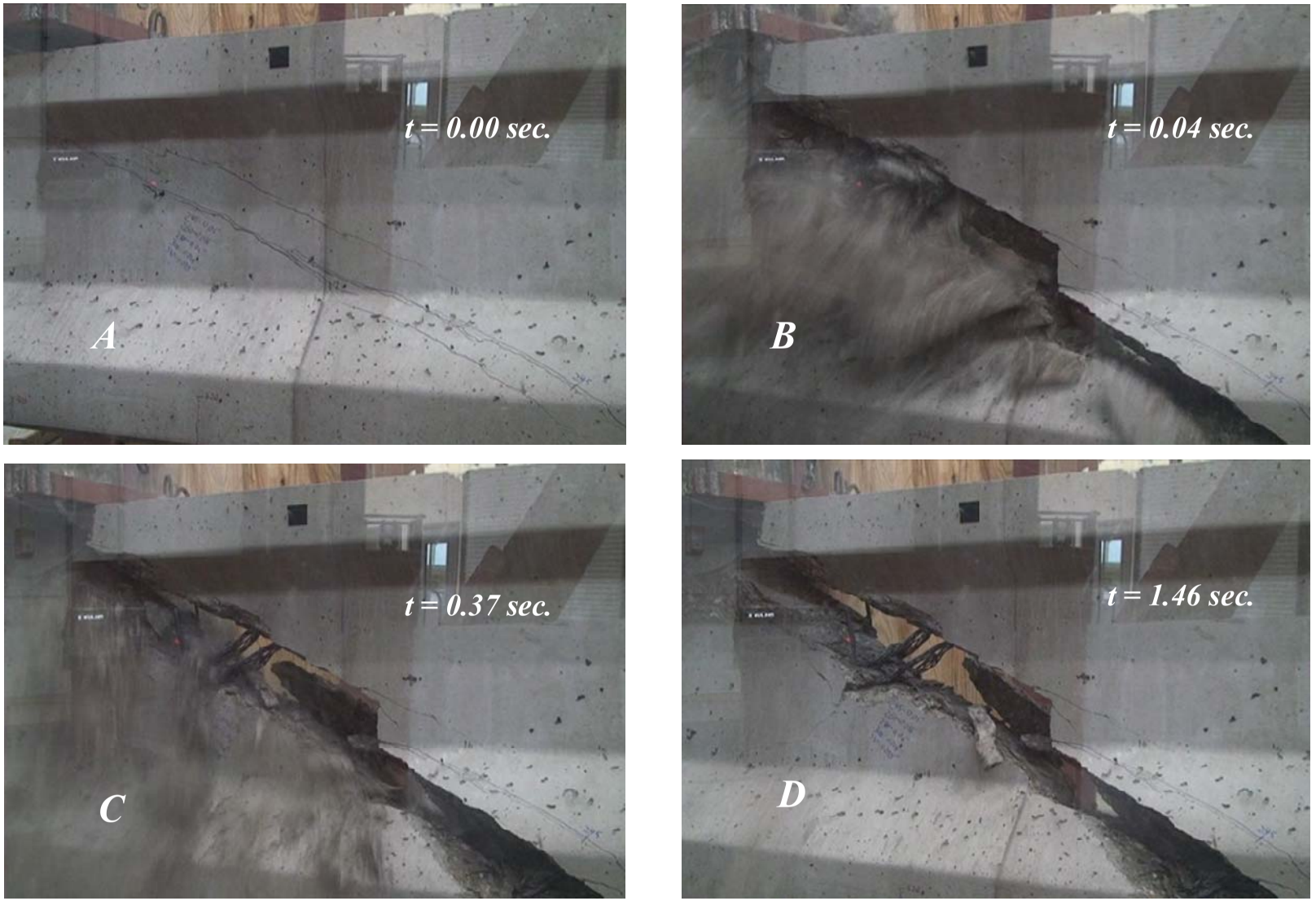

Figure 5.12 Diagonal Tension Failure: Specimen CB-60-1

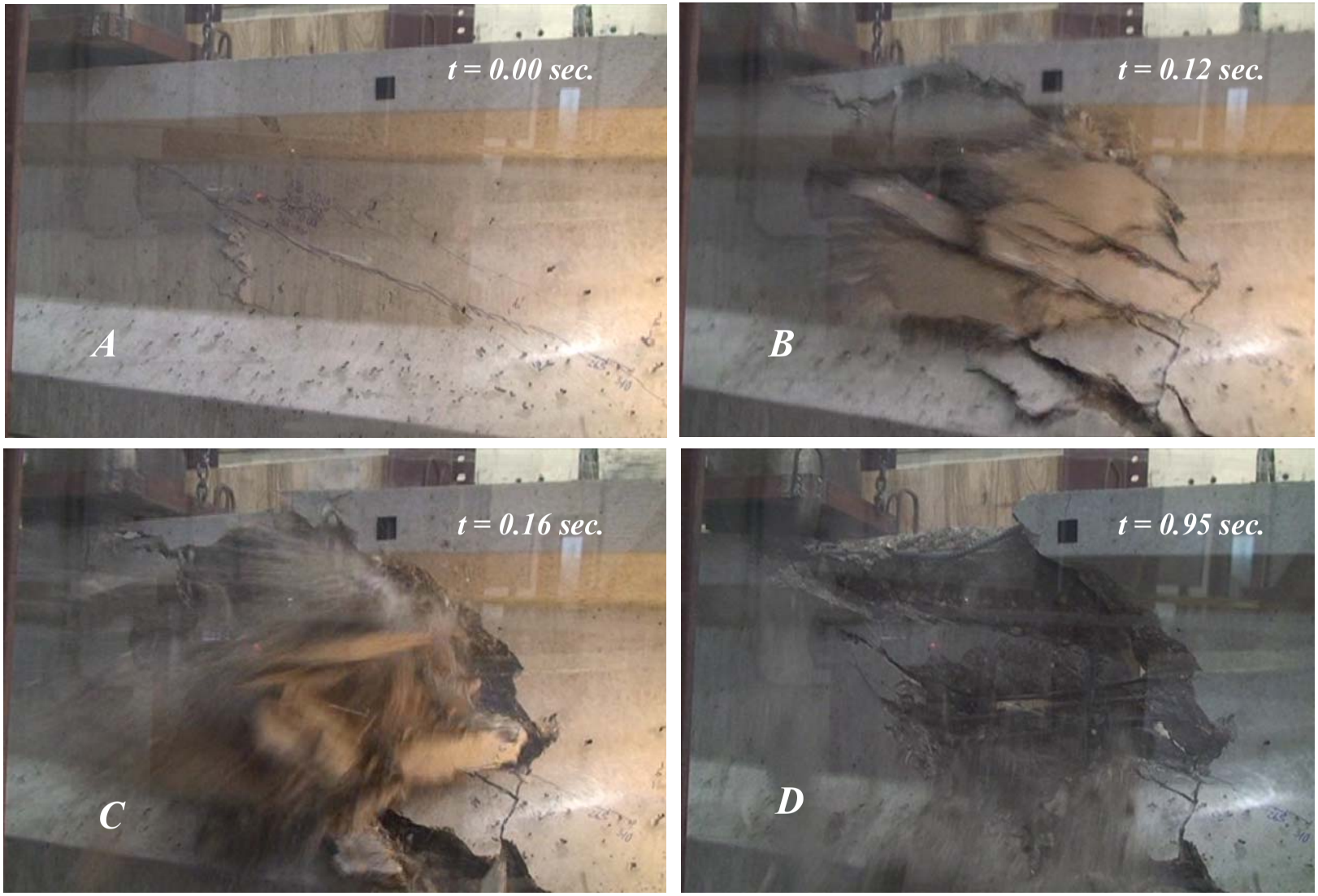

Figure 5.13 Web Crushing Failure: Specimen CD-60-2

Once failure occurred, the test specimen was unloaded. The maximum reading the load cell recorded during the test was documented and the total shear in the critical section was calculated using Equation 5-1. Once the maximum load was recorded and the load-deflection data were taken from the computer, the cleanup process began to make the setup ready for the next test. A summary of the measured shear capacities is provided in Table 5.2.

5.2.3 Diagonal Cracking Shear Calculations

The theoretical diagonal cracking shears were calculated by using the shear design provisions of ACI 318-08 and the AASHTO LRFD (2007) simplified procedure. The ACI 318 and AASHTO LRFD provisions for shear strength of prestressed concrete members were discussed in depth in Section 2.2.1. In ACI 318-08, the concrete shear strength contribution to a prestressed member is said to be the lesser of the shear needed to transform a flexural crack into a diagonal crack, V_{ci}, or the shear needed to form a diagonal web crack, V_{cw}. Similarly, in the simplified shear design procedure in AASHTO LRFD (2007), the shear strength of concrete is defined as the lesser of V_{ci} and V_{cw} as well. For the shear span of six feet used in the experimental program, the shear span to depth ratio was rather small (a/d = 2.22), which made web-shear cracking more critical ($V_{cw} < V_{ci}$). As such, the V_{cw} equations, discussed in Chapter 2, governed. The equations for V_{cw} in ACI 318-08 (f'_c in Equation 5-2 in units of psi) and the AASHTO LRFD (2007) simplified procedure (f'_c in Equation 5-3 in units of ksi) are repeated here for convenience, respectively.

$$V_{cw} = (3.5\sqrt{f'_c} + 0.3 f_{pc}) b_w d_p + V_p \qquad \textbf{\textit{Equation 5-2}}$$

$$V_{cw} = (0.06\sqrt{f'_c} + 0.30 f_{pc}) b_v d_v + V_p \qquad \textbf{\textit{Equation 5-3}}$$

For the beams tested in this study, the theoretical web-shear crack was assumed to occur at the critical section for shear. A complete sample calculation of a diagonal

web-cracking shear can be found in Appendix B. The calculated diagonal cracking shear between beams of the same series would only change depending on the effective prestress force in the strands (beyond the scope of this discussion) and the compressive strength of the concrete. Concrete cylinders were tested in accordance with American Society for Testing and Materials (ASTM C39) specifications. Six cylinders were shipped by each fabricator along with the first beam from each casting line. Three cylinders were tested on the day of testing for the first beam and three were tested on the day of testing for the last beam on each casting line. In this way, the compressive strength of concrete used to fabricate each test specimen could be evaluated by interpolating the strength of concrete between the aforementioned days of testing. The change in concrete compressive strength for beams on a casting line was usually minimal. The maximum change in strength was 700 psi (Fabricator B, $0.70f'_{ci}$ group). However, knowing the exact strength of the concrete at the time of testing was essential to calculate the diagonal cracking shears accurately. In addition to the concrete compressive strength, another factor that could have changed the predicted cracking load was the shear span. As such, careful placement of the beam to ensure that the shear span was exactly six feet in each test was crucial. The estimated cracking shears are summarized in Table 5.3.

Table 5.3 Calculated Diagonal Cracking Shears

Fabricator	Specimen Designation	Calculated Diagonal Cracking Shear, V_{cw} (kips)		Measured Diagonal Cracking Shear, V_{crack} (kips)
		ACI 318	AASHTO LRFD	
Fabricator B (Series 1)	CB-60-1	189	137	228
	CB-60-2	191	138	219
	CB-70-1	189	137	219
	CB-70-4	187	136	232
	CB-70-5	187	135	219
	CB-70-6	187	135	229
Fabricator C (Series 2)	CC-70-1	212	161	224
	CC-70-2	213	161	228
	CC-65-3	217	164	232
	CC-65-4	217	164	237
	CC-60-1	216	164	215
	CC-60-2	216	164	210
Fabricator D (Series 2)	CD-70-1	220	167	241
	CD-70-2	221	167	246
	CD-65-3	212	162	250
	CD-65-4	218	165	246
	CD-60-1	221	167	241
	CD-60-2	221	167	246

5.2.4 Shear Capacity Calculations

The calculation of the shear capacity for each beam specimen was carried out in a manner similar to that of the previously discussed diagonal cracking shear estimates. The nominal shear strength of a prestressed concrete member is defined in ACI 318-08 and the AASHTO LRFD (2007) simplified procedure as the summation of the concrete and steel contributions to shear strength:

$$V_n = V_c + V_s \qquad \textit{Equation 5-4}$$

The ACI 318 and AASHTO LRFD equations for the shear strength provided by transverse reinforcement, given in Equations 5-5 and 5-6, respectively, were discussed in Section 2.2.1.

$$V_s = \frac{A_v f_{yt} d}{s} \qquad \textit{Equation 5-5}$$

$$V_s = \frac{A_v f_y d_v \cot\theta}{s} \qquad \textit{Equation 5-6}$$

As discussed in Chapter 2, the transverse steel contribution to the nominal shear strength, V_s, depends on the size and spacing of the stirrups, the yield strength of the stirrups, and the effective depth of the prestressing reinforcement. The AASHTO LRFD (2007) equation (Equation 5-6) also depends on the angle of diagonal cracks. The ACI 318-08 equation, however, assumes a diagonal crack angle of 45 degrees for all calculations. A sample calculation for the shear strength provided by transverse reinforcement by both codes is provided in Appendix B. From the V_s calculation, the contribution from the steel was summed with the contribution from the concrete (V_{cw}) to calculate the nominal shear strength of the test specimens. The calculated shear capacities of the test specimens are summarized in Table 5.4.

Table 5.4 Calculated Nominal Shear Capacities

Fabricator	Specimen Designation	Calculated Nominal Shear Capacity*, V_n (kips)		Measured Shear Capacity, V_{test} (kips)
		ACI 318	AASHTO LRFD	
Fabricator B (Series 1)	CB-60-1	222	190	365
	CB-60-2	224	191	359
	CB-70-1	221	190	359
	CB-70-4	220	188	356
	CB-70-5	220	188	340
	CB-70-6	219	187	374
Fabricator C (Series 2)	CC-70-1	245	214	372
	CC-70-2	246	214	408
	CC-65-3	249	217	382
	CC-65-4	250	217	395
	CC-60-1	248	216	379
	CC-60-2	248	216	378
Fabricator D (Series 2)	CD-70-1	253	219	398
	CD-70-2	254	219	409
	CD-65-3	250	215	389
	CD-65-4	250	218	403
	CD-60-1	253	219	401
	CD-60-2	254	219	413

*$V_n = V_{cw} + V_s$

5.3 COMPARISON OF TEST RESULTS

In this research study, the shear behavior of 18 TxDOT Type-C beams was studied using a shear span to depth ratio of 2.22. The primary variable in the experimental program was the maximum compressive stress in each beam at the time of prestress transfer. The strand pattern (Series 1 versus Series 2) and coarse aggregate used (crushed limestone versus hard river gravel) were other variables. In this section, data from all 18 tests will be comparatively evaluated by examining 1) the load deflection data, 2) the ratio of measured to estimated diagonal cracking shear 3), the ratio of measured to estimated shear capacity, 4) the diagonal crack widths, 5) the diagonal crack angles, and 6) the coarse aggregate type.

5.3.1 Load-Deflection Data

For each shear test performed (with exception of the first test from Fabricator D - Specimen CD-70-1), deflection was measured at midspan of the beam using a linear potentiometer. After the first shear test, when a linear potentiometer was damaged at the point of the load, it was determined that for equipment safety reasons, the linear potentiometer should not be placed around the area of the beam that was failing. As such, the linear potentiometer was moved to the midspan of the beam for the next 17 tests (Figure 5.14). When plotted against the applied load (P in Figure 5.14) on one vertical axis and the shear at the critical section (V in Figure 5.14) on another vertical axis, the deflection appears as seen in Figure 5.15 through Figure 5.17. The value of 11.8 kips on the secondary vertical axis of the load-deflection plots represents the shear from the self weight of the beam. The plots are intended solely to show the brittle nature of the shear failures and were not used for making comparisons about shear strength or stiffness of individual beams. As can be seen in the graphs, failure occurred suddenly without yielding of the longitudinal steel, which would be found in a ductile flexural failure. Accompanying each plot is a photograph of the specimen directly after failure. Figure 5.14 shows the locations of the applied load and the measured deflection for the shear tests as well as the location that each photograph was taken from.

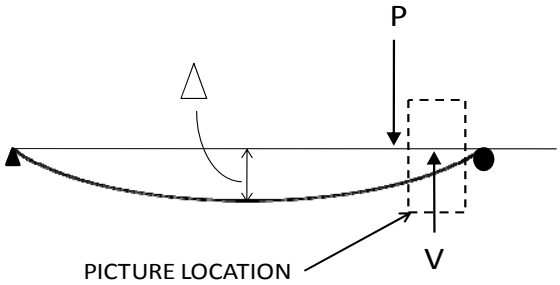

a) All specimens except Specimen CD-70-1

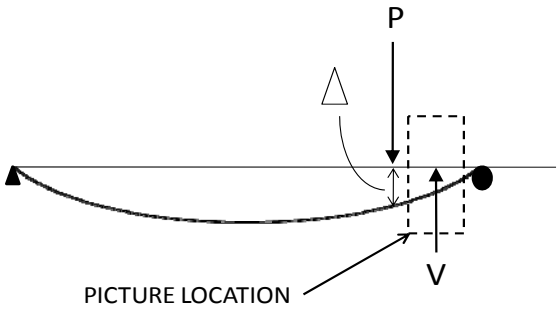

b) Specimen CD-70-1

Figure 5.14 Key for Load-Deflection Plots

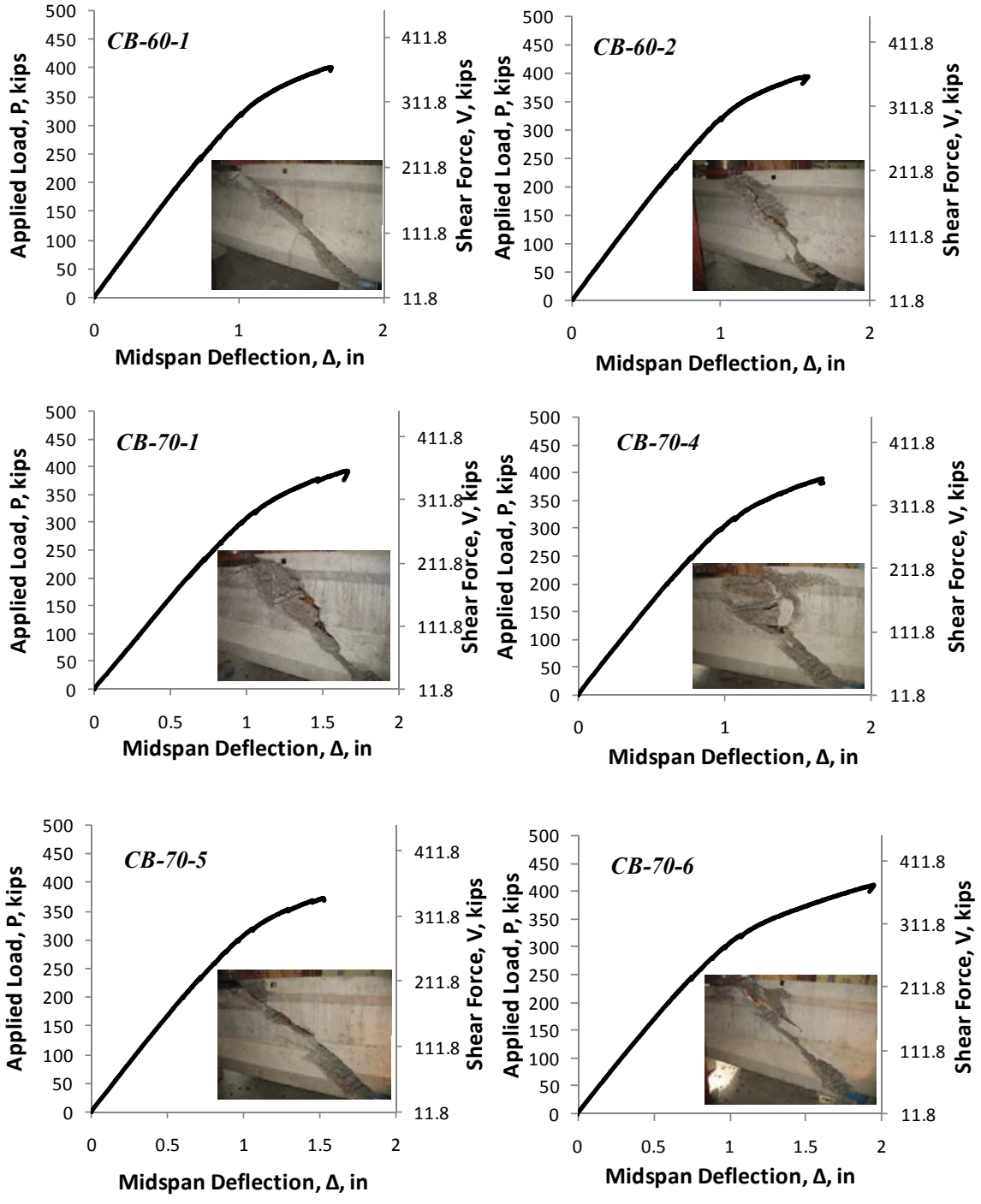

Figure 5.15 Load Deflection Plots – Fabricator B

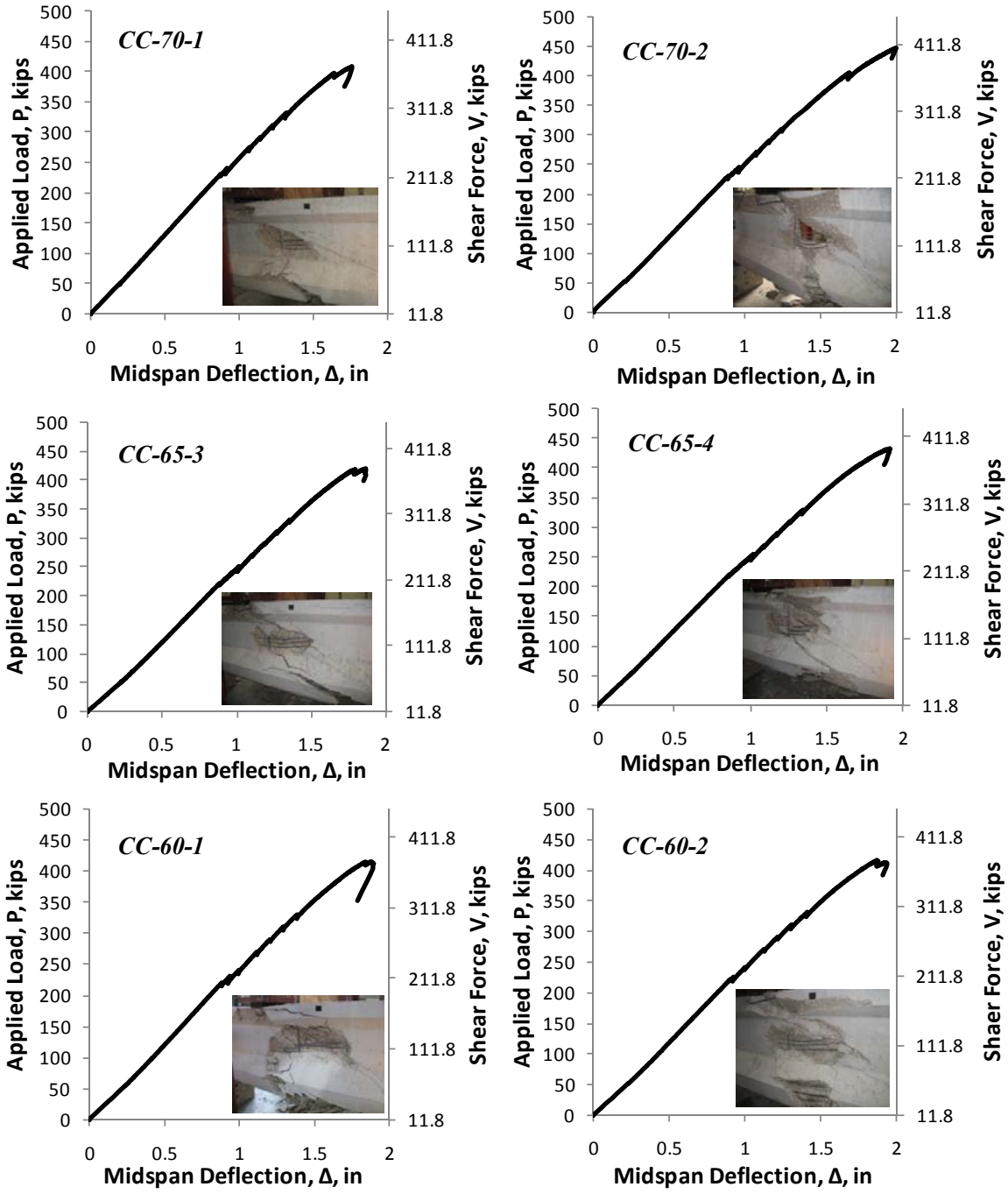

Figure 5.16 Load Deflection Plots – Fabricator C

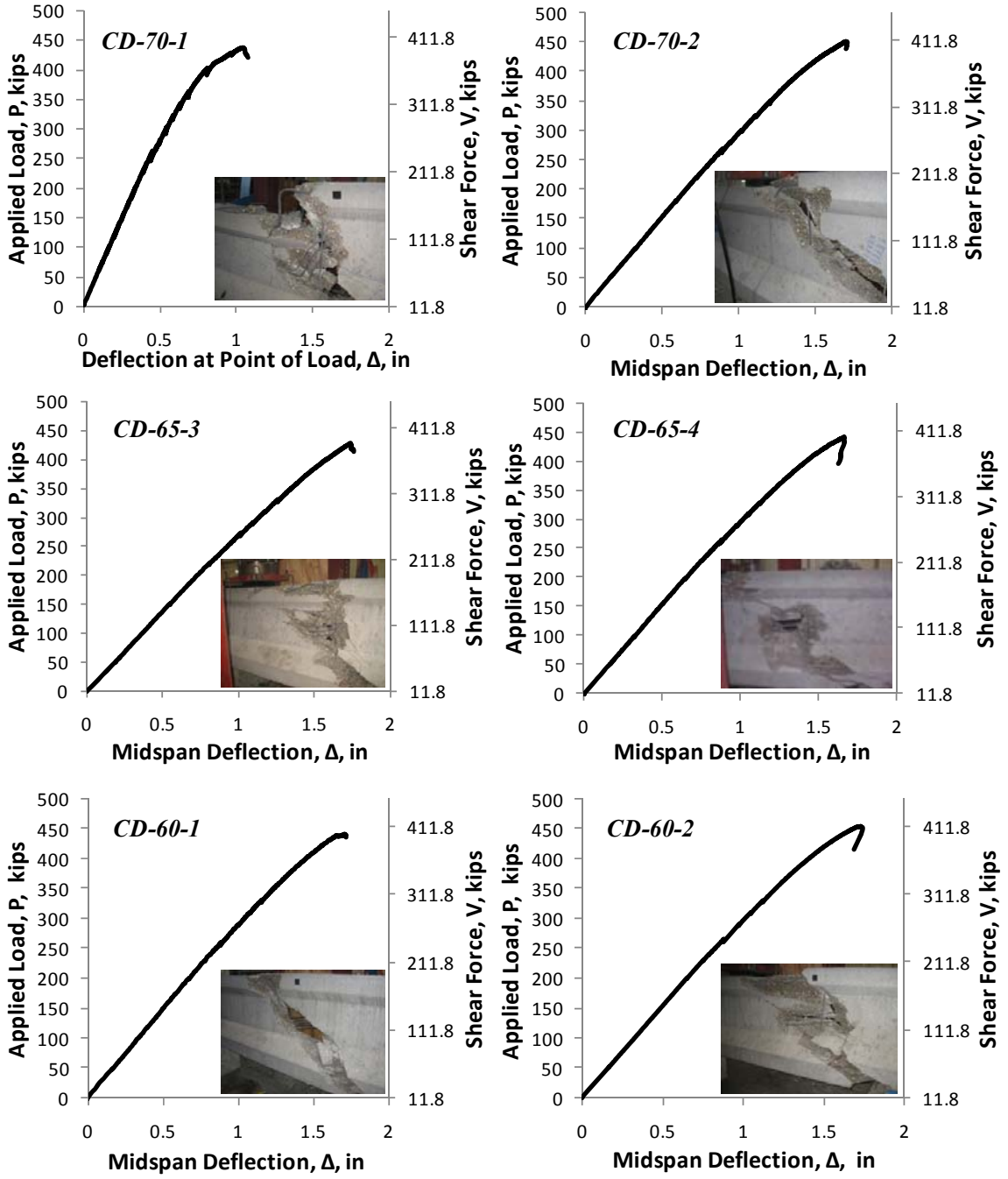

Figure 5.17 Load Deflection Plots – Fabricator D

5.3.2 Measured and Calculated Diagonal Cracking Shears

The ratio of the measured to the estimated diagonal cracking shear is an important parameter in the study of the shear strength of prestressed concrete members for the following reasons. First, in design, service level shear forces can be compared to the web-shear cracking strength of prestressed concrete members to assess if a prestressed concrete beam will develop shear cracks under service loads. As discussed in Chapter 2, the use of V_{cw} expressions (in particular that of ACI 318-08) yield conservative and reasonably accurate estimates of diagonal cracking shears. The accuracy and conservativeness of V_{cw} equations should not be compromised by a change in the allowable maximum compressive stresses at prestress transfer. Second, for members with shear reinforcement, the load at which the first diagonal crack forms is approximately equal to the concrete contribution to shear strength. A comparison of this load to that obtained through the use of the V_{cw} expressions will be used to assess the accuracy and conservativeness of the code equations. The diagonal cracking shears were calculated for all 18 shear test specimens and compared to the experimentally measured shears. Table 5.5 illustrates the ratio of measured to estimated diagonal cracking shears for both the ACI 318-08 and AASHTO-LRFD (2007) specifications and the values are plotted against the ratio of maximum compressive stress in concrete to compressive strength at prestress transfer in Figure 5.18 and Figure 5.19.

Table 5.5 Ratio of Measured to Calculated Diagonal Cracking Shears

Fabricator	Specimen Designation	$V_{crack}/V_{cw,ACI}$	$V_{crack}/V_{cw,AASHTO}$
Fabricator B (Series 1)	CB-60-1	1.20	1.66
	CB-60-2	1.15	1.58
	CB-70-1	1.16	1.60
	CB-70-4	1.24	1.71
	CB-70-5	1.17	1.62
	CB-70-6	1.23	1.70
Fabricator C (Series 2)	CC-70-1	1.05	1.39
	CC-70-2	1.07	1.39
	CC-65-3	1.07	1.42
	CC-65-4	1.09	1.44
	CC-60-1	0.99	1.31
	CC-60-2	0.97	1.29
Fabricator D (Series 2)	CD-70-1	1.09	1.45
	CD-70-2	1.11	1.47
	CD-65-3	1.18	1.54
	CD-65-4	1.13	1.49
	CD-60-1	1.09	1.45
	CD-60-2	1.11	1.47
Statistics	Maximum	1.24	1.71
	Minimum	0.97	1.29
	Average	1.12	1.50
	Standard Dev.	0.07	0.12
	COV	0.07	0.08

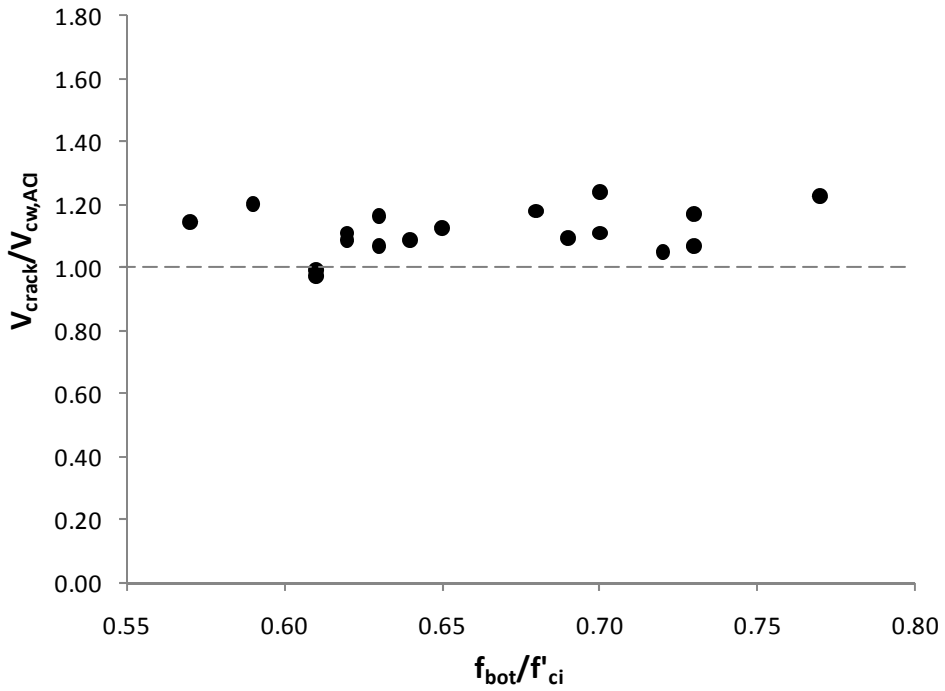

Figure 5.18 Ratio of Measured to Estimated Cracking Shears, ACI 318-08

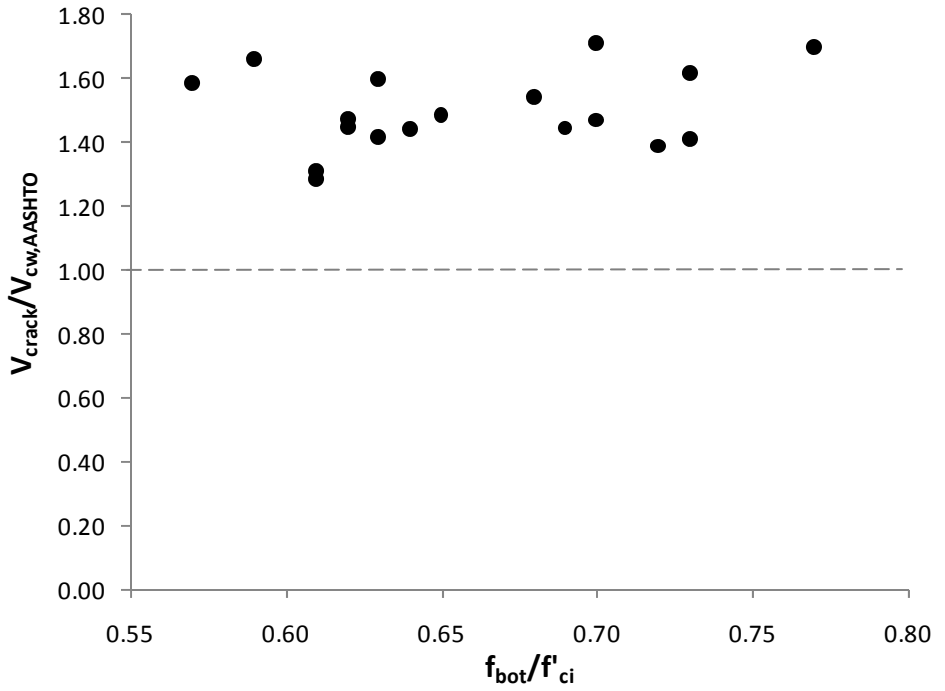

Figure 5.19 Ratio of Measured to Estimated Cracking Shears, AASHTO LRFD (2007)

As seen in Figure 5.18, the diagonal cracking shears estimated by ACI 318-08 have the right amount of accuracy and conservatism. The minimum ratio was 0.97 and the maximum was 1.24, with an average of 1.12 and a standard deviation of 0.07. In addition, there appears to be no visible relationship between the accuracy of the diagonal cracking shear estimate and the compressive stress in concrete at prestress transfer (Figure 5.18). If there was any negative effect of high compressive stresses at release on the formation of the initial diagonal crack, there would be a downward trend in the data points with increasing compressive stresses at prestress transfer. As seen in Figure 5.18 and Figure 5.19, even if the two low points (0.97 and 0.99 for ACI 318-08, which both came from $0.61f'_{ci}$ beams) were considered as abnormalities, there would still be no obvious or strong downward trend, proving that the compressive stress in concrete at release had no effect on the diagonal cracking shears.

On average, the AASHTO LRFD (2007) simplified procedure V_{cw} expression proved to underestimate the cracking loads of the beams by 50 percent (Figure 5.19). The maximum ratio was 1.71 and the minimum was 1.29, with a standard deviation was 0.13. While the AASHTO LRFD (2007) V_{cw} expression proved to be overly-conservative, its use showed that the initial diagonal cracking shear is independent of the compressive stress in concrete at prestress transfer.

When the diagonal cracking shear data from the shear tests conducted under TxDOT Project 5197 are added to the 65 data points for web-shear failures obtained from the University of Texas Prestressed Concrete Shear Database (PCSD, Section 2.4), the plots in Figure 5.20 and Figure 5.21 are obtained. The data points from TxDOT Project 5197 appear to fit well with the historical data and do not represent a low or high point in the figures. Further discussion on the impacts of the TxDOT Project 5197 tests on the PCSD are provided in the next section (5.3.3).

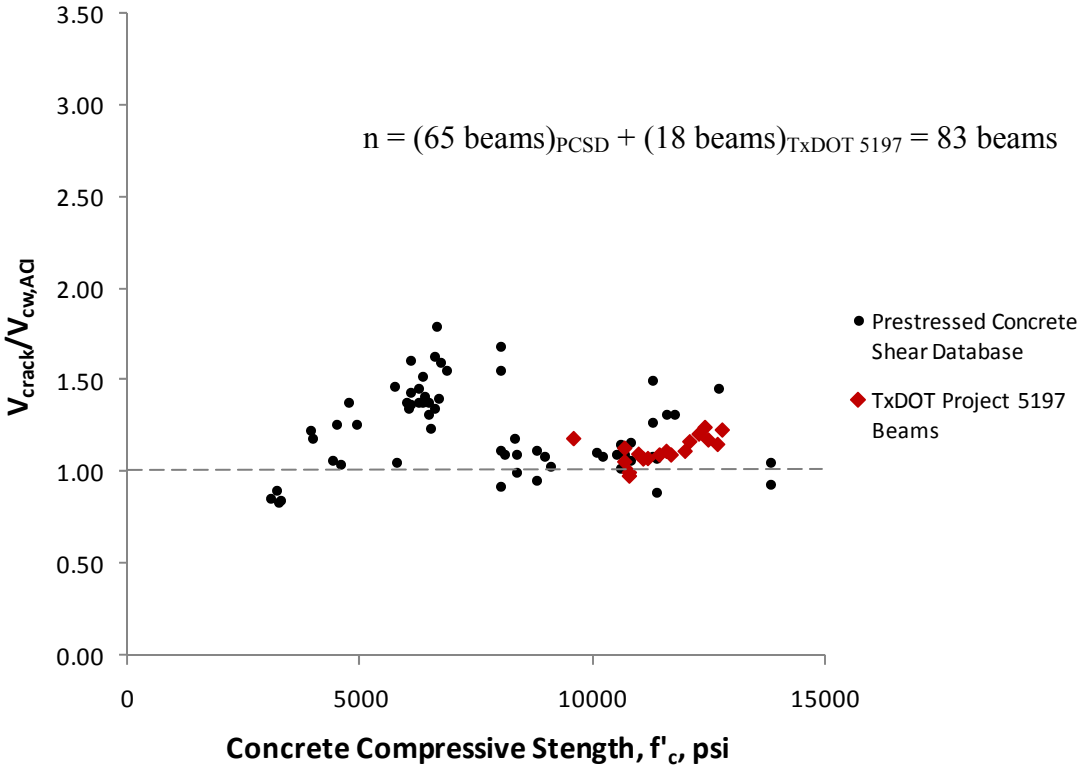

Figure 5.20 Ratio of Measured to Calculated Diagonal Cracking Shear, ACI 318-08

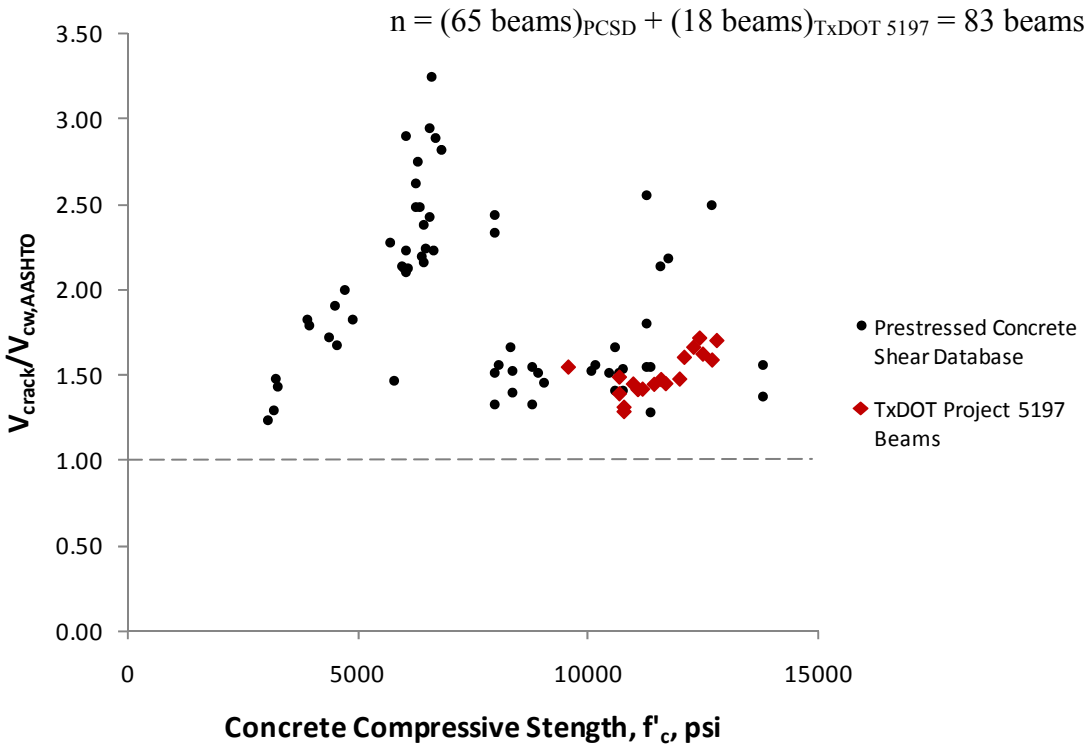

Figure 5.21 Ratio of Measured to Calculated Diagonal Cracking Shear, AASHTO LRFD (2007)

5.3.3 Measured and Calculated Shear Capacities

The ratio of the measured to calculated shear capacity is another important parameter in the study of the shear strength of prestressed concrete members (for the reasons previously discussed). By comparing the experimental and calculated shear capacities of all 18 test specimens, an opinion can be formed as to whether or not the maximum compressive stress in concrete at prestress transfer affects the ultimate shear strength of prestressed concrete members. Table 5.6 shows the ratio of measured to calculated shear capacity for test specimens and the ratios are plotted against the ratio of maximum compressive stress in concrete to compressive strength at prestress transfer in Figure 5.22 and Figure 5.23.

Table 5.6 Ratio of Measured to Calculated Shear Capacities

Fabricator	Specimen Designation	$V_{test}/V_{n,ACI}$	$V_{test}/V_{n,AASHTO}$
Fabricator B (Series 1)	CB-60-1	1.64	1.92
	CB-60-2	1.60	1.88
	CB-70-1	1.62	1.89
	CB-70-4	1.62	1.89
	CB-70-5	1.55	1.81
	CB-70-6	1.70	1.99
Fabricator C (Series 2)	CC-70-1	1.52	1.74
	CC-70-2	1.66	1.91
	CC-65-3	1.53	1.76
	CC-65-4	1.58	1.82
	CC-60-1	1.52	1.75
	CC-60-2	1.52	1.75
Fabricator D (Series 2)	CD-70-1	1.57	1.81
	CD-70-2	1.61	1.86
	CD-65-3	1.55	1.81
	CD-65-4	1.61	1.85
	CD-60-1	1.58	1.83
	CD-60-2	1.63	1.88
Statistics	Maximum	1.70	1.99
	Minimum	1.52	1.74
	Average	1.59	1.84
	Standard Dev.	0.05	0.07
	COV	0.03	0.04

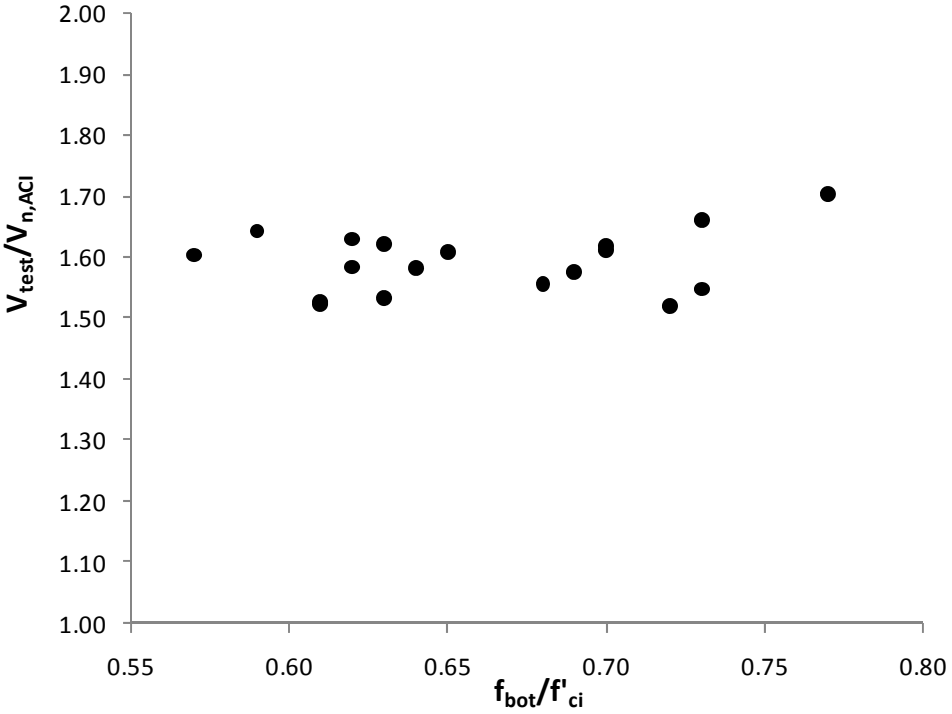

Figure 5.22 Ratio of Measured to Calculated Shear Capacity, ACI 318-08

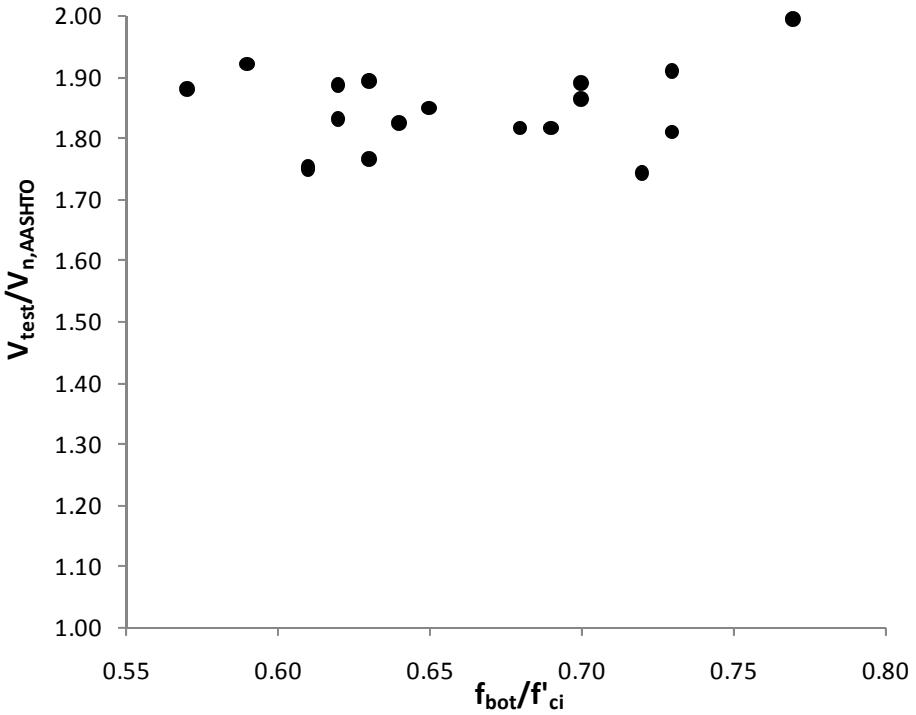

Figure 5.23 Ratio of Measured to Calculated Shear Capacity, AASHTO LRFD (2007)

As seen in Figure 5.22 and Figure 5.23, the shear capacity estimates from ACI 318-08 and AASHTO LRFD (2007) were conservative. When ACI 318-08 provisions were used to calculate shear capacity, the average ratio of experimental to calculated shear capacity for the 18 test specimens was 1.59. The maximum ratio obtained was 1.70 and the minimum was 1.52, resulting in a standard deviation of 0.05 and showing that the use of ACI 318-08 provisions resulted in fairly consistent estimates of shear capacity. Although these strength estimates can be viewed as overly-conservative it is important not to reach such conclusions prior to putting the data in context with the Prestressed Concrete Shear Database. When AASHTO LRFD (2007) provisions were used to calculate shear capacity, the average strength ratio was 1.84, showing that AASHTO LRFD (2007) provisions are even more conservative than ACI 318-08 provisions when estimating shear capacity. However, like ACI 318-08, the strength estimates were fairly consistent, with a maximum of 1.99 and a minimum of 1.74, yielding a standard deviation of 0.07.

Reasons for the inconsistencies between the two codes were previously discussed in depth in Chapter 2. Both specifications calculate the nominal shear capacity as the sum of the concrete and stirrup contributions. However, these components are calculated differently, as discussed in Sections 5.2.3 and 5.2.4. AASHTO LRFD (2007) provisions are more accurate for estimating shear carried by transverse reinforcement because the actual diagonal cracking angle is estimated, whereas the ACI 318-08 provisions assume a conservative diagonal cracking angle of 45 degrees. The angle of diagonal cracking estimated by AASHTO LRFD (2007) for the test specimens was 29 degrees (Appendix B) for both series of beams, which was a more accurate estimate of the actual diagonal crack angles (Section 5.3.5) than 45 degrees. The shear carried by the stirrups using AASHTO LRFD (2007) was 52.6 kips and the shear carried by the stirrups using ACI 318-08 was 32.4 kips ($V_{s,ACI} < V_{s,AASHTO}$). The ACI 318-08 equation for V_s proves to be more conservative than the AASHTO LRFD (2007) equation. However, since the V_{cw} equation in ACI 318-08 is more accurate than the V_{cw} equation in AASHTO LRFD

(2007) ($V_{cw,AASHTO} < V_{cw,ACI}$), as discussed in Section 5.3.2, AASHTO LRFD (2007) still produces more conservative estimates than ACI 318-08 for nominal shear capacity .

In order for an argument to be made that high stresses in concrete at prestress transfer negatively affect the shear capacity of prestressed concrete beams, a downward trend would have to be observed in Figure 5.22 and Figure 5.23. For a downward trend to exist, the ratios of measuredd to calculated shear capacity in the 0.60 range would have to be noticeably higher than ratios in the 0.70 range. By examining the data in plotted in Figure 5.22 and Figure 5.23, it is obvious that no such trends exist. Independent of the maximum compressive stress in concrete at prestress transfer, the ACI 318-08 and AASHTO LRFD (2007) provisions for the shear strength of prestressed concrete members are conservative.

When the data from the shear tests conducted under TxDOT Project 5197 are added to the 65 data points for web-shear failures obtained from the University of Texas Prestressed Concrete Shear Database (Section 2.4), the plots given in Figure 5.24 and Figure 5.25 are obtained. These figures show that the data from the current research study are in reasonable agreement with the historical data for ACI 318-08 and AASHTO LRFD (2007). In addition, Figure 5.24 and Figure 5.25 clearly indicate that the shear tests performed under TxDOT Project 5197 did not yield the low data points seen in the figures. This fact is important for two reasons. First, regardless of the different maximum compressive stresses used at prestress transfer, shear strengths of beams fabricated in three different precast plants were higher than most other beams tested in shear over the last 50 years. Second, code provisions should not be based on the results of one research study. Comprehensive databases should be used to calibrate or recalibrate code provisions. In this context, it can be seen that both design code provisions for nominal shear capacity ($V_n=V_c+V_s$) are reasonably conservative. ACI 318-08 provisions minimize scatter and reduce seemingly unnecessary conservatism. However, AASHTO LRFD (2007) provisions seem to have more conservatism than necessary.

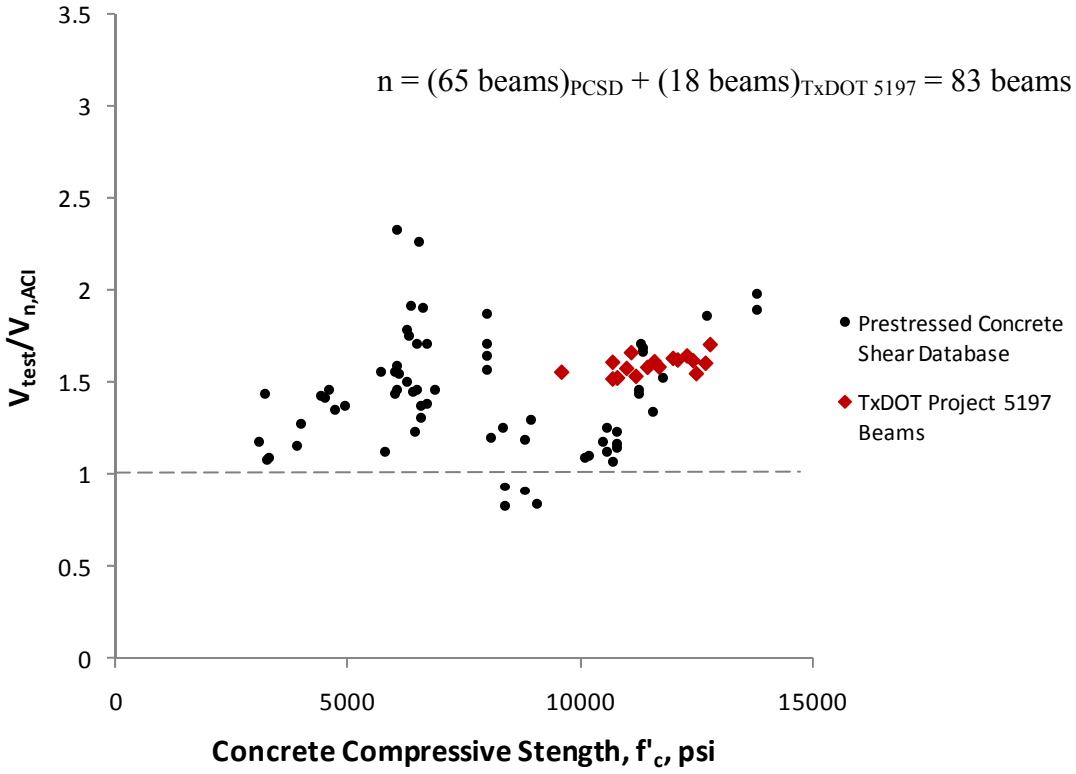

Figure 5.24 Ratio of Measured to Calculated Shear Capacity, ACI 318-08

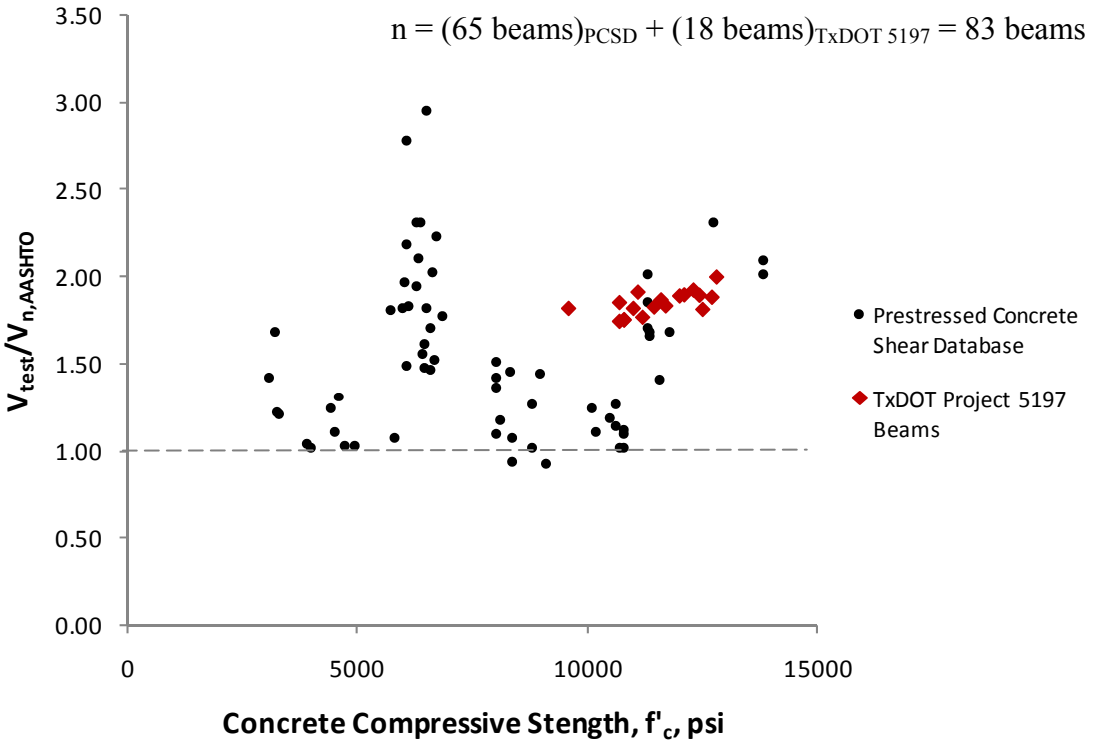

Figure 5.25 Ratio of Measured to Calculated Shear Capacity, AASHTO LRFD (2007)

5.3.4 Diagonal Crack Widths

For each shear test, the growth of the first diagonal crack was recorded and measured using a crack comparator card (Figure 5.2). Once the web-shear crack formed, the initial crack width (usually in the range of 0.007 to 0.013 inches) was immediately measured. From there, the crack width was measured at each load stage as discussed in Section 5.2.2. After the final load stage, it was deemed unsafe to stand next to the beam to measure crack widths. On average, crack widths were recorded at five different load stages for each beam and plotted in Figure 5.26 through Figure 5.28. The key given in Figure 5.14 is applicable to the three plots. Crack widths were measured to determine if there was any relationship in the diagonal crack widths to the ratio of maximum compressive stress in concrete to compressive strength at prestress transfer.

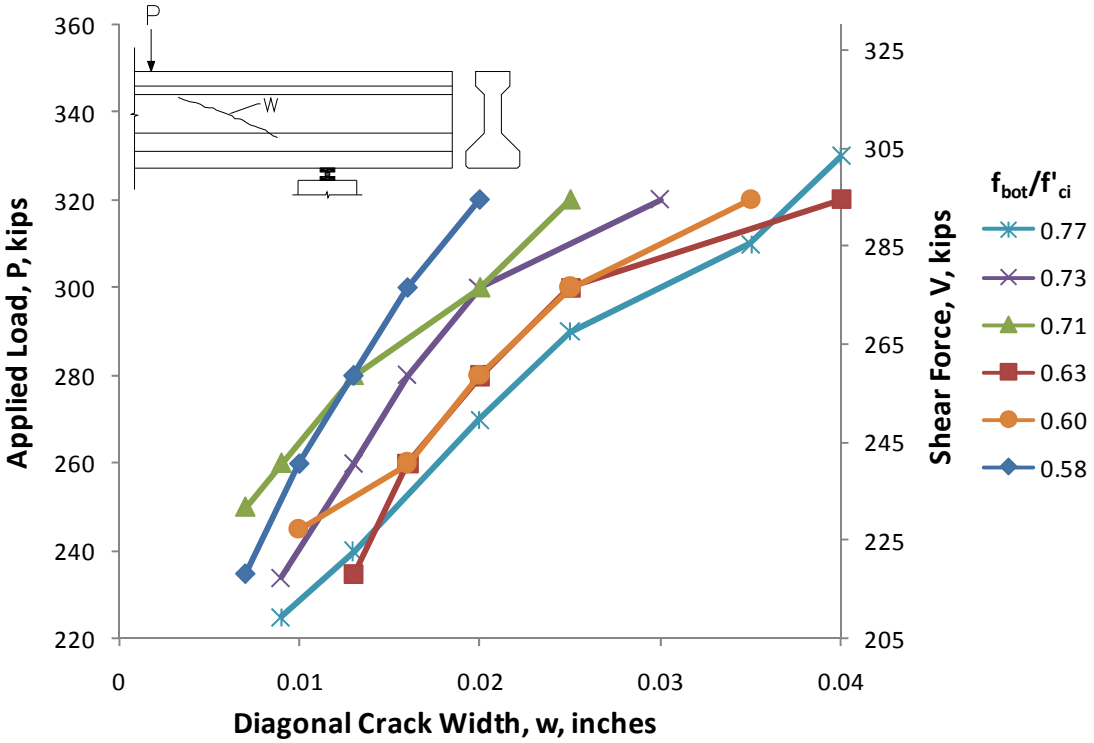

Figure 5.26 Crack Width Plots – Fabricator B

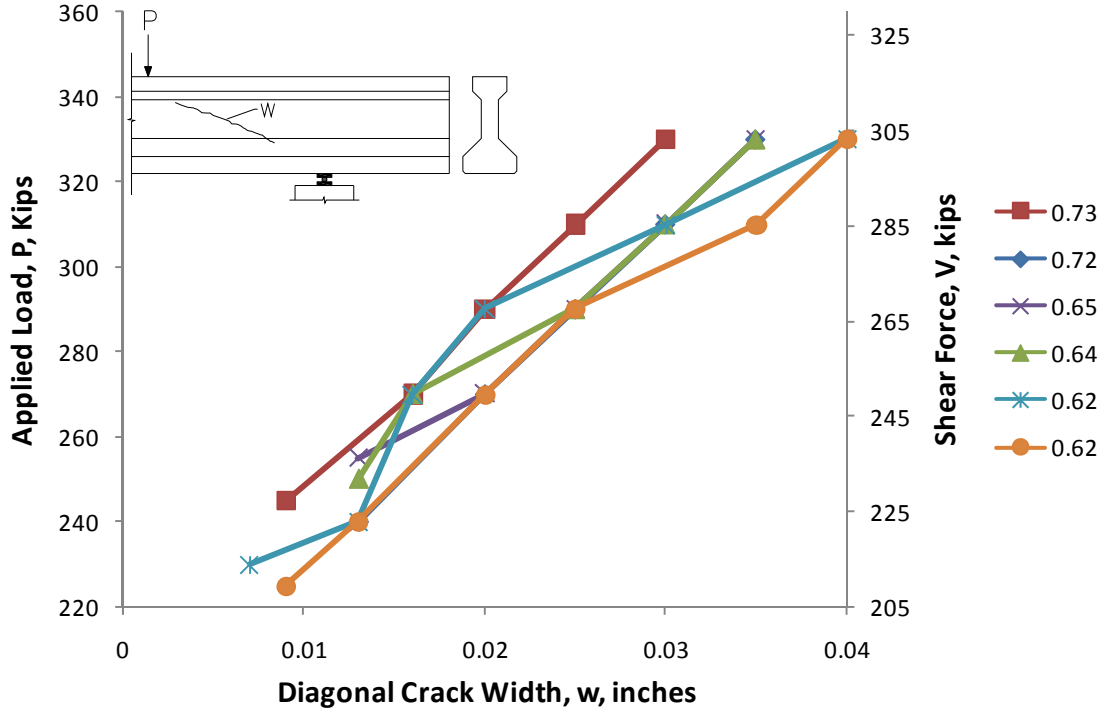

Figure 5.27 Crack Width Plots – Fabricator C

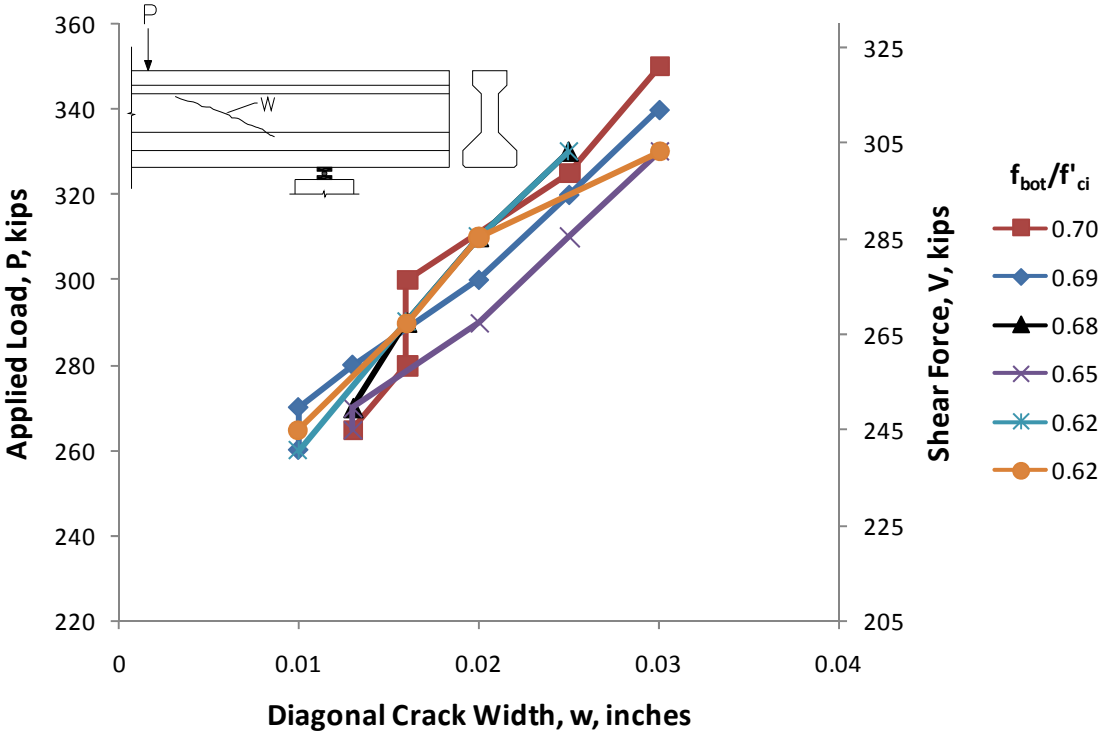

Figure 5.28 Crack Width Plots – Fabricator D

As can be observed in Figure 5.26 through Figure 5.28, there appears to be no obvious relationship between the diagonal crack width growth and the maximum compressive stress at prestress transfer. The data points in the above figures are connected by solid straight lines. If the lines did not cross and followed clear trends, it could be stated that there was a relationship between the two axes, but the lines cross each other too frequently to validate any argument for such a relationship. The above figures clearly show that releasing the stress in the strands early is not indicative of earlier or more severe diagonal web-shear cracking. Additionally, if the plots were normalized to show the ratio of diagonal cracking load to maximum applied load on the vertical axis, the same lack a of trend exists.

5.3.5 Inclination of Diagonal Cracks

The inclination of the diagonal web-shear crack of a prestressed concrete beam can be used to determine the number of stirrups that can be utilized to calculate V_s as per the AASHTO LRFD (2007) specifications. The inset diagrams in Figure 5.29 through Figure 5.31 show how the angle from the horizontal was measured. A smaller crack angle from the horizontal means that more stirrups may be utilized in calculating stirrup contribution to shear strength than a larger crack angle. In the case of this research study, shear reinforcement was spaced at 24 inches, thus making the effects of the crack angle somewhat insignificant because only two stirrups were located in the region between the point of the load and the support. Typical measured diagonal crack angles ranged from about 22 to 27 degrees. Since the angles measured were small and crossed two stirrups in all cases, both stirrups in the shear span were utilized in the tests. However, the stirrup contribution to shear strength from ACI 318-08 assumes a diagonal crack inclination of 45 degrees, which doesn't include two stirrups in the test specimens. The estimate of 29 degrees from AASHTO LRFD (2007) provides a more accurate crack angle, as discussed in Section 5.3.3. In contrast, the ACI 318-08 assumption of 45 degrees is more conservative than the diagonal crack inclination estimate of 29 degrees from AASHTO LRFD (2007). The variations in crack angle are plotted in Figure 5.29 through Figure 5.31.

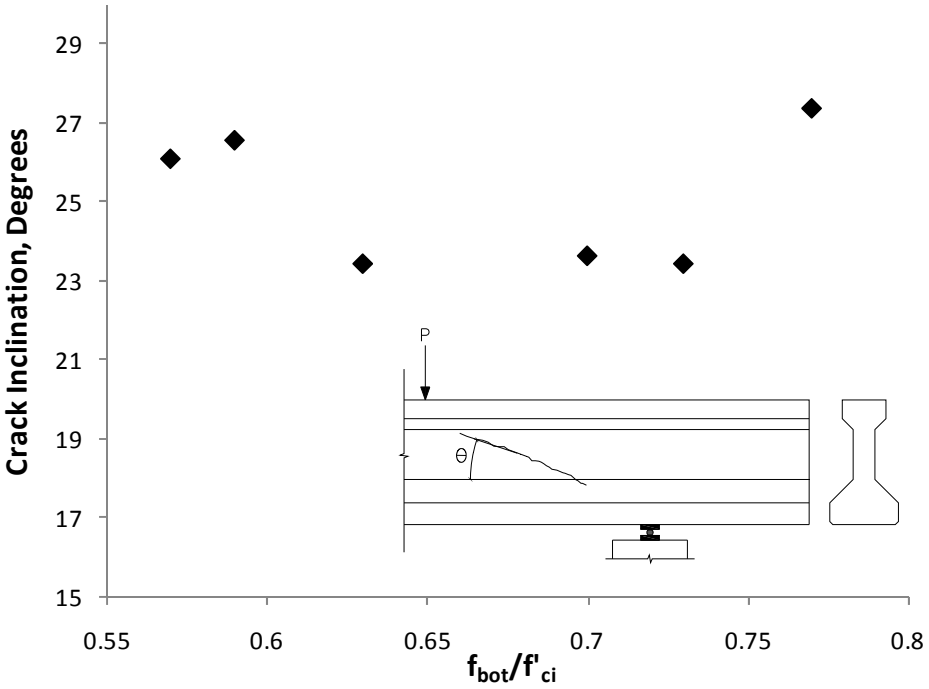

Figure 5.29 Crack Angle Plots – Fabricator B

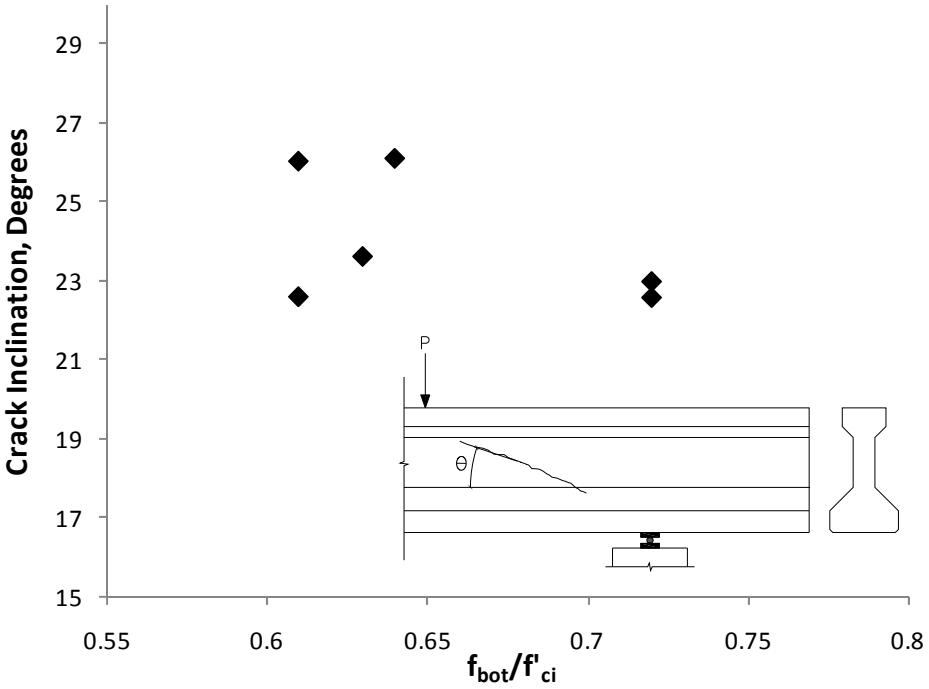

Figure 5.30 Crack Angle Plots – Fabricator C

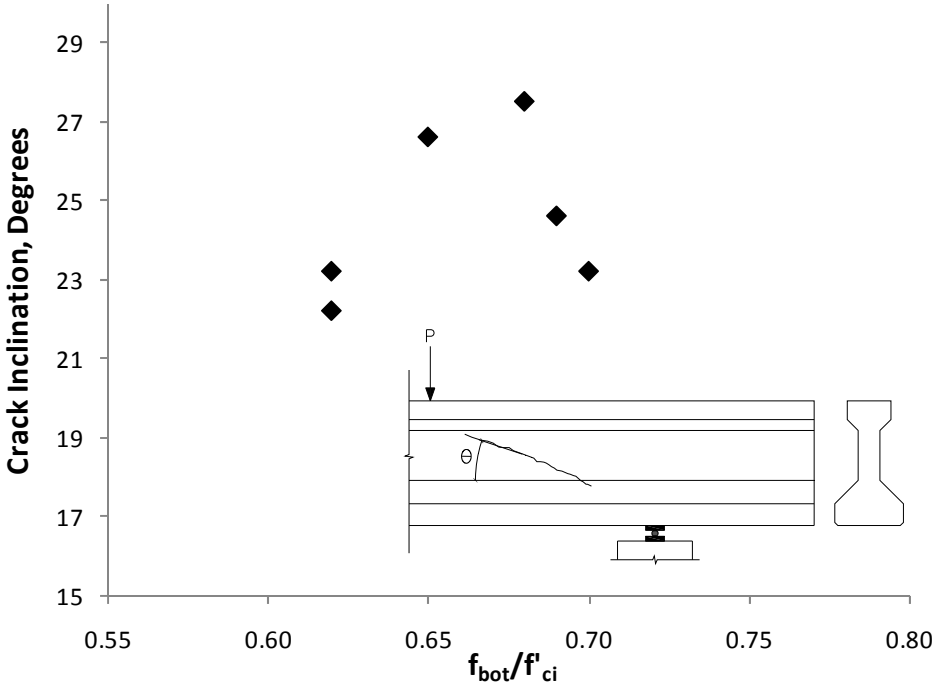

Figure 5.31 Crack Angle Plots – Fabricator D

The data in the above figures show that the maximum compressive stress in concrete at prestress transfer did not seem to have an effect on the diagonal cracking angle. Another important observation is that the use of AASHTO LRFD (2007) provisions in estimating the angle of diagonal cracking and the 45 degree assumption of ACI 318-08 were both conservative for all 18 shear tests regardless of the maximum compressive stress at release.

5.3.6 Coarse Aggregate Type

Series 2 beams were produced by fabricators C and D with the only difference in beam fabrication specifications being the type of coarse aggregate that was used in the concrete mixtures. Fabricator C used crushed limestone (CL) to produce Class H concrete (as per TxDOT Specifications) whereas Fabricator D used hard river gravel (HRG). Fabricator B also used hard river gravel to produce Series 1 beams.

When the average diagonal cracking loads of all test specimens are compared, there exists a difference between the behavior of beams fabricated with concrete made with the different coarse aggregates types. The first diagonal cracking shears of all test specimens were normalized with respect to the web-shear cracking expressions of ACI 318-08 and AASHTO LRFD (2007) and presented in Figure 5.32 and Figure 5.33. As can be observed in these plots, for comparable levels of maximum compressive stress at prestress transfer, beams made with concrete containing crushed limestone cracked under slightly lower shear forces than beams made with concrete containing hard river gravel. In addition, two of the beams fabricated with crushed limestone as the coarse aggregate failed to give conservative results for diagonal cracking shears. The average ratios of measured to estimated diagonal cracking shear are shown in Table 5.7 separated by coarse aggregate type.

Similarly, the normalized nominal shear capacities of all test specimens are given in Figure 5.34 and Figure 5.35. As seen in these plots, there is still a noticeable difference between the data from two types of coarse aggregate, but the disparity is somewhat reduced. Nevertheless, beams made with concrete containing hard river gravel displayed greater shear strengths than their crushed limestone counterparts. However, all shear capacities were conservatively estimated using ACI 318-08 and AASHTO LRFD (2007) shear design provisions. Lastly, it is important to recognize that for both coarse aggregate types there are no discernable negative impacts of increasing the allowable compressive stress at prestress transfer. The average ratios of measured to estimated shear capacity are also shown in Table 5.7.

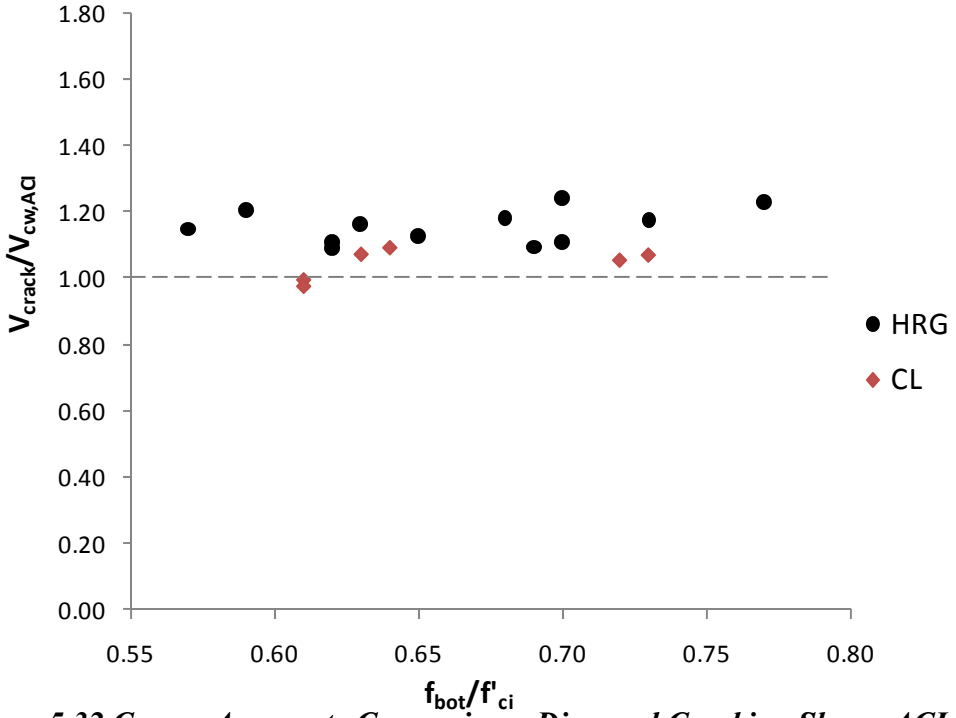

Figure 5.32 Coarse Aggregate Comparison: Diagonal Cracking Shear, ACI 318-08

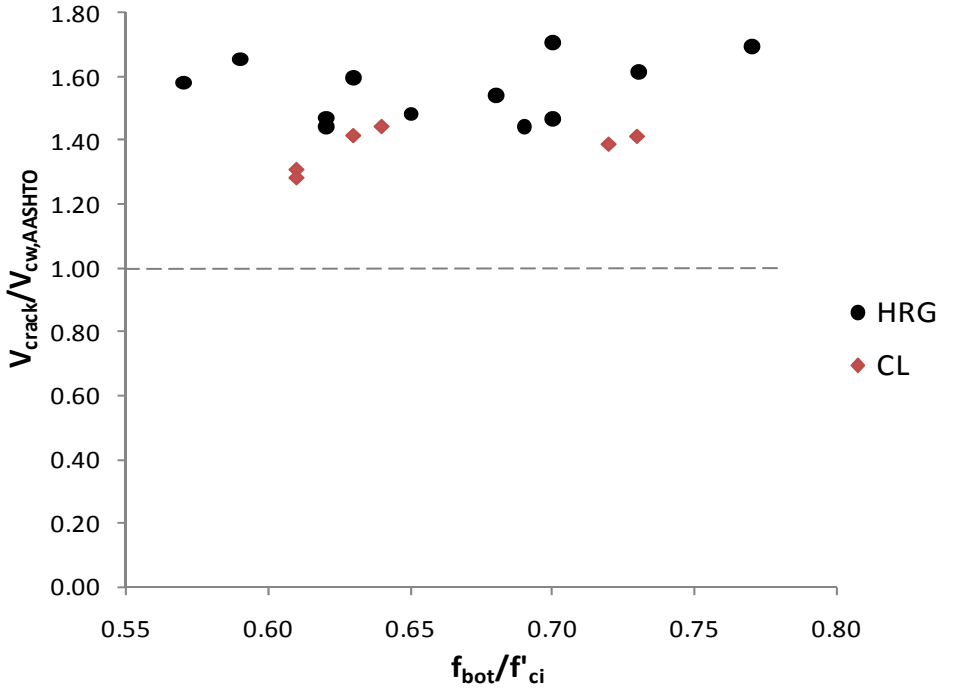

Figure 5.33 Coarse Aggregate Comparison: Diagonal Cracking Shear, AASHTO LRFD (2007)

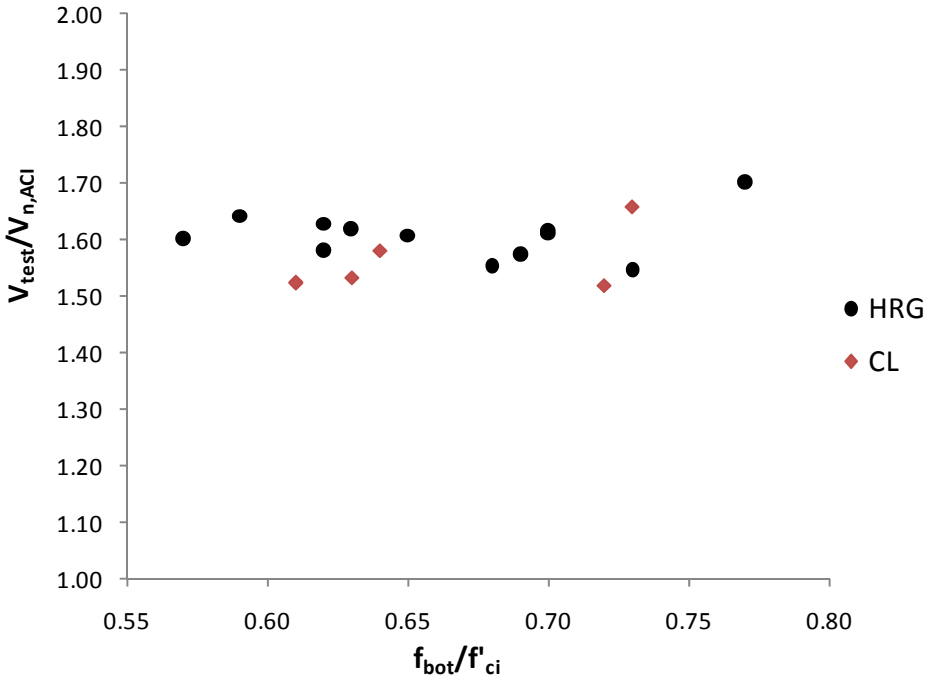

Figure 5.34 Coarse Aggregate Comparison: Shear Capacity, ACI 318-08

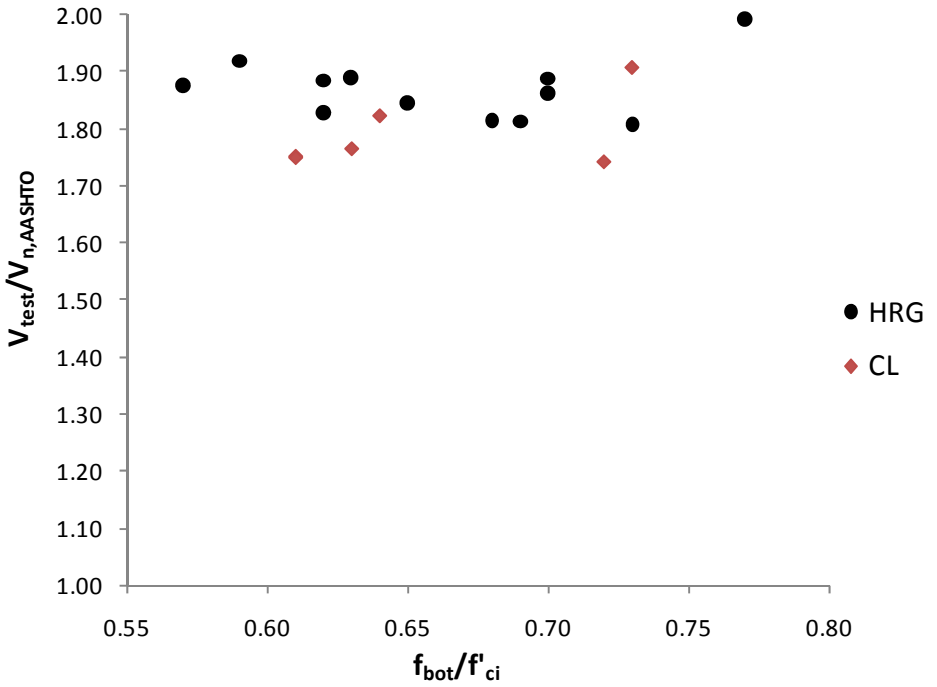

Figure 5.35 Coarse Aggregate Comparison: Shear Capacity, AASHTO LRFD (2007)

Table 5.7 Comparison Between Coarse Aggregate Types

Coarse Aggregate	Average Diagonal Cracking Shear Ratio		Average Shear Strength Ratio	
	$V_{crack}/V_{cw,ACI}$	$V_{crack}/V_{cw,AASHTO}$	$V_{test}/V_{n,ACI}$	$V_{test}/V_{n,AASHTO}$
Crushed Limestone	1.04	1.38	1.56	1.79
Hard River Gravel	1.15	1.56	1.61	1.87

5.4 SUMMARY

As part of the experimental investigation summarized in this thesis, 18 TxDOT C-beams were tested in shear. The purpose of the tests was to evaluate the impact of increasing the allowable compressive stress at prestress transfer on the performance of prestressed concrete members in shear. All 18 beams experienced diagonal web-shear cracking before any flexural cracks formed and subsequently failed in shear. The diagonal cracking shears and shear capacities were estimated using the shear design provisions of ACI 318-08 and the AASHTO LRFD (2007) simplified procedure. Of the 18 beams tested, nine failed due to diagonal tension and nine failed due to web crushing.

The results of the tests indicate that higher allowable compressive stresses at release had no negative effect on the initial diagonal cracking shears or shear capacities of the prestressed concrete beams tested. ACI 318-08 and AASHTO LRFD (2007) equations for nominal shear strength were both conservative for members subjected to compressive stresses at release greater than the current allowable limit. ACI 318-08 provisions were found to be more accurate in estimating diagonal cracking shears and shear capacities than AASHTO LRFD (2007). In addition, ACI 318-08 provisions appeared to be sufficiently conservative and AASHTO LRFD (2007) provisions were more conservative. Lastly, the beams fabricated with hard river gravel as the coarse aggregate proved to be slightly stronger in shear than the beams fabricated with crushed limestone.

CHAPTER 6
Summary, Conclusions, and Recommendations

6.1 SUMMARY OF THE RESEARCH PROGRAM

This research study was conducted at the Phil M. Ferguson Structural Engineering Laboratory at the University of Texas at Austin to investigate the effects of increasing the allowable compressive stress in concrete at prestress transfer on the shear performance of prestressed concrete beams. The study was a continuation of previous research conducted at the University of Texas that looked into the effects of high compressive stresses in concrete at release on the flexural performance of prestressed concrete beams (Phase I of TxDOT Project 5197). The currenty study (Phase II) was initiated based on the recommendations of Birrcher and Bayrak (2007).

A comprehensive study of literature dedicated to prestressed concrete shear research revealed that release stresses at prestress transfer had not been studied by previous researchers. To investigate the issue, beams fabricated for this research project were subjected to compressive stresses in excess of the allowable compressive stress limit of $0.60f'_{ci}$ in AASHTO LRFD (2007).

In Phase II of the research project, 45 TxDOT Type-C beams were fabricated. In the shear performance evaluation, 18 of the C-beams were tested at a shear span of six feet (a/d = 2.22) in a test setup designed to create a web-shear failure of the test specimens. The beams were fabricated by three different precast plants in Texas and featured maximum compressive stresses at release ranging from $0.57f'_{ci}$ to $0.77f'_{ci}$. The diagonal cracking shears and shear capacities were estimated using the shear deigns provisions of ACI 318-08 and the AASHTO LRFD (2007) simplified procedure. The actual diagonal cracking shears and shear capacities were experimentally evaluated. For all beams, the measured diagonal cracking shears and shear capacities were compared to their estimated quantities to evaluate the feasibility of raising the allowable compressive

stress at release from $0.60f'_{ci}$ to $0.65f'_{ci}$ or $0.70f'_{ci}$. The results of the shear tests indicated that the compressive stress in concrete at prestress transfer had no negative effect on diagonal cracking shears or shear capacities. The ACI 318-08 provision for V_{cw} proved to be accurate and conservative whereas the AASHTO LRFD (2007) provision tended to underestimate the diagonal cracking shear substantially in some cases. In addition, ACI 318-08 and AASHTO LRFD (2007) equations for nominal shear capacity were both conservative for the beams tested in shear.

6.2 CONCLUSIONS AND RECOMMENDATIONS

The impact of increasing the allowable compressive stress at release on the shear performance of prestressed concrete girders was evaluated in the current study. The conclusions and recommendations of the current study in regards to this aspect of prestressed concrete member behavior are discussed herein. Unless otherwise noted, the following conclusions are based solely from the experimental data of the current study:

1) The ACI 318-08 equation for web-shear cracking strength proved to be accurate and conservative for beams subjected to maximum compressive stresses at release in excess of the current allowable limit. On the other hand, the AASHTO LRFD (2007) equation for V_{cw} proved to be somewhat over-conservative for all beams tested. The compressive stress in concrete at release also had no effect on the inclination or width of the diagonal cracks, and as such, they did not influence the accuracy or conservativeness of the V_{cw} expressions in estimating diagonal cracking shears.
2) Shear failure of all beams tested occurred in the form of diagonal tension or web crushing, which are both viewed as web-shear failures. All beams fabricated with crushed limestone as the coarse aggregate failed by web crushing, along with three of the beams fabricated with hard river gravel as the coarse aggregate. Nine beams fabricated with hard river gravel failed in diagonal tension. The mode of failure was affected by the coarse aggregate type, but not by the maximum compressive stresses in concrete at release. In

general, the beams fabricated with hard river gravel were capable of carrying higher loads than the beams fabricated with crushed limestone, but the ACI 318-08 and AASHTO LRFD (2007) shear design provisions for nominal shear strength were conservative in estimating the shear strength of beams fabricated with both types of aggregates. In addition, no adverse effects of subjecting the beams to maximum compressive stresses in excess of $0.60f'_{ci}$ was encountered.

3) Based on the experimental results reported in this thesis, an increase in the allowable maximum compressive stress in concrete in the end regions of prestressed concrete beams at prestress transfer to $0.65f'_{ci}$ or $0.70f'_{ci}$ can be justified.

6.3 RECOMMENDATIONS FOR FUTURE WORK

In regards to determining the shear capacity of prestressed concrete members, additional testing should be carried out on beams released after the current allowable limit with different cross sections, such as box beams, to confirm the findings of this research project.

APPENDIX A
Bursting Cracks in End Regions

Cracks forming from bursting, spalling, and splitting stresses in the end regions were monitored for all 45 C-beams fabricated in Phase II of the research study. These cracks are referred to as "bursting cracks" in this thesis to study the cracking in the end regions. Bursting cracks were present at both ends of the beams and were mapped on the beams with a black marker. The maximum width of each individual bursting crack was measured with a crack comparator card (as described in Chapter 4 and Chapter 5) and recorded. The maximum crack width usually did not exceed 0.005 inches. If the crack was too small to call 0.005 inches, it was labeled as "hairline," since the smallest denomination of crack width on the crack comparator card was 0.005 inches. Each side of each end of the beam was photographed for all 45 beams, leading to 180 photographs (45 specimens x 2 ends x 2 sides). The crack locations, lengths, and widths from the photographs were then used to produce drawings of the end regions. The crack maps for each beam are shown in this appendix.

Similarities in bursting crack lengths, widths, and patterns were shown between beams of the same series. The bursting cracks were dependent upon the amount of prestressing force. Series 2 beams, which featured 10 more strands and higher prestressing forces than Series 1 beams, typically had wider bursting cracks. The locations of the bursting cracks also changed by prestressing force. Bursting cracks in Series 1 beams (fabricators A and B) had distinctly different locations than bursting cracks in Series 2 beams (fabricators C and D), as seen in the crack maps that follow. The coarse aggregate type had no visible effect on the bursting cracks. In addition, the maximum compressive stress at release also had no visible effects on the bursting cracks. The beams released at high compressive release stresses did not have distinctly different bursting crack characteristics as beams released at lower stresses. As such, the drawings

that follow indicate that the bursting crack lengths, widths, and patterns of the C-beam specimens analyzed were not affected by the allowable compressive stress in concrete at release. Figure A.1 below provides a key to the figures that follow.

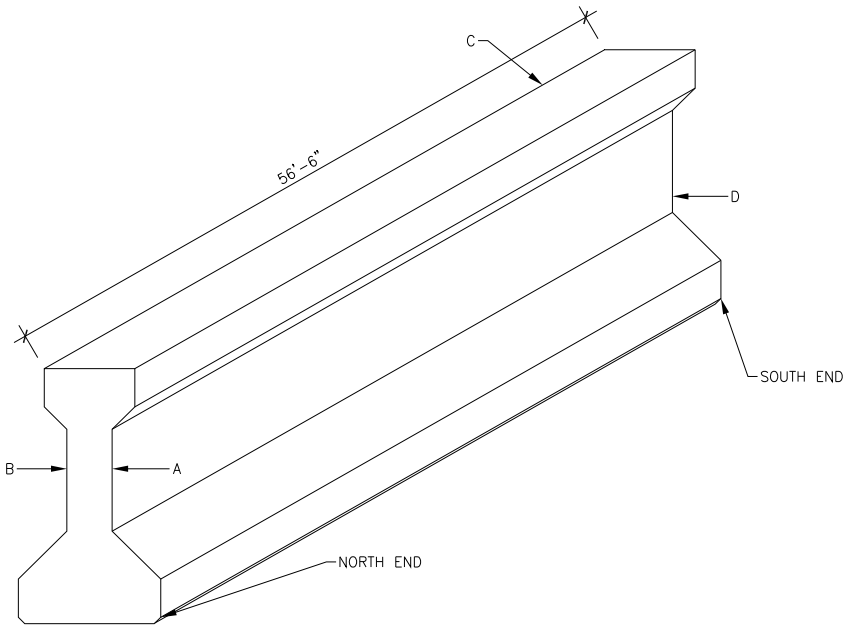

Figure A.1 Bursting Crack Location Key

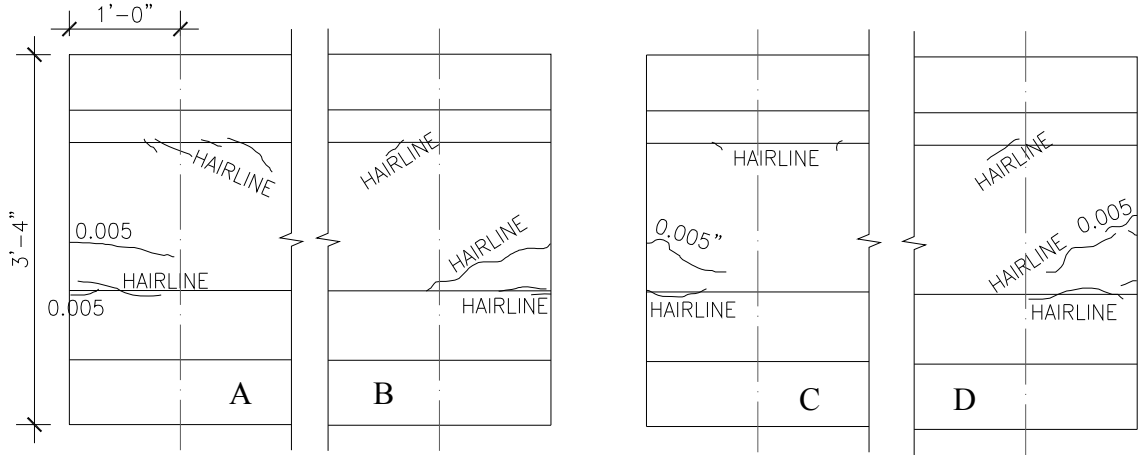

North End South End

Fabricator A – Specimen CA-70-1

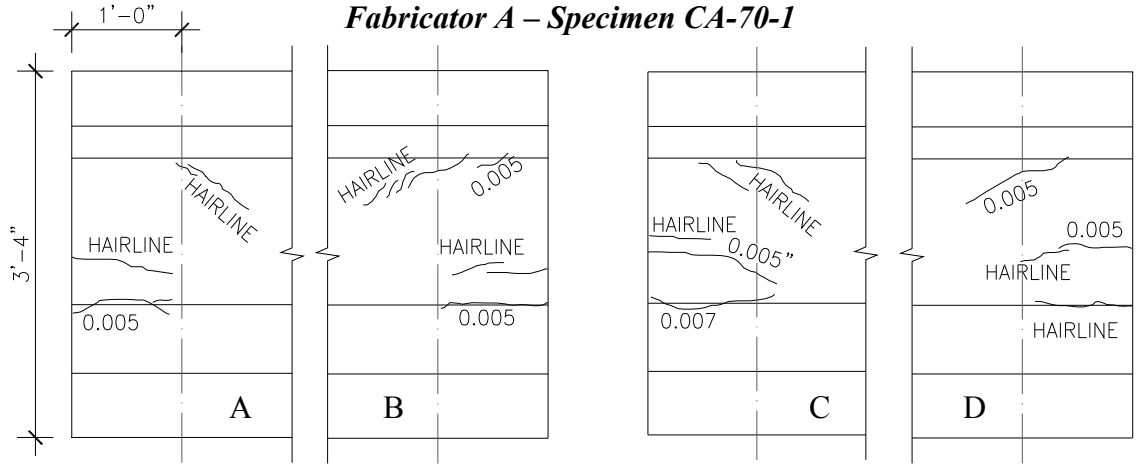

North End South End

Fabricator A – Specimen CA-70-2

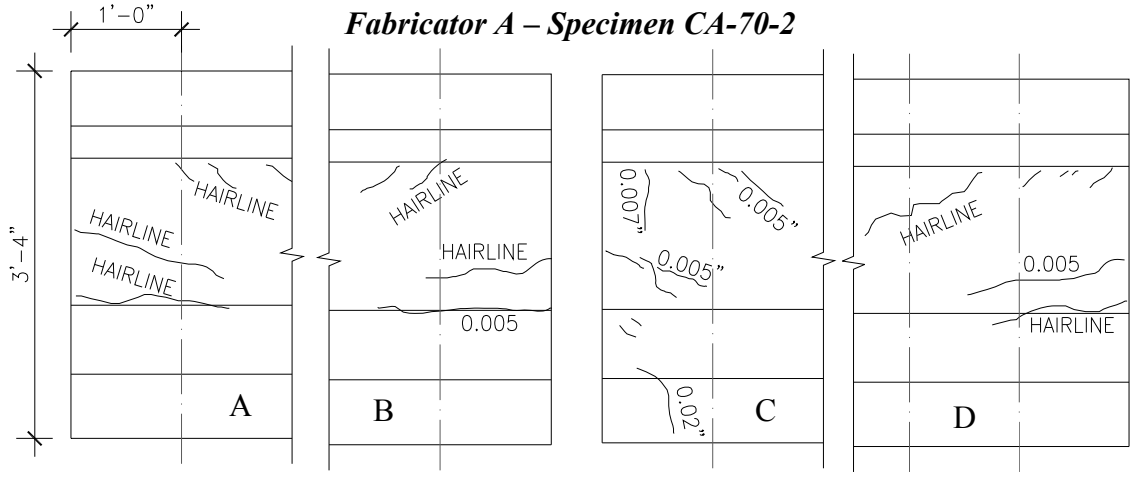

North End South End

Fabricator A – Specimen CA-70-3

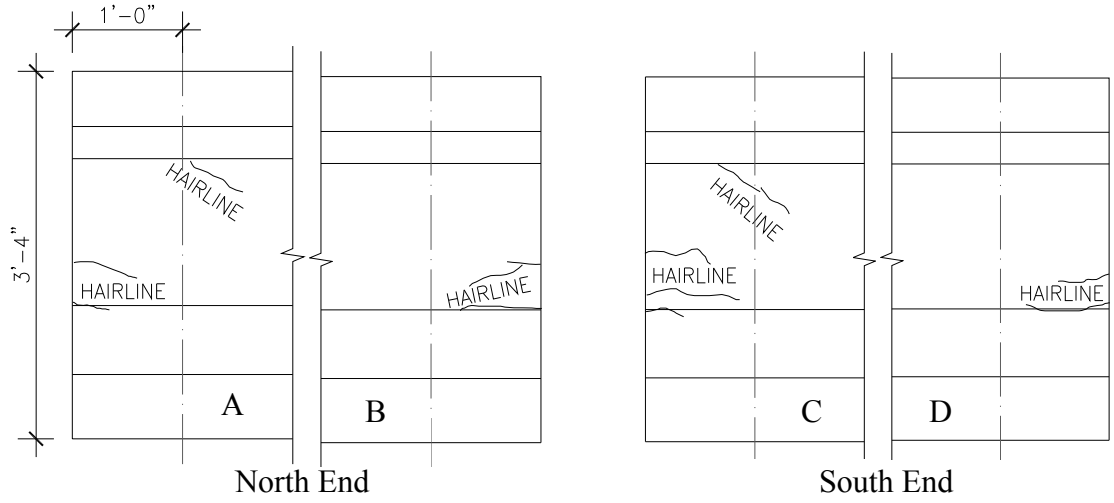

Fabricator A – Specimen CA-65-1

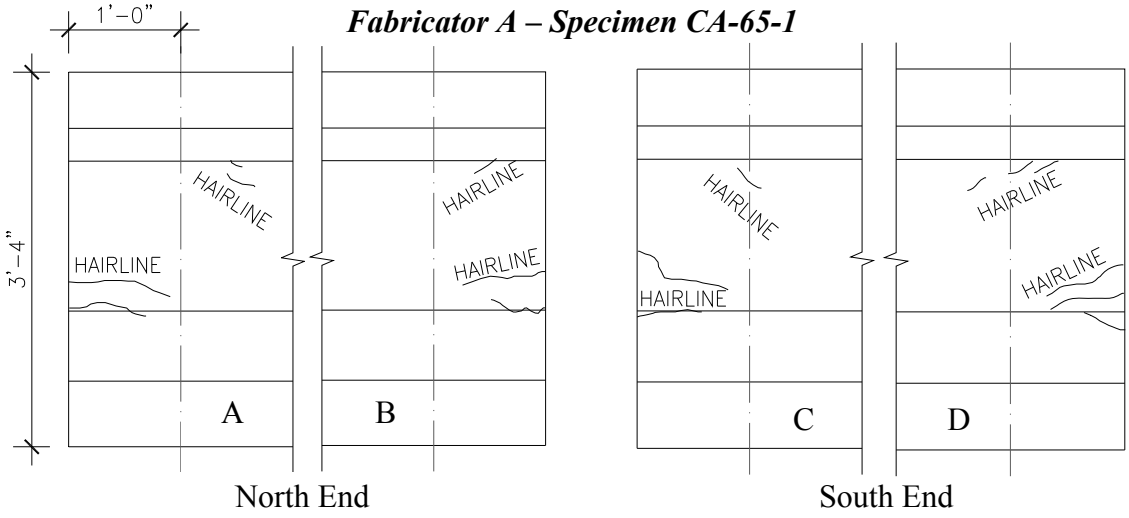

Fabricator A – Specimen CA-65-2

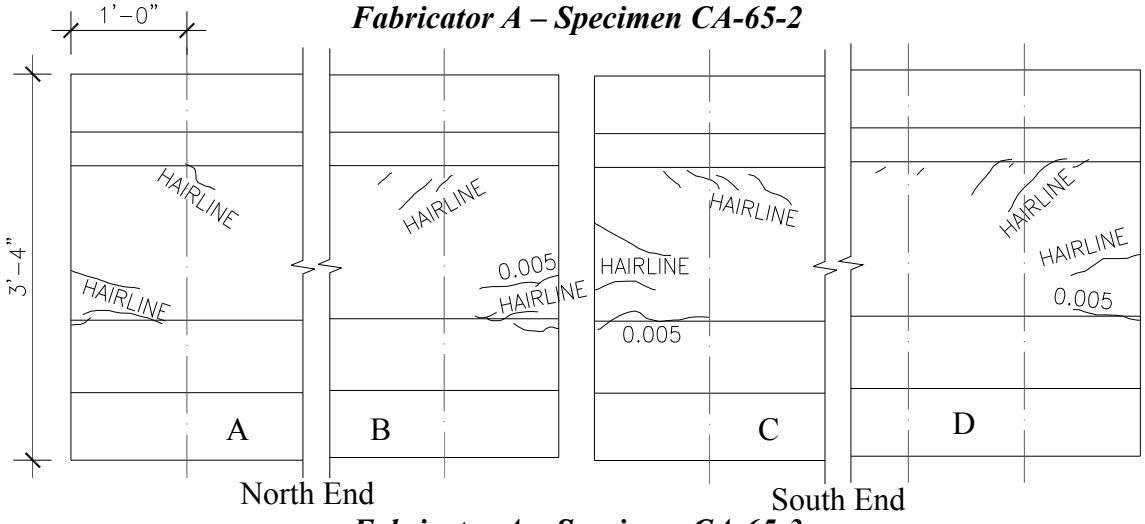

Fabricator A – Specimen CA-65-3

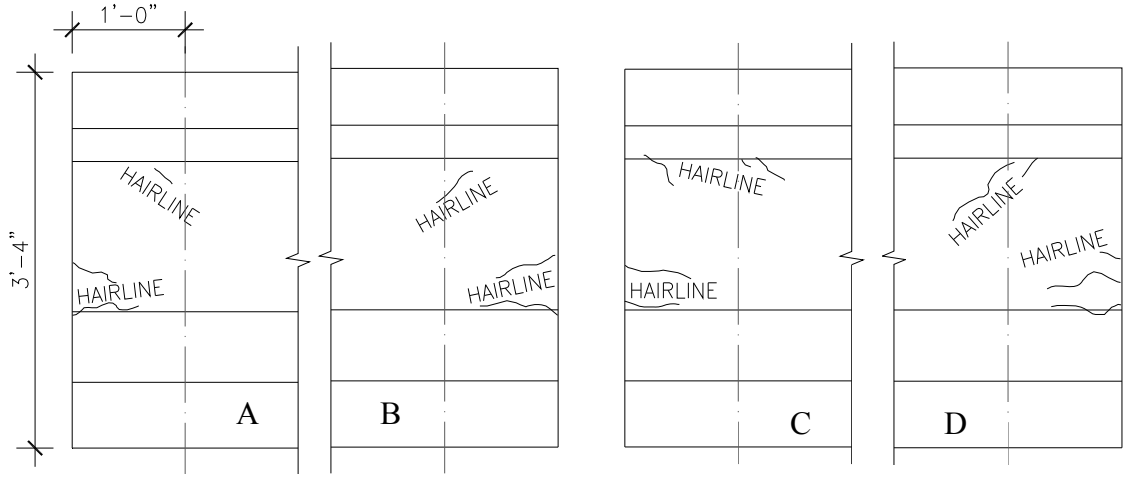

Fabricator A – Specimen CA-65-4

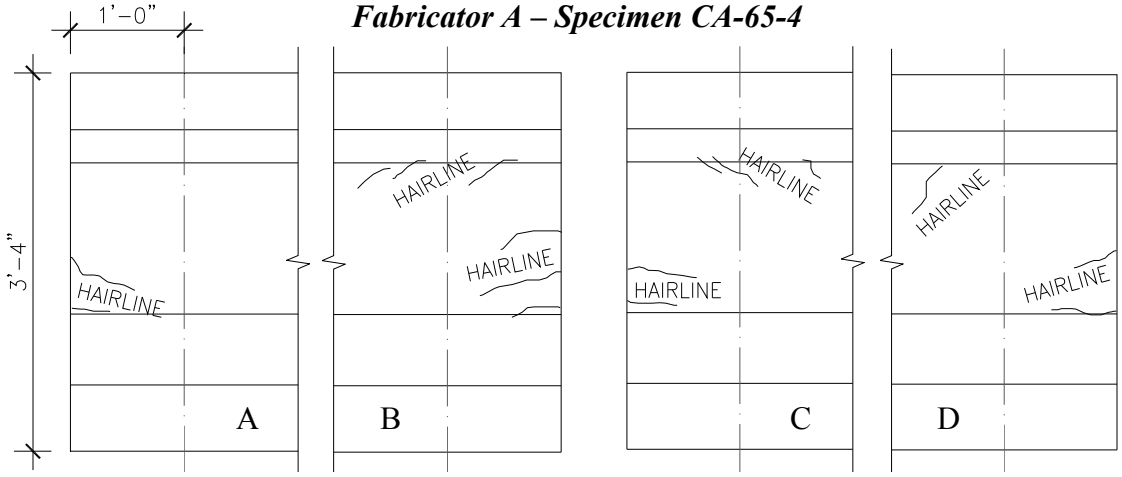

Fabricator A – Specimen CA-65-5

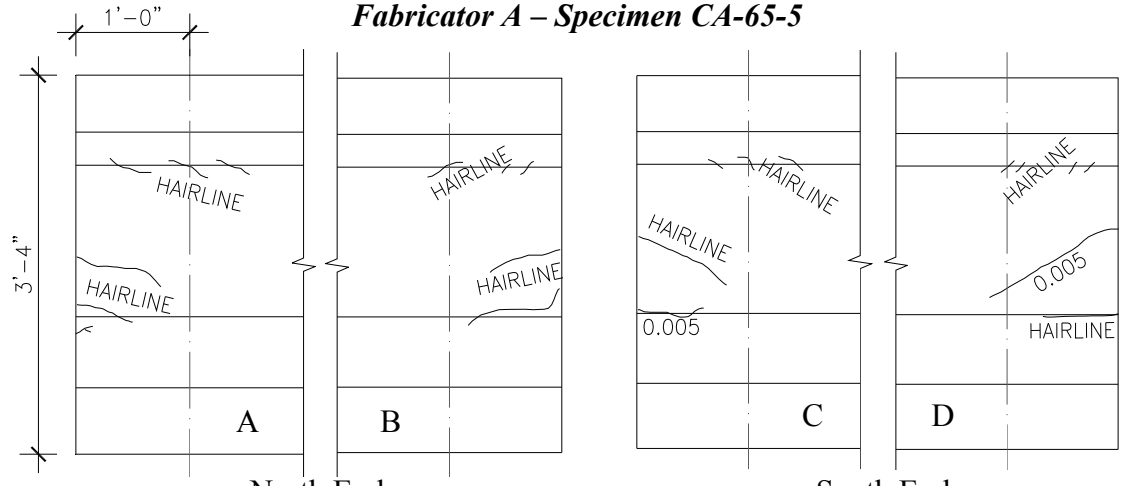

Fabricator A – Specimen CA-65-6

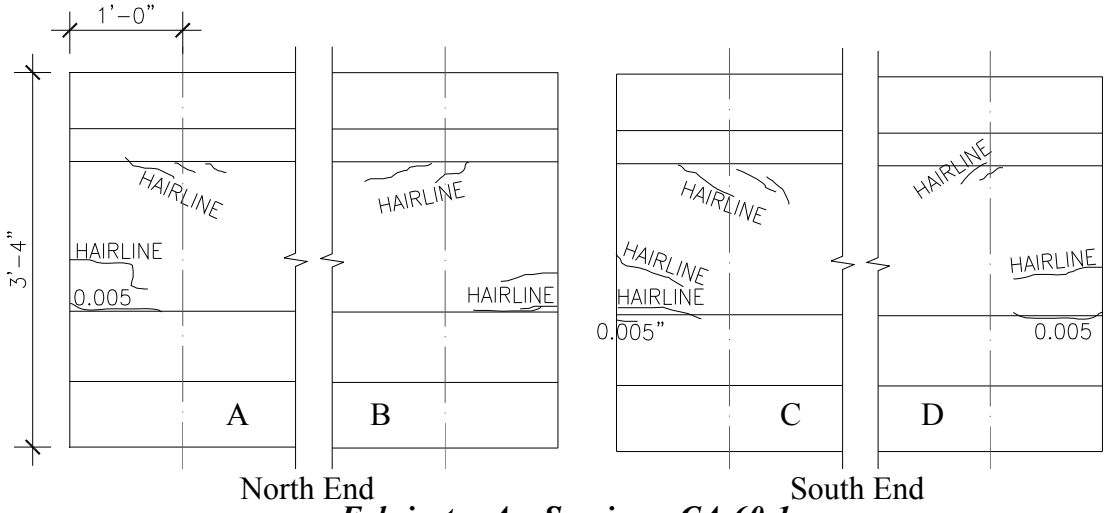

Fabricator A – Specimen CA-60-1

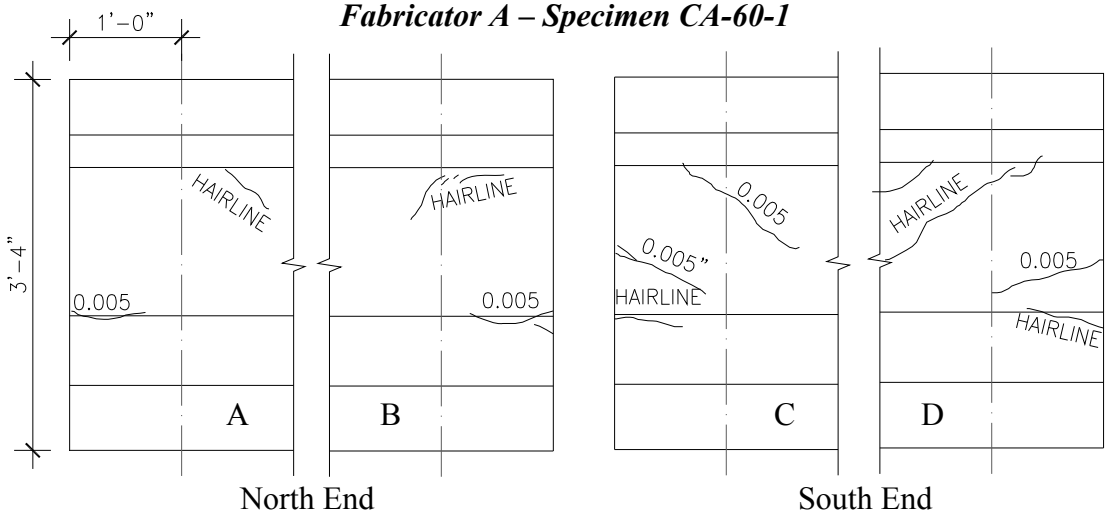

Fabricator A – Specimen CA-60-2

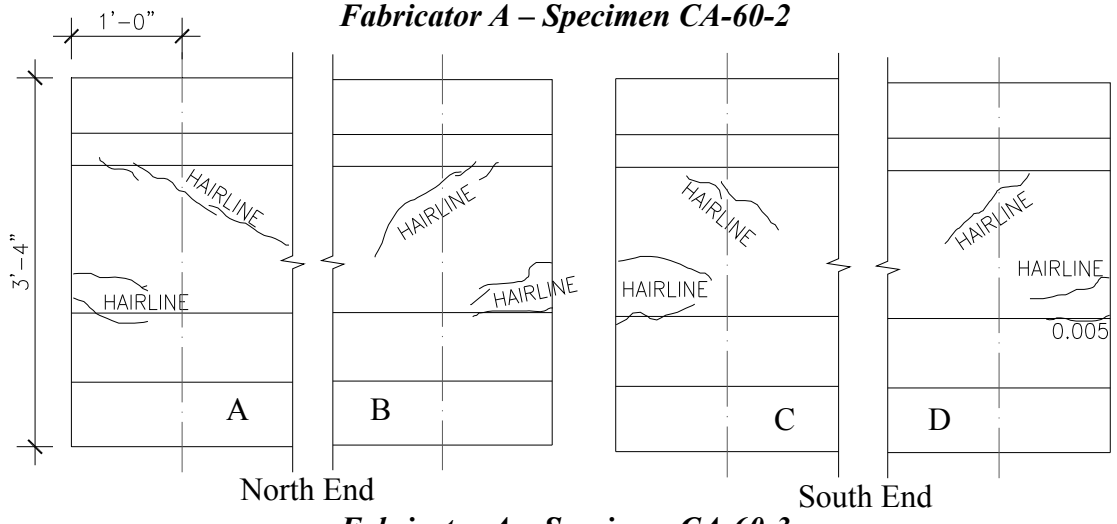

Fabricator A – Specimen CA-60-3

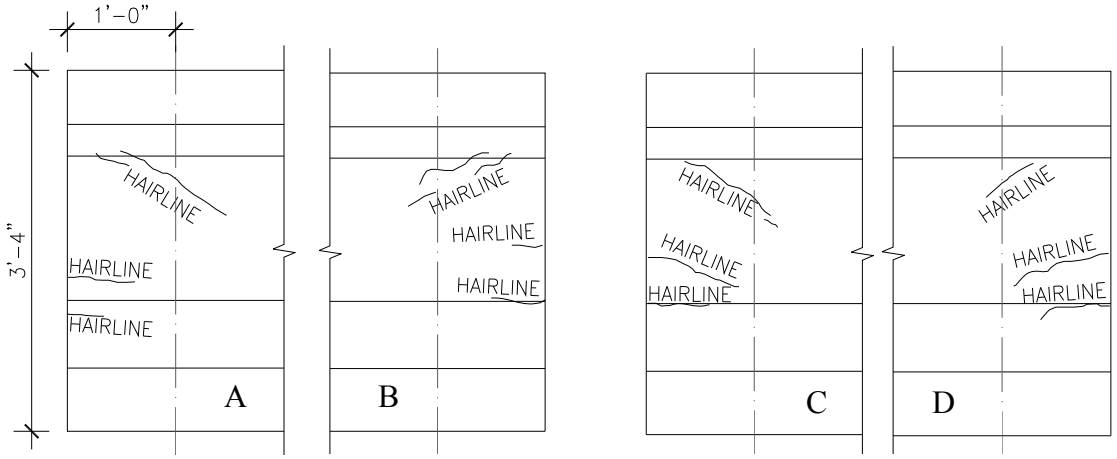

Fabricator B – Specimen CB-70-1

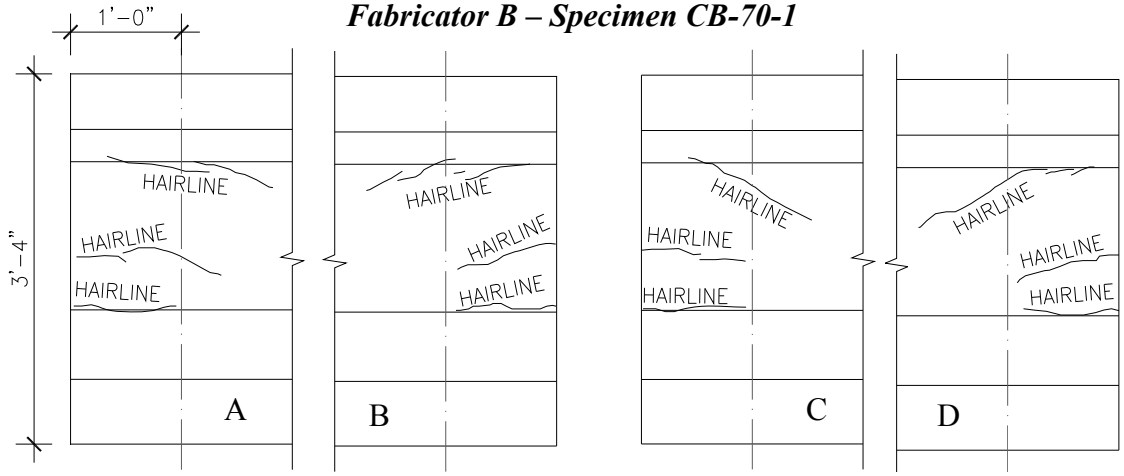

Fabricator B – Specimen CB-70-2

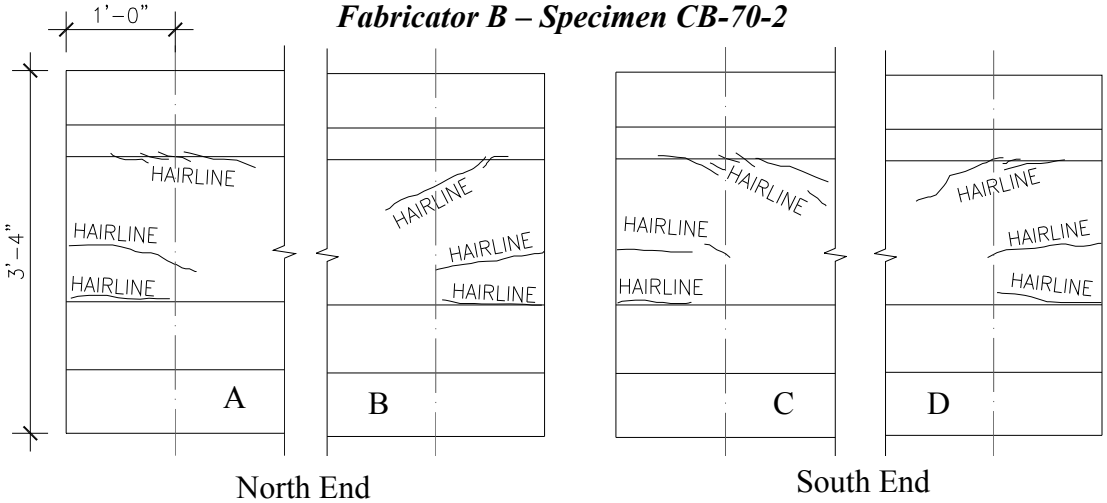

Fabricator B – Specimen CB-70-3

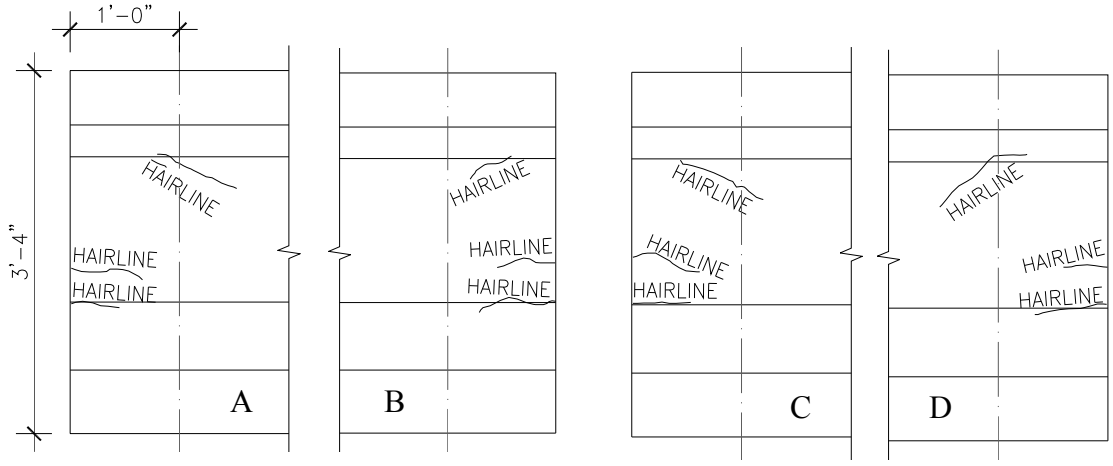

Fabricator B – Specimen CB-70-4

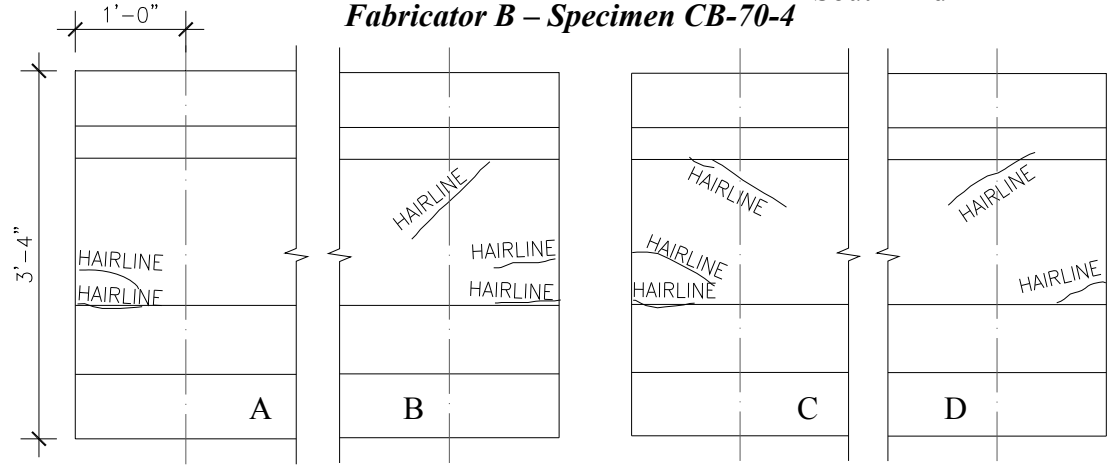

Fabricator B – Specimen CB-70-5

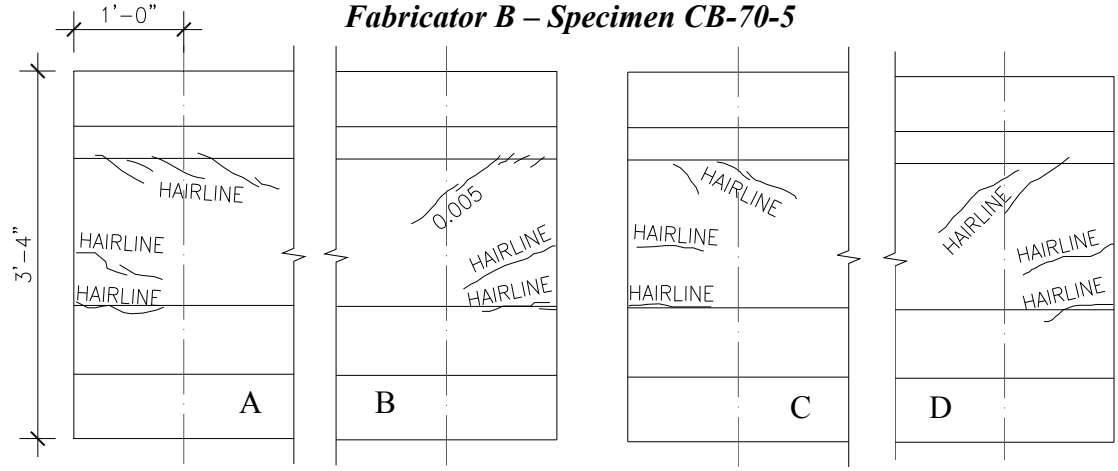

Fabricator B – Specimen CB-70-6

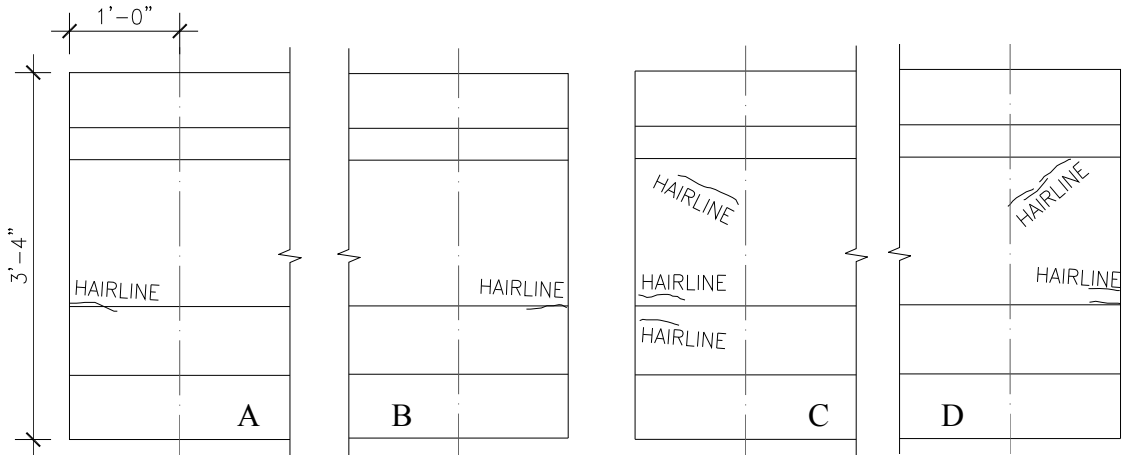

Fabricator B – Specimen CB-60-1

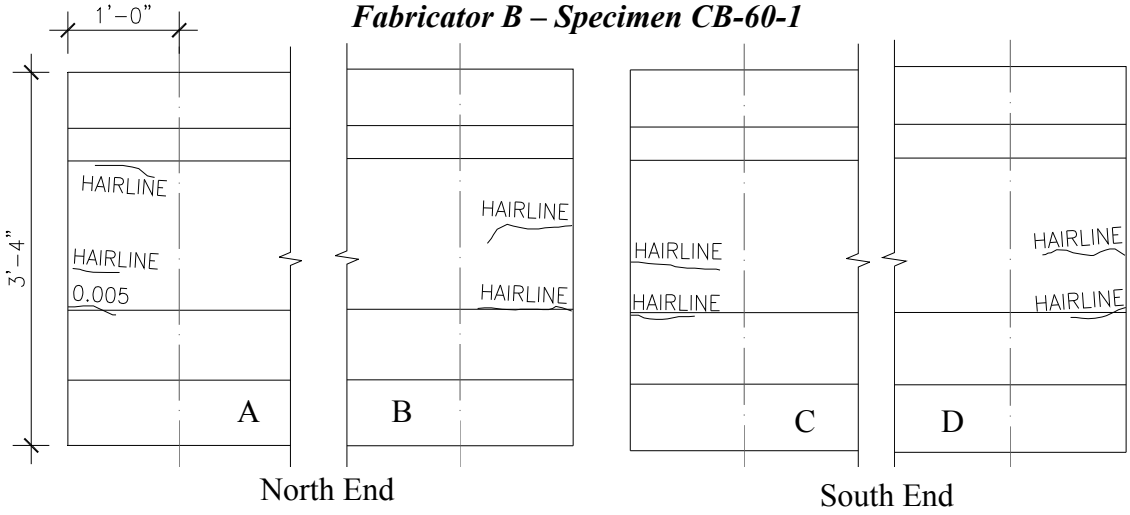

Fabricator B – Specimen CB-60-2

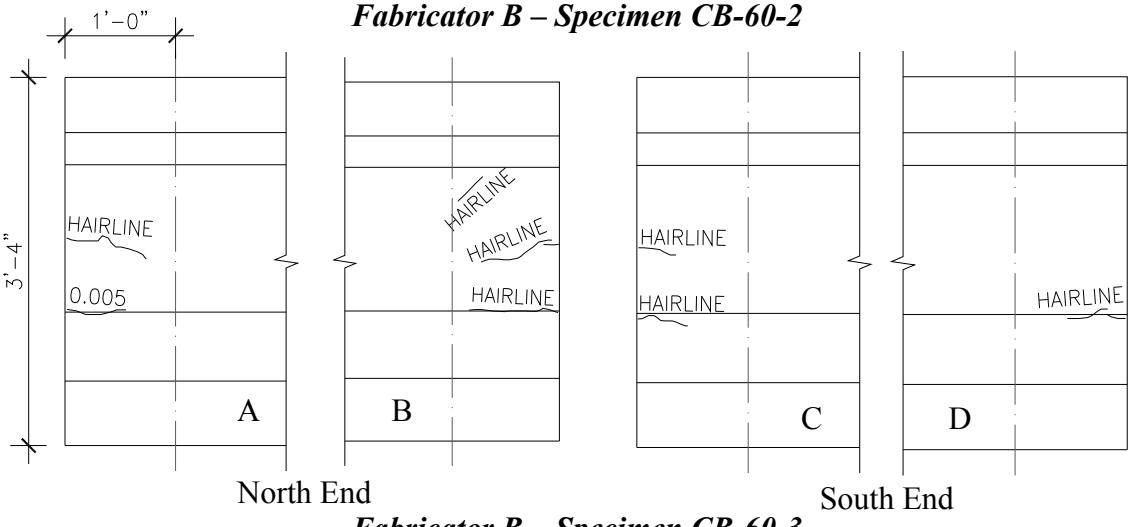

Fabricator B – Specimen CB-60-3

Fabricator C – Specimen CC-70-1

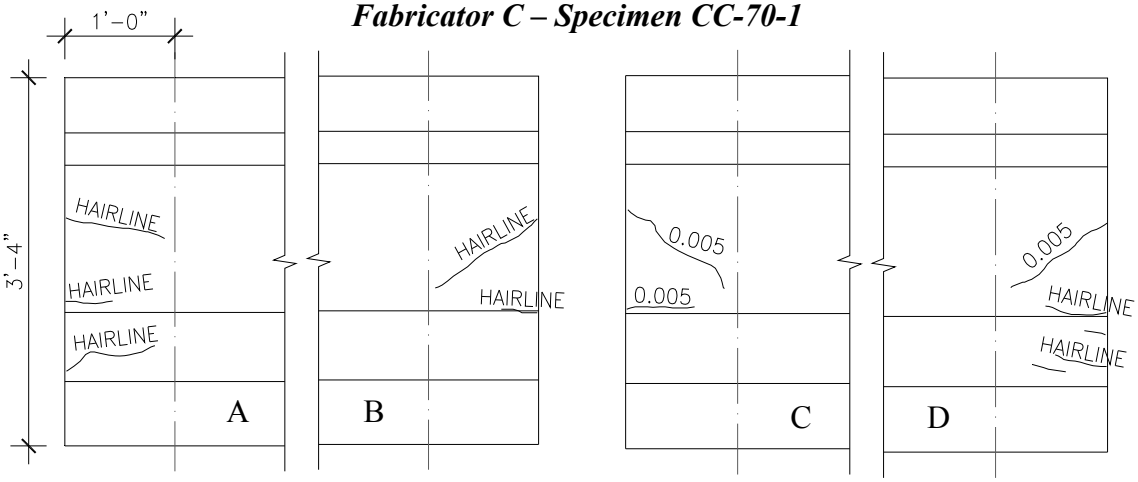

Fabricator C – Specimen CC-70-2

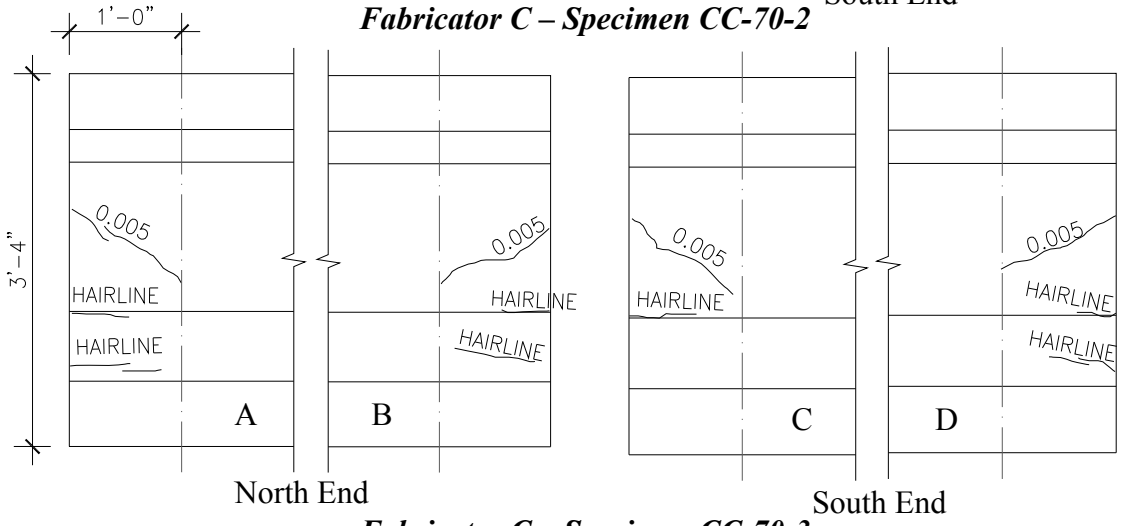

Fabricator C – Specimen CC-70-3

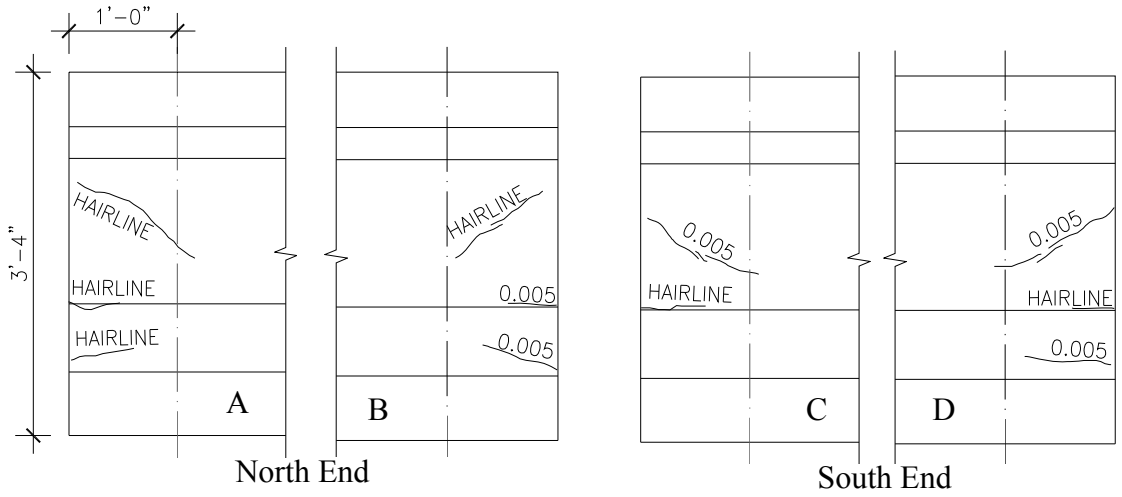

Fabricator C – Specimen CC-65-1

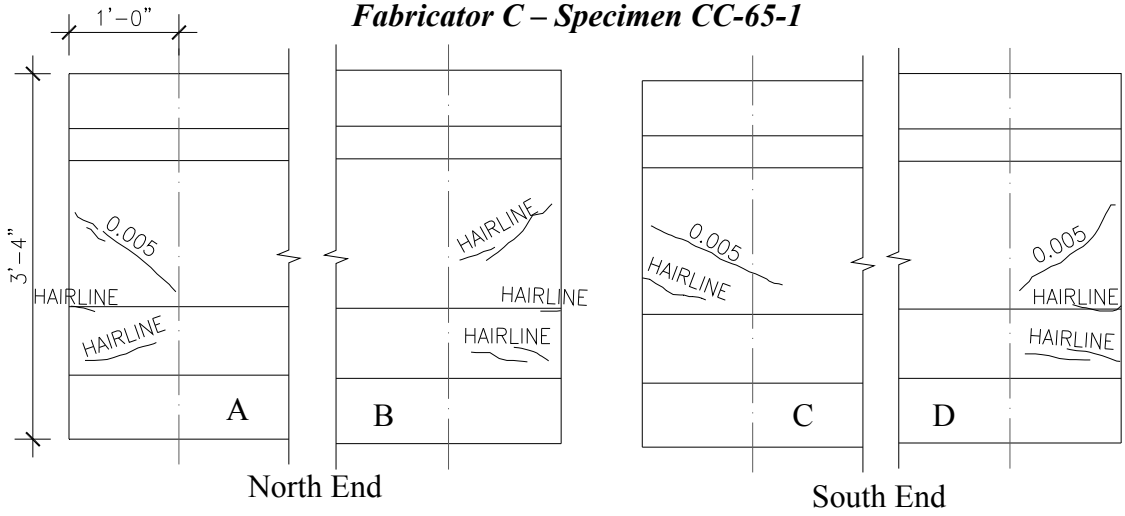

Fabricator C – Specimen CC-65-2

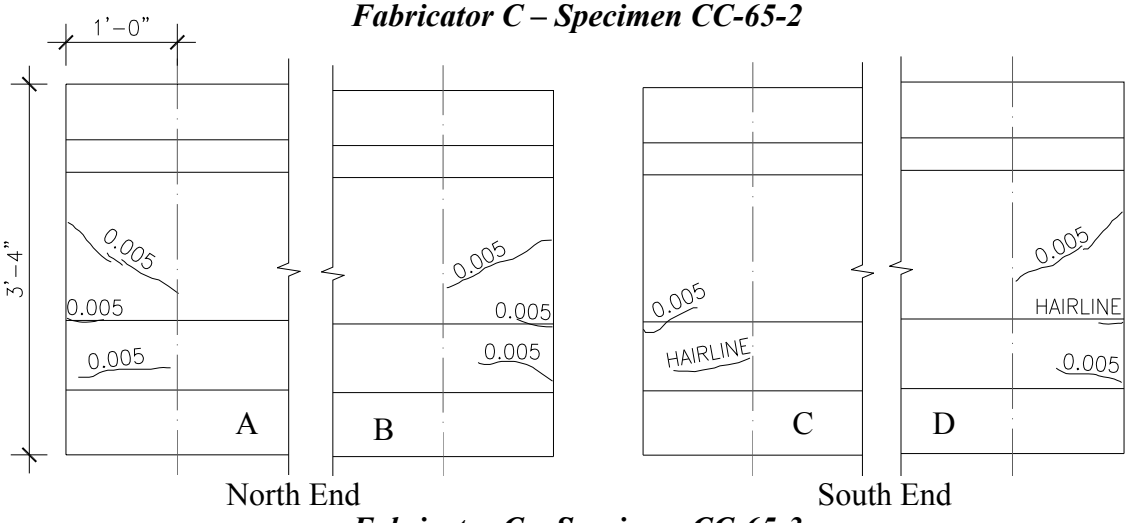

Fabricator C – Specimen CC-65-3

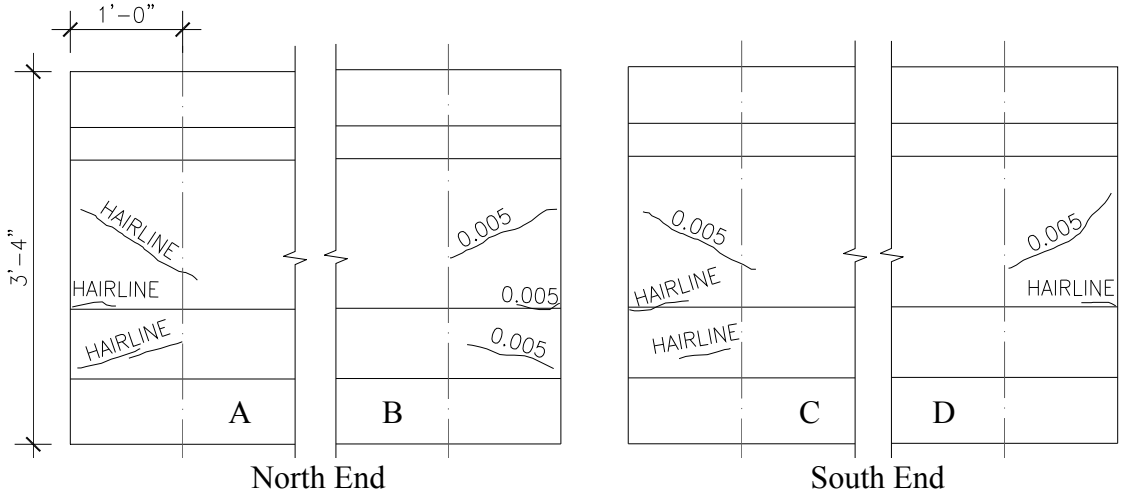

Fabricator C – Specimen CC-65-4

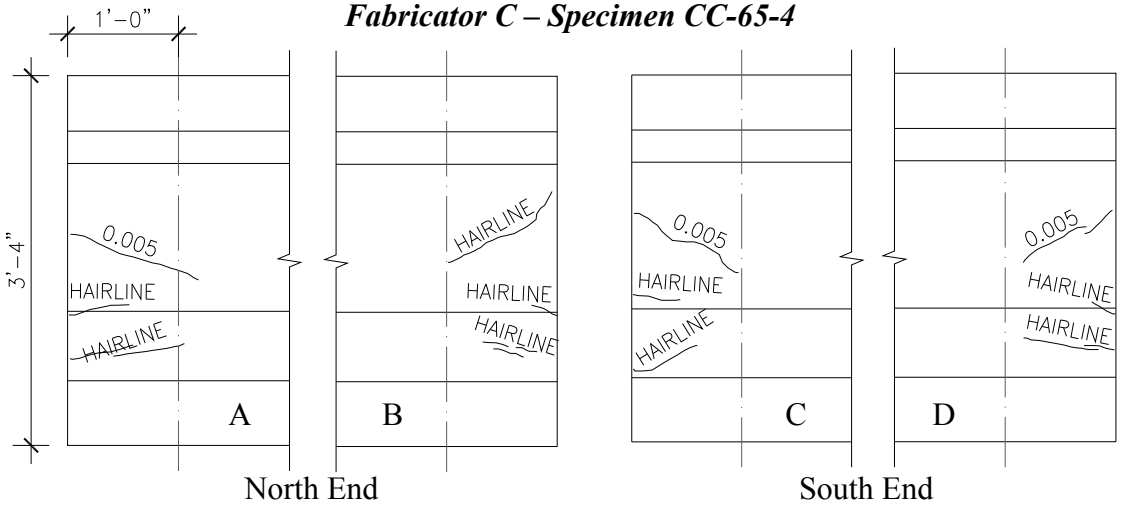

Fabricator C – Specimen CC-65-5

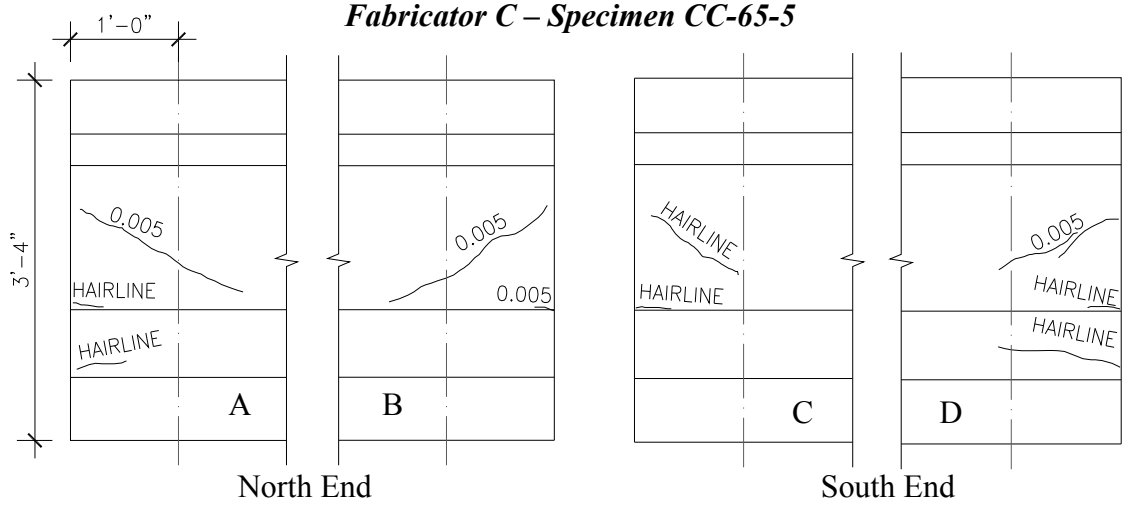

Fabricator C – Specimen CC-65-6

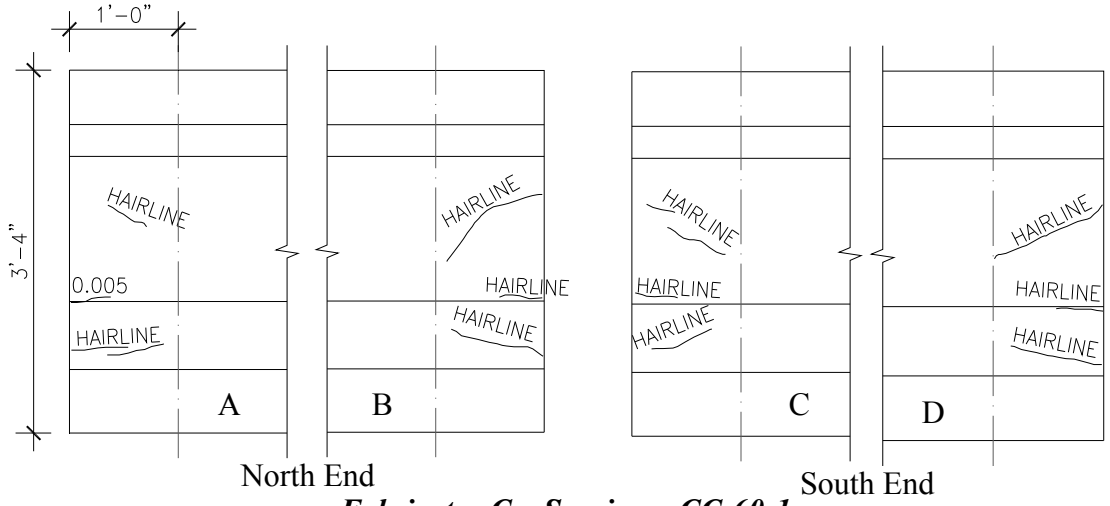

Fabricator C – Specimen CC-60-1

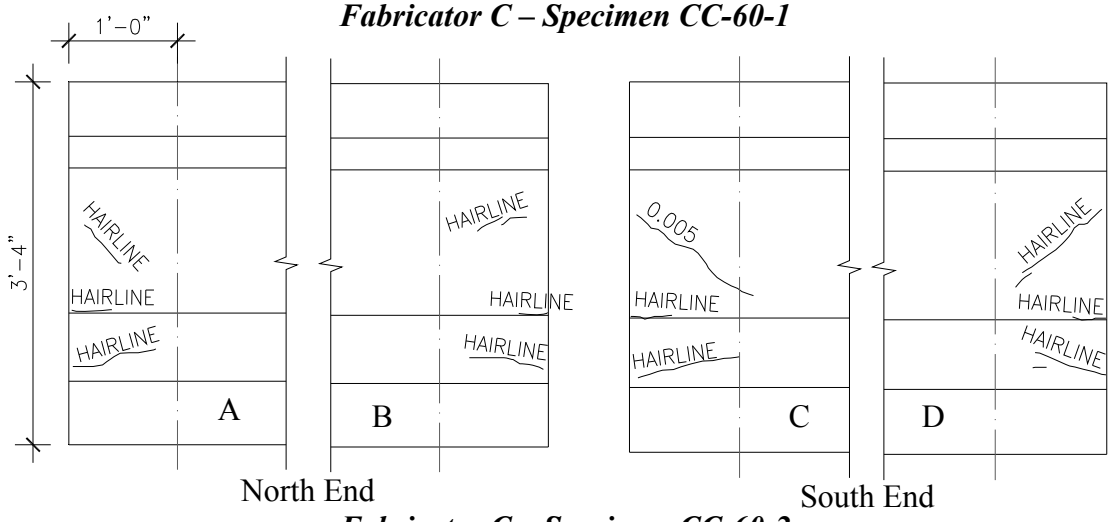

Fabricator C – Specimen CC-60-2

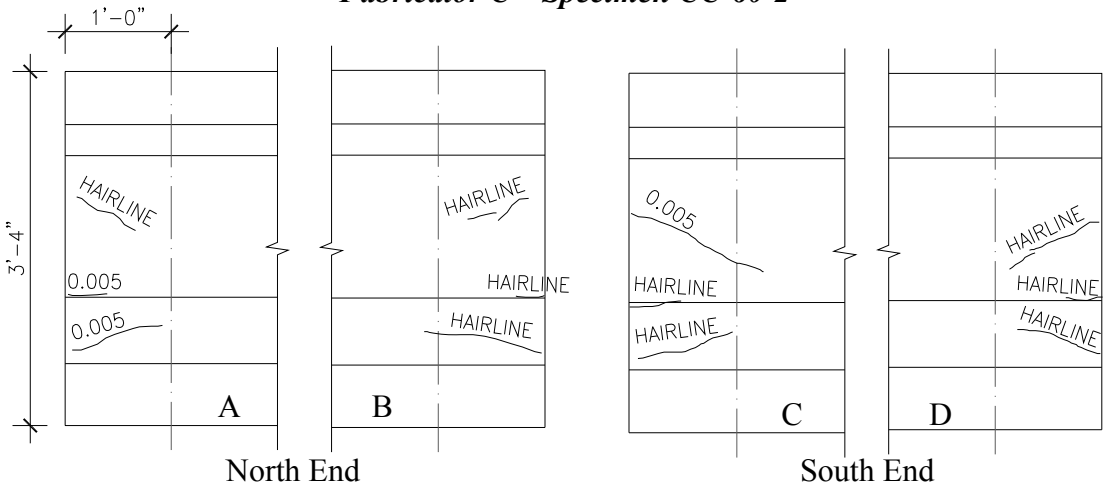

Fabricator C – Specimen CC-60-3

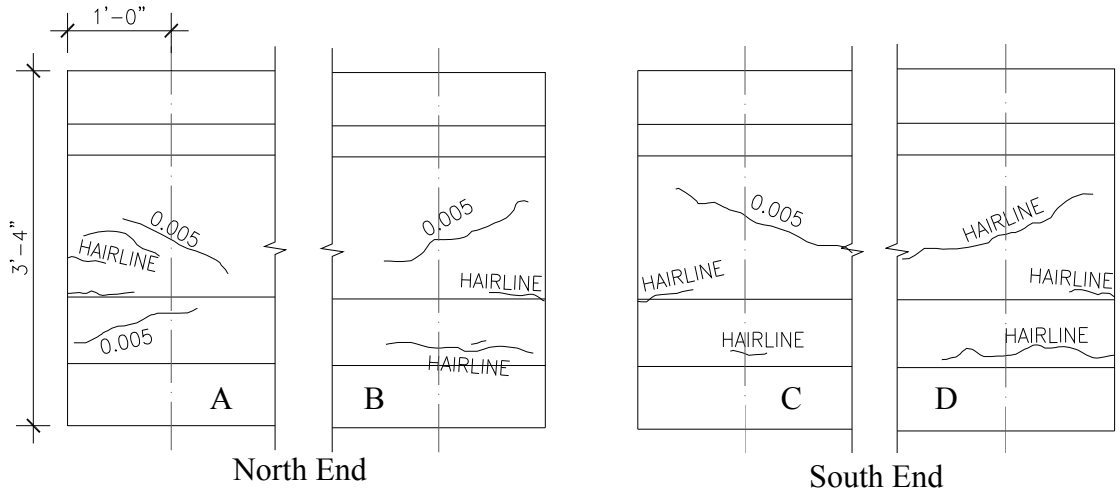

Fabricator D – Specimen CD-70-1

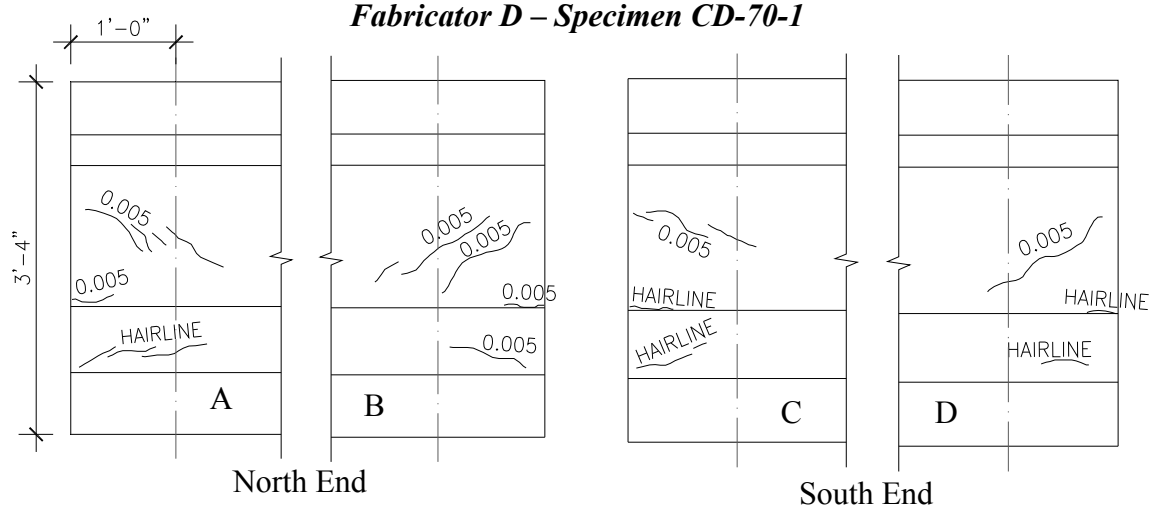

Fabricator D – Specimen CD-70-2

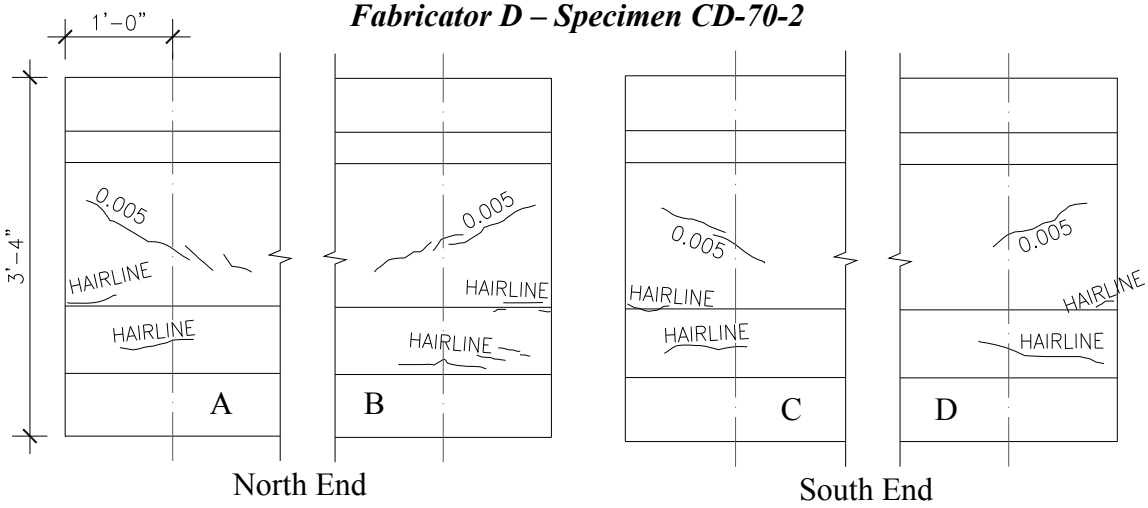

Fabricator D – Specimen CD-70-3

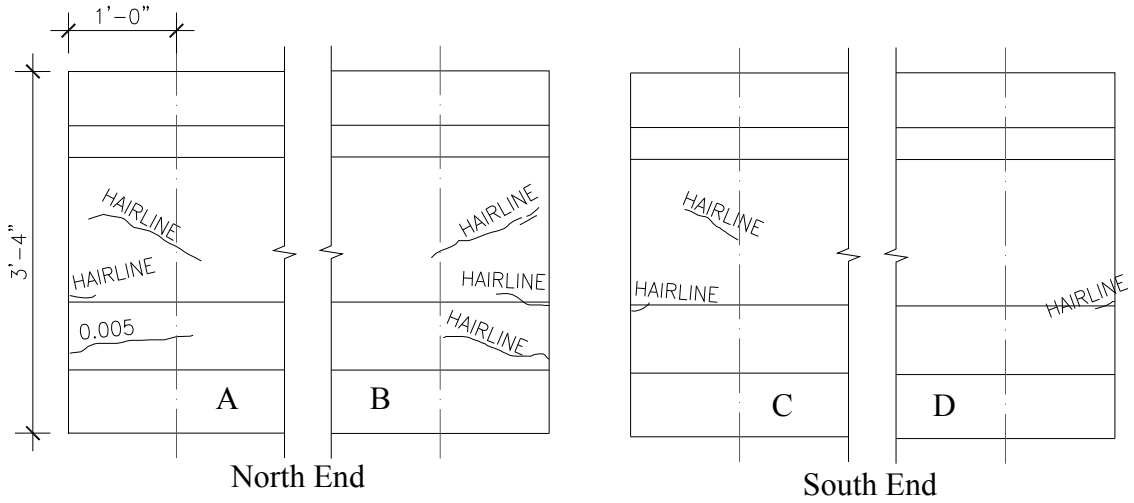

Fabricator D – Specimen CD-65-1

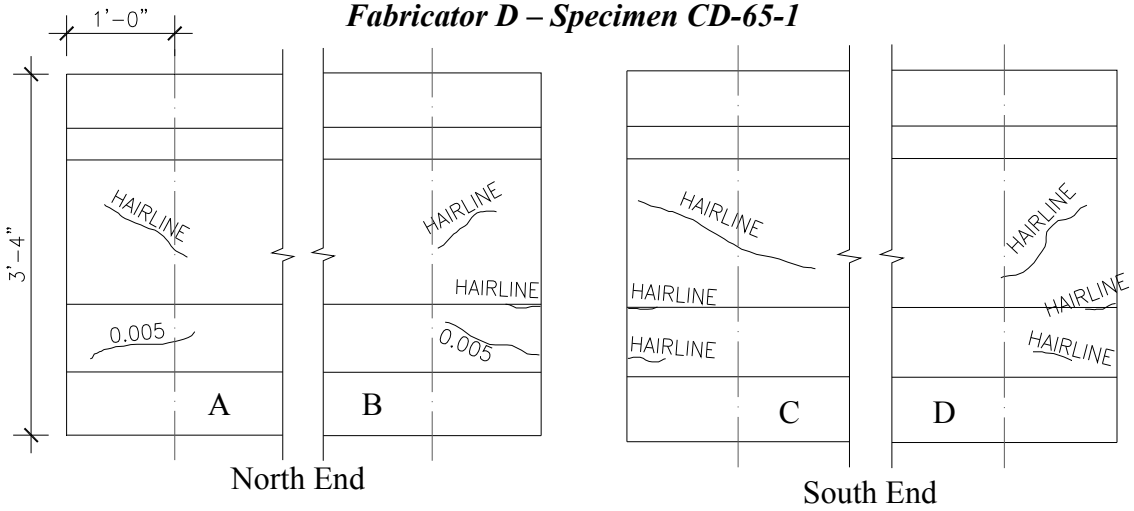

Fabricator D – Specimen CD-65-2

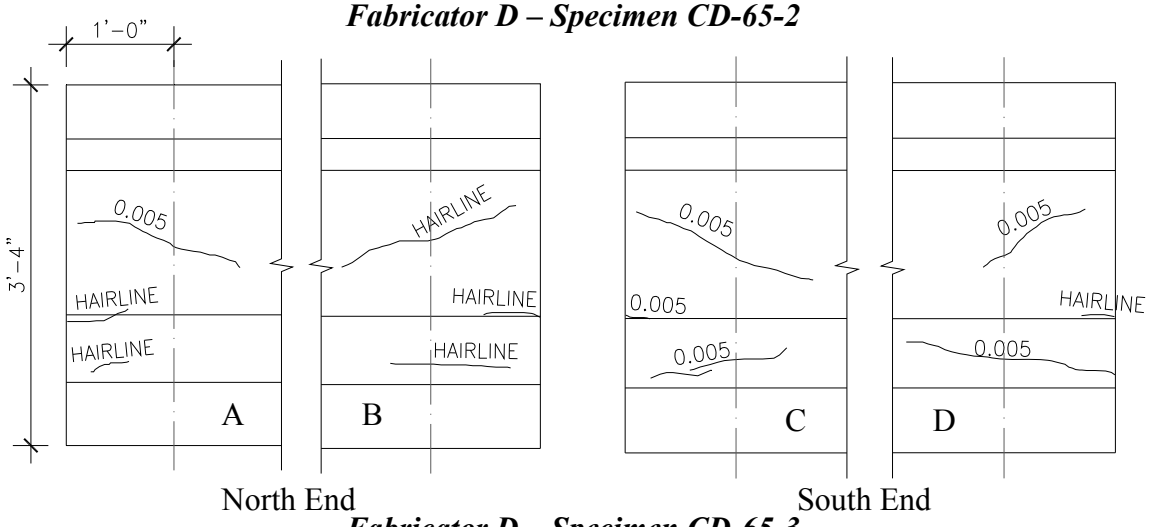

Fabricator D – Specimen CD-65-3

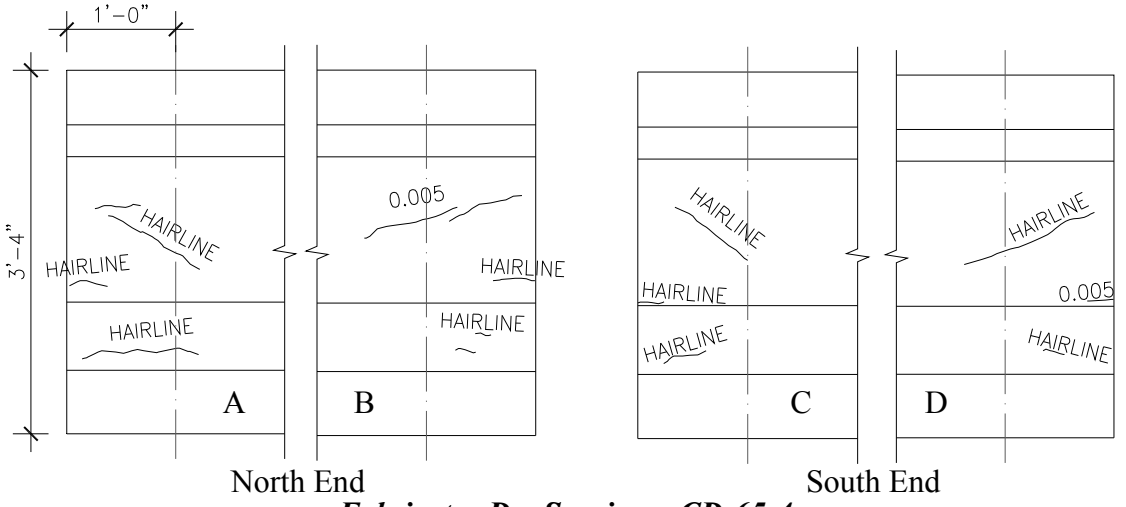

North End South End

Fabricator D – Specimen CD-65-4

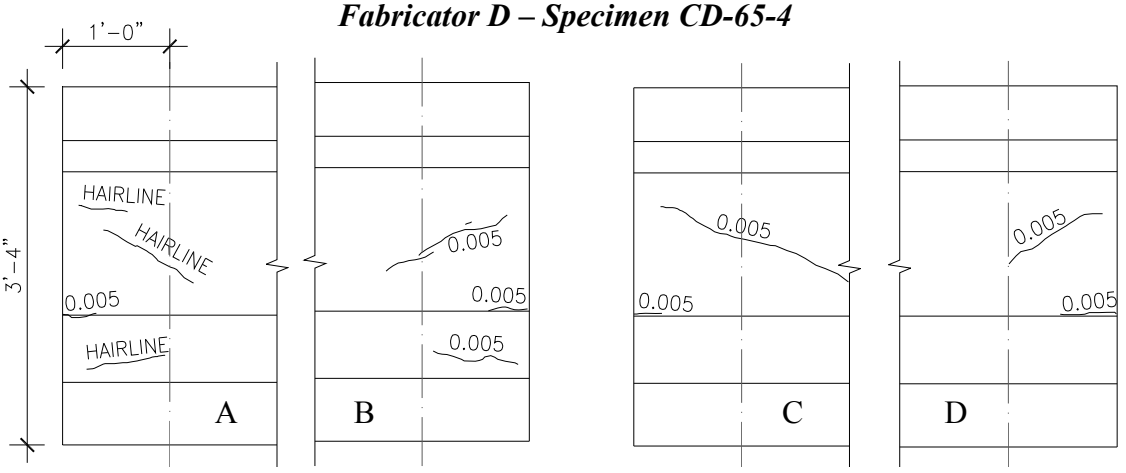

North End South End

Fabricator D – Specimen CD-65-5

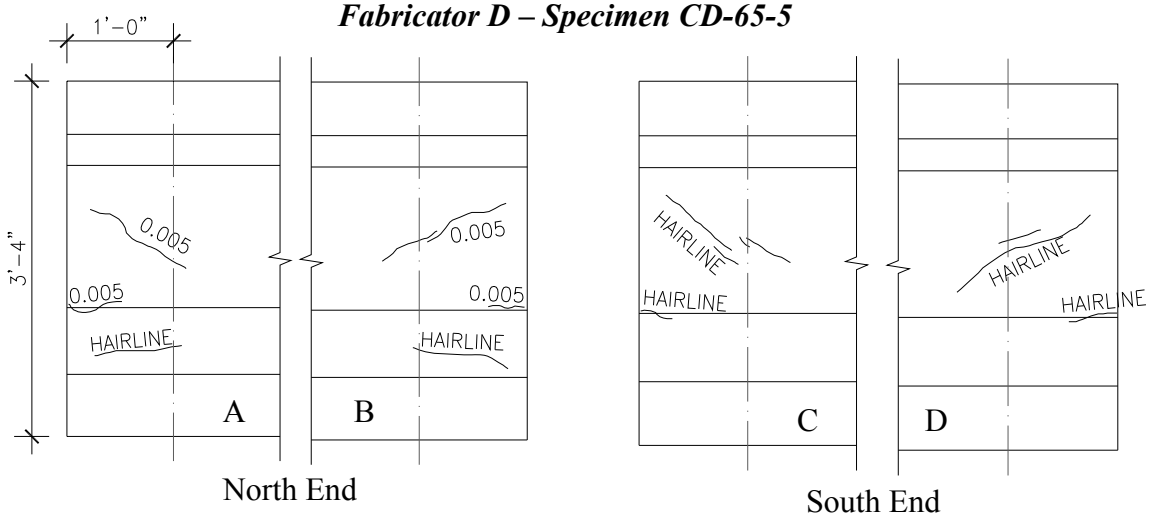

North End South End

Fabricator D – Specimen CD-65-6

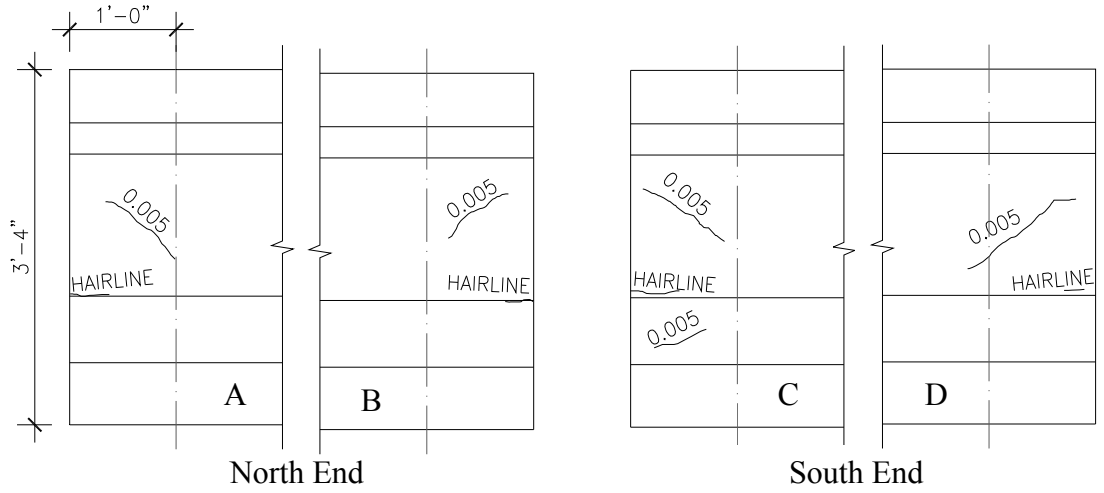

Fabricator D – Specimen CD-60-1

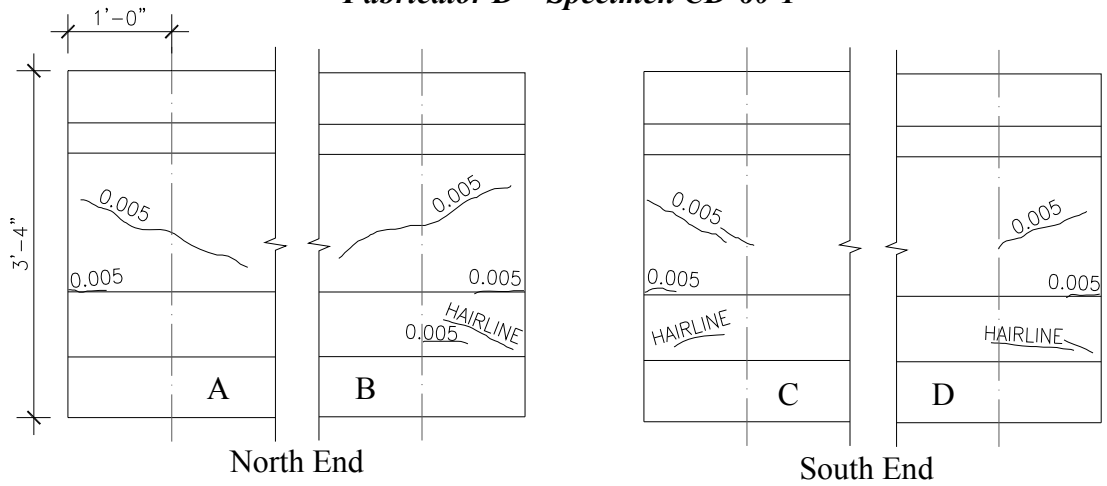

Fabricator D – Specimen CD-60-2

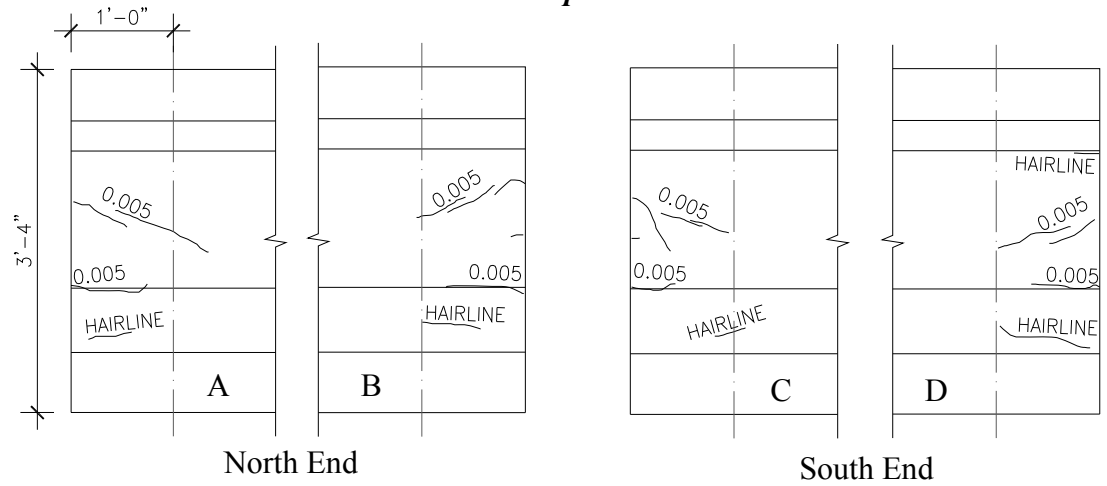

Fabricator D – Specimen CD-60-3

APPENDIX B

Sample Calculations and Data Recording Documents

Sample Calculation - Shear Resisted by Self Weight of Member and Applied Load

Input:

self weight of beam $sw := 0.516 \frac{kip}{ft}$

Length of beam $L_b := 56.5 \cdot ft$

Length of beam between supports $L_s := 51.5 ft$

Right overhang $O_R := 4.25 \cdot ft$

Left overhang $O_L := 9 in$

Right Reaction $R_R := \frac{sw \cdot L_b \cdot \left(\frac{L_b}{2} - O_L \right)}{L_s}$ $R_R = 15.568 \cdot kip$

Left Reaction $R_L := sw \cdot L_b - R_R$ $R_L = 13.586 kip$

A shear force diagram for the self weight of the member can be seen in Figure B.1.

The critical shear occurs at the section halfway between the point of the applied load (six feet to the left of the support on the right) and the point of the support on the right, or L=49.25 ft.

Working backwards from the point of the support where V=13.38 kips

shear at critical section $V_{sw} := 13.38 \cdot kip - (sw \cdot 3 ft)$

$V_{sw} = 11.832 \cdot kip$

The applied Load, P (assumed to be unity in this calculation), is applied at a section six feet from the support on the right, as seen in Figure B.1

$L_P := 46.25 \cdot ft$ $P := 1 \cdot kip$

Right Reaction $R_{R2} := P \cdot \frac{(L_P - O_L)}{L_s}$ $R_{R2} = 0.883 \cdot kip$

$R_{L2} := P - R_{R2}$ $R_{L2} = 0.117 \cdot kip$

$V_{applied}(P) := 0.88 \cdot P$

Thus the total shear at the critical section under any applied load is:

$Vcrit(P) := 0.88 \cdot P + V_{sw}$

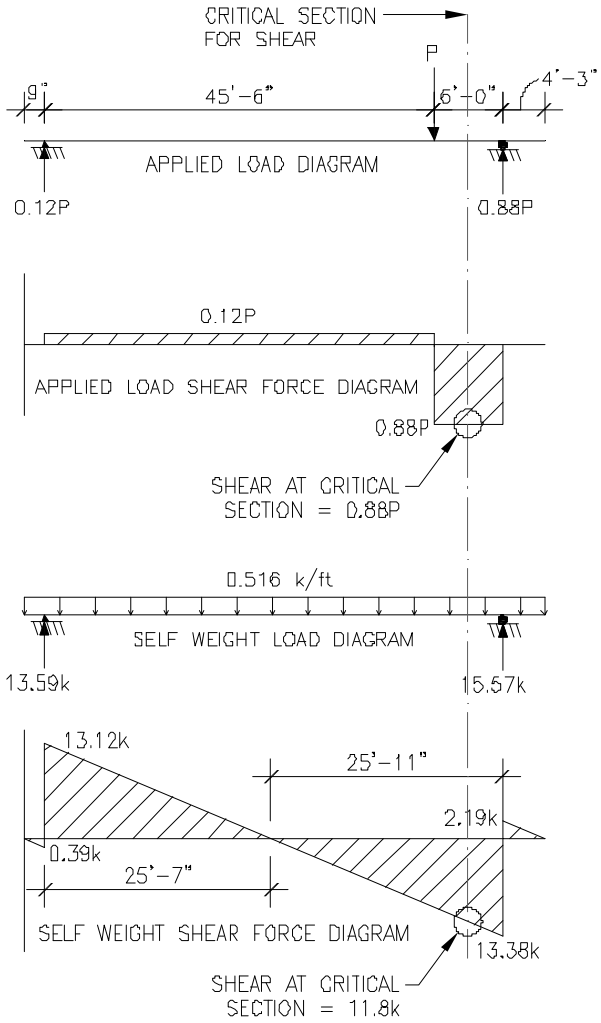

Figure B.1 Diagram of Loading and Shear Force Diagram for Each Load Case

Sample Calculation - Web-Shear Cracking Strength - ACI 318-08 (Specimen CC-70-1)

Input:

Length of beam between supports	$L_b := 51.5 \cdot ft$
Length to Loading Point	$L_L := 45.5 \cdot ft$
height of beam section	$h := 40 \cdot in$
Compressive strength of Concrete	$f_c := 10700 \cdot psi$
width of web	$b_w := 7 \cdot in$
Net Cross-sectional area of beam	$A_{net} := 490.9 \cdot in^2$
Cross sectional area of single strand	$a_s := 0.153 \cdot in^2$
Total number of strands for Series 2 beam	$n := 36$
Number of harped strands for Series 2 beam	$n_h := 6$
Stress in strands after all losses	$f_s := 160.6 \cdot ksi$
Section Properties	$y_t := 22.91 \cdot in$
	$y_b := 17.09 \cdot in$

The critical shear occurs at the section halfway between the point of the load and the point of the support, or L=48.5 ft

Calculate total area of steel	$A_s := a_s \cdot n$	$A_s = 5.508 \cdot in^2$
Calculate effective prestressing force	$P_{eff} := f_s \cdot A_s$	$P_{eff} = 884.585 \cdot kip$
Calculate f_{pc}	$f_{pc} := \frac{P_{eff}}{A_{net}}$	$f_{pc} = 1.802 \cdot ksi$

Calculate verticle component of prestressing force, given the angle of inclination of the harped strands. This angle is 2.87 degrees for a series 2 beam

$$V_p := \sin\left(\frac{2.87 \cdot \pi}{180}\right) \cdot P_{eff} \cdot \frac{n_h}{n} \qquad V_p = 7.382 \cdot kip$$

Calculate depth to prestressing steel at the section L=48.5 ft

eccentricity at section = 9.53 inches $e_s := 9.53 \cdot in$

depth to prestress $d_p := e_s + y_t$

$d_p = 32.44 \cdot in$

check if depth is less than 0.8h

$check := 0.8 \cdot h$

$check = 32 \cdot in$

depth is not less than 0.8h so the effective depth is equal to

$d := d_p$

$d = 32.44 \cdot in$

Calculate web-shear cracking strength

$$V_{cw} := \left(3.5 \cdot \sqrt{f_c} \cdot psi^{\frac{1}{2}} + 0.3 \cdot f_{pc}\right) \cdot b_w \cdot d + V_p$$

$V_{cw} = 212.352 \cdot kip$

Sample Calculation - Web-Shear Cracking Strength - AASHTO LRFD (Specimen CC-70-1)

Input:

Length of beam between supports	$L_b := 51.5 \cdot ft$
Length to Loading Point	$L_L := 45.5 \cdot ft$
height of beam section	$h := 40 \cdot in$
Compressive strength of Concrete	$f_c := 10700 \cdot psi$
width of web	$b_w := 7 \cdot in$
Net Cross-sectional area of beam	$A_{net} := 490.9 \cdot in^2$
Cross sectional area of single strand	$a_s := 0.153 \cdot in^2$
Total number of strands for Series 2 beam	$n := 36$
Number of harped strands for Series 2 beam	$n_h := 6$
Stress in strands after all losses	$f_s := 164.51 \cdot ksi$
Section Properties	$y_t := 22.91 \cdot in$
	$y_b := 17.09 \cdot in$

The critical shear occurs at the section halfway between the point of the load and the point of the support, or L=48.5 ft

Calculate total area of steel	$A_s := a_s \cdot n$	$A_s = 5.508 \cdot in^2$
Calculate effective prestressing force	$P_{eff} := f_s \cdot A_s$	$P_{eff} = 906.121 \cdot kip$
Calculate f_{pc}	$f_{pc} := \frac{P_{eff}}{A_{net}}$	$f_{pc} = 1.846 \cdot ksi$

Calculate verticle component of prestressing force, given the angle of inclination of the harped strands. This angle is 2.87 degrees for a series 2 beam

$$V_p := \sin\left(\frac{2.87 \cdot \pi}{180}\right) \cdot P_{eff} \cdot \frac{n_h}{n} \qquad V_p = 7.562 \cdot kip$$

Calculate depth to prestressing steel at the section L=48.5 ft

eccentricity at section = 9.53 inches $e_s := 9.53 \cdot in$

depth to prestress $d_p := e_s + y_t$ $d_p = 32.44 \cdot in$

Calculate AASHTO LRFD shear depth, d_v

shear depth is the maximum of 0.9 times the depth to prestresssing steel, 0.72 times height of section, and depth to prestressing steel minus depth of compression block in flexure divided by 2

depth of compression block in flexure $a := 10.63 \cdot in$

$\frac{d_p - a}{2} = 10.905 \cdot in$ $0.9 \cdot d_p = 29.196 \cdot in$ $0.72 \cdot h = 28.8 \cdot in$

$d_v := 29.20 \cdot in$

Calculate web-shear cracking strength (units conversion in concrete strength already made)

$$V_{cw} := \left(1.9 \cdot \sqrt{f_c \cdot psi}^{\frac{1}{2}} + 0.3 \cdot f_{pc}\right) \cdot b_w \cdot d_v + V_p$$

$V_{cw} = 160.921 \cdot kip$

Sample Calculation - Shear Strength of Transverse Reinforcement - ACI 318-08 (Specimen CC-70-1)

Input:

Cross sectional area of double legged #4 stirrup $a_s := 0.4 \cdot in^2$

yield strength of stirrup $f_y := 60 \cdot ksi$

depth to prestressing steel (from V_{cw} calculation) $d := 32.44 \cdot in$

Spacing of stirrups $s_s := 24 \cdot in$

Calculate shear resistance provided by the stirrups

$$V_s := \frac{a_s \cdot f_y \cdot d}{s_s}$$

$V_s = 32.44 \cdot kip$

Sample Calculation - Shear Strength of Transverse Reinforcement - ACI 318-08 (Specimen CC-70-1)

Additional input:

shear depth (from V_{cw} calculation) $d_v := 29.20 \cdot in$

compressive strength of concrete $f_c := 10.7 \cdot ksi$

f_{pc} (from V_{cw} calculation) $f_{pc} := 2.08 \cdot ksi$

cot(θ), for $V_{ci} > V_{cw}$

$$\cot_\theta := 1.0 + 3 \cdot \left(\frac{f_{pc}}{\sqrt{f_c} \cdot ksi^{\frac{1}{2}}} \right)$$ less than or equal to 1.8

$\cot_\theta = 2.908$ 1.8 governs, thus:

$\cot\theta := 1.8$ and θ = the inverse tangent of 1/1.8

$\theta := 29deg$

Calculate shear resistance provided by the stirrups

$$V_S := \frac{a_s \cdot f_y \cdot d_v \cdot \cot\theta}{s_s}$$

$V_S = 52.56 \cdot kip$

Sample Calculation - Compressive Stress at Release (Specimen CC-70-1)

Input:

Length of Beam $L_b := 56.5 \cdot ft$

Length to strand hold down points: $L_{HD} := 23.25 \cdot ft$

height of beam section $h := 40 \cdot in$

Compressive strength of Concrete at Release $f_{ci} := 5382 \cdot psi$

width of web $b_w := 7 \cdot in$

Gross Cross-sectional area of beam $A_g := 494.9 \cdot in^2$

Gross Moment of Inertia of beam $I_g := 82602 \cdot in^4$

Weight of beam per unit length $w_{sw} := 0.516 \cdot \frac{kip}{ft}$

Cross sectional area of single strand $a_s := 0.153 \cdot in^2$

diameter of single strand $d_b := 0.5 \cdot in$

Total Number of strands for Series 2 beam $n := 36$

Stress in strands after losses not including time-dependent losses $f_s := 184.33 \cdot ksi$

Section Properties $y_t := 22.91 \cdot in$

$y_b := 17.09 \cdot in$

Strand Eccentricities $e_{end} := 8.76 \cdot in$

$e_{center} := 11.09 \cdot in$

Maximum compressive stress at release in end regions occurs at transfer length

Calculate Transfer Length (AASHTO LRFD 2007) $L_t := 60 \cdot d_b$

$L_t = 2.5\,ft$

Eccentricity at transfer length $e_t := e_{end} + \frac{e_{center} - e_{end}}{L_{HD}} \cdot L_t$

$e_t = 9.011 \cdot in$

Calculate dead load moment due to self-weight of beam at transfer length

$$M_D := w_{sw} \cdot \left(\frac{L_t}{2}\right) \cdot \left(L_b - L_t\right)$$

$$M_D = 417.96 \cdot in \cdot kip$$

Calculate bottom fiber compressive stress at hold down points

Calculate total area of steel $A_s := a_s \cdot n$ $A_s = 5.508 \cdot in^2$

Calculate effective prestressing force $P_{eff} := f_s \cdot A_s$ $P_{eff} = 1.015 \times 10^3 \cdot kip$

$$f_{bot} := \frac{-P_{eff}}{A_g} - \frac{P_{eff} \cdot y_b \cdot e_t}{I_g} + \frac{M_D \cdot y_b}{I_g}$$

$f_{bot} = -3.858 \cdot ksi$ negative sign indicates compression

Calculate ratio of bottom fiber compressive stress to compressive strength in concrete at prestress transfer

$$percentage := \frac{f_{bot}}{-f_{ci}} \qquad percentage = 0.717$$

$f_{bot} := 0.72 f_{ci}$

Sample Shear Test Data Sheet (Specimen CB-70-6)

Date:		
Left Overhang		in
Span		in
Right Overhang		in
Total		in
Concrete Strength		psi
Bottom Fiber Stress		f'_c

Cracking and Ultimate Load Calculation (ACI)				
Reaction on Right	0.882	P	historical data	
Reaction on Left	0.118	P	x1.5	AASHTO
Expected Max Load	**269**	kips	**403**	**227**
Expected Crack Load	232	kips		
Expected V_{ci} Crack	489	kips		
Expected V_{cw} Crack	**232**	kips		**168**
Estimate Flex Failure	460	kips		

Load	Maximum Crack Width

Actual First Cracking Load		k
Actual Ultimate Load		k

Actual Web Shear Crack		k

Shear Strength Ratio:	$V_{test}/V_{n,ACI}$	**0.00**	$V_{test}/V_{n,AASHTO}$	**0**
Web Cracking Ratio:	$V_{crack}/V_{c,ACI}$	**0.00**	$V_{crack}/V_{c,AASHTO}$	**0**

APPENDIX C

Shop Drawings

C.1 Beam Fabrication Specifications

C.2 Rebar Data Sheet

C.3 Series 1 Beam Shop Drawings

C.4 Series 2 Beam Shop Drawings

C1: Project 5197 Extension

Beam Fabrication Specifications

1. Each fabricator will schedule a prefabrication meeting before fabricating any beams.

2. Each fabricator will submit a concrete mix design to be approved by TxDOT before beam fabrication. The approved mix design will be used to fabricate all 12 beams provided from each fabricator.

3. A ±2% prestressing force and elongation tolerance will be required for all fabricated beams.

4. Each fabricator will start by producing three (3) beams at 0.7f'c. This will be followed by six (6) beams at 0.65f'c and three (3) beams at 0.6f'c.

5. Twenty-four (24) cylinders shall be fabricated with each beam. Of the twenty-four (24), six (6) shall be shipped to the University of Texas with each beam. The remaining eighteen (18) cylinders shall be used to target the required release strength.

6. All cylinders shall be sure-cured.

7. All cylinders shall be marked with the corresponding beam mark (i.e. C70-1) and the date of casting.

8. Approximately six (6) hours after the beam is cast, two (2) cylinders shall be tested in compression every hour. As soon as the strength of the cylinders reaches within

1000-psi of the targeted strength at release, two (2) cylinders shall be tested every thirty (30) minutes or as needed to appropriately achieve the required release strength.

9. When the targeted strength is achieved, all prestressing force shall be transferred to the beam within fifteen (15) minutes.

10. After the beam has been released, two (2) cylinders will be tested in compression.

11. Each Fabricator will report the concrete strength immediately before and immediately after prestress transfer. The time at which the concrete strength was determined will also be reported.

12. Lifting Loops on each beam shall be located 5.75 feet from the end of the beam and be no higher than 5 inches from the top face of the beam. Additional lifting loops may be added if deemed necessary by the fabricator.

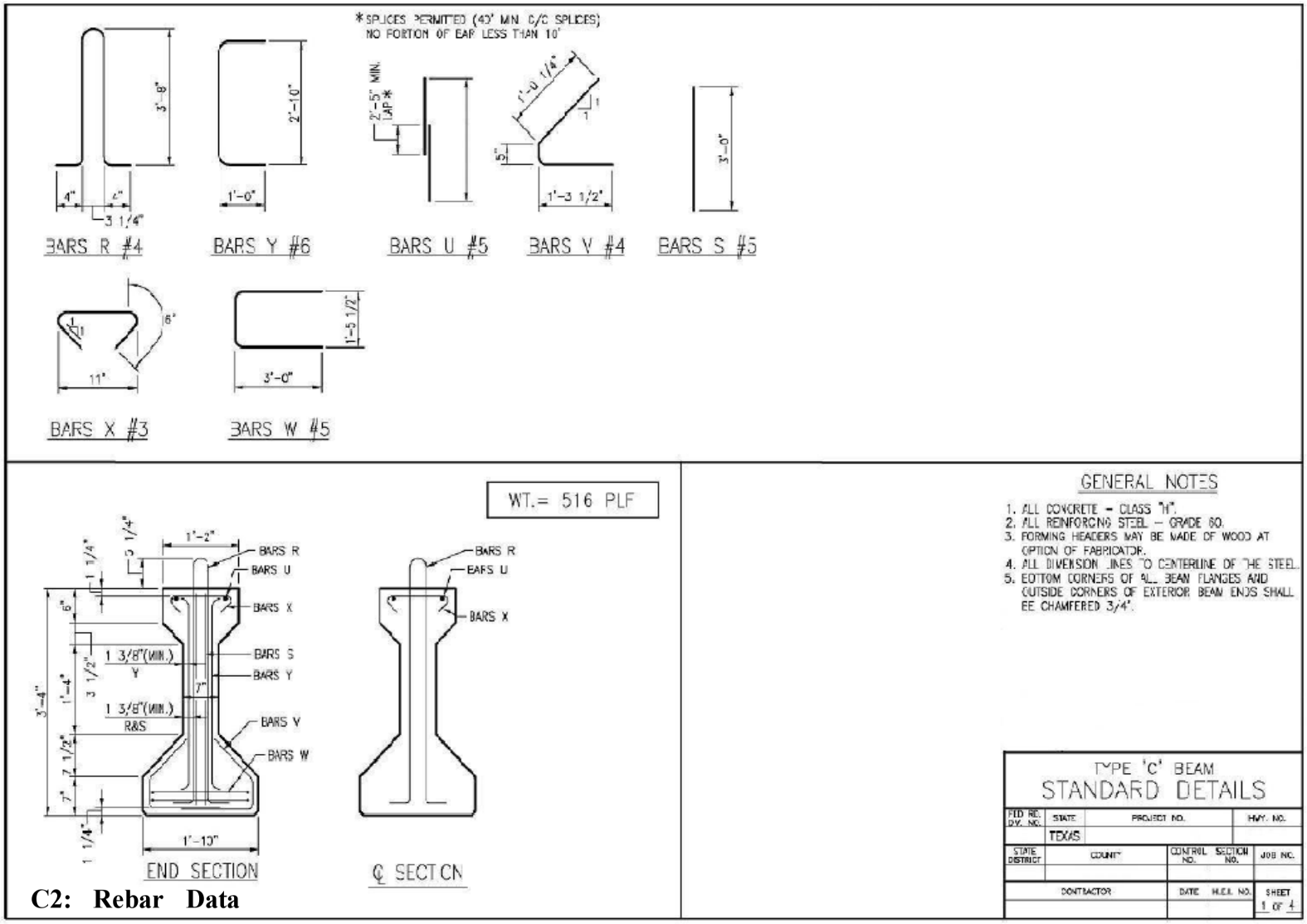

C2: Rebar Data

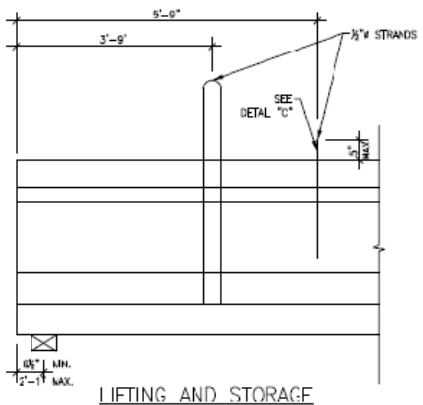

LIFTING AND STORAGE

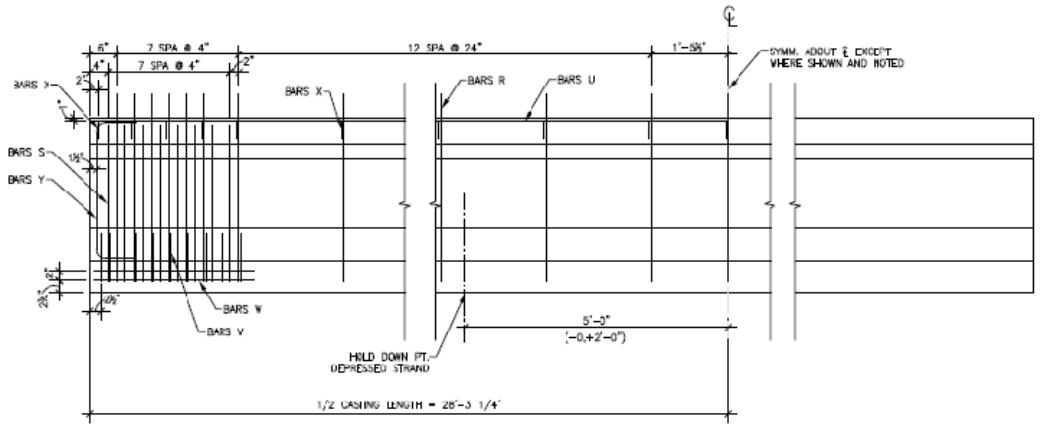

ELEVATION

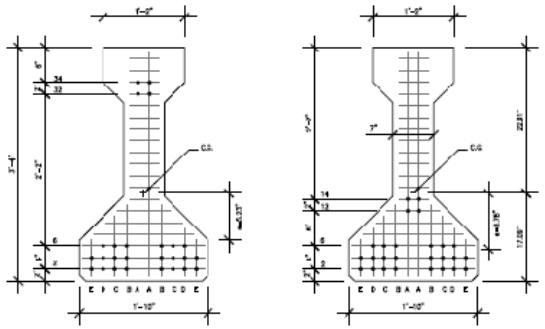

END SECTION

℄ SECTION

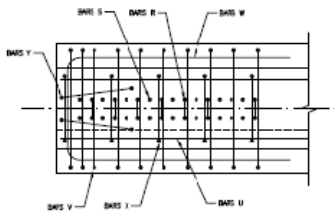

DETAIL A

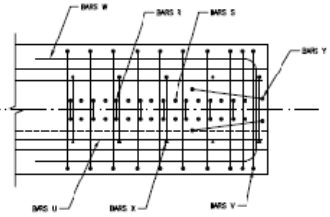

DETAIL B

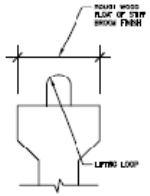

DETAIL "C"

REINFORCING BAR SCHEDULE								
BEAM MARK	NO. BEAMS REQ'D.	R #4	X #3	V #4	S #5	W #5	Y #6	U #5
C-70-1	3	4'	35	40	32	4	4	2
	TOTALS	123	105	120	96	12	12	6

U-BAR LENGTH = 58'-3"

STRAND PATTERN	
NO. OF STRANDS	26-½"ø, 270K LOLAX @ 31.0 K/STR.
NO. STRAIGHT	22
NO. DEFLECTED	4 @ A28
RELEASE STRENGTH	3900 – 4100 PSI*
COARSE AGGREGATE	RIVER GRAVEL
CLASS OF CONCRETE	H

* Strength at release within this range is critical. See attached document detailing beam fabrication and cylinder testing.

STRAND PATTERN 26D4 @ A28 (TYPE C BEAM)				
FED. RD. DIV. NO.	STATE	PROJECT NO.		HWY. NO.
NA	TEXAS	TxDOT PROJECT 5197		NA
STATE DISTRICT	COUNTY	CONTROL NO.	SECTION NO.	JOB NO.
AUSTIN	TRAVIS			
VALLEY PRESTRESSED		DATE		SHEET 2 OF 4
UNIVERSITY OF TEXAS – FSEL		FEB. '08		

C3: Series 1 Beam Shop Drawings

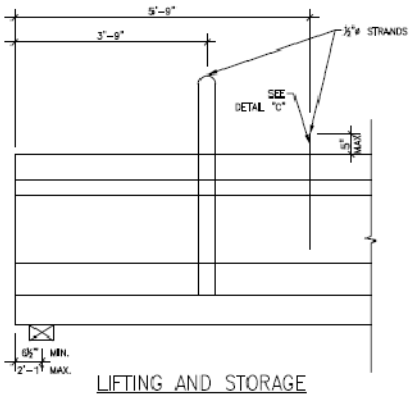

LIFTING AND STORAGE

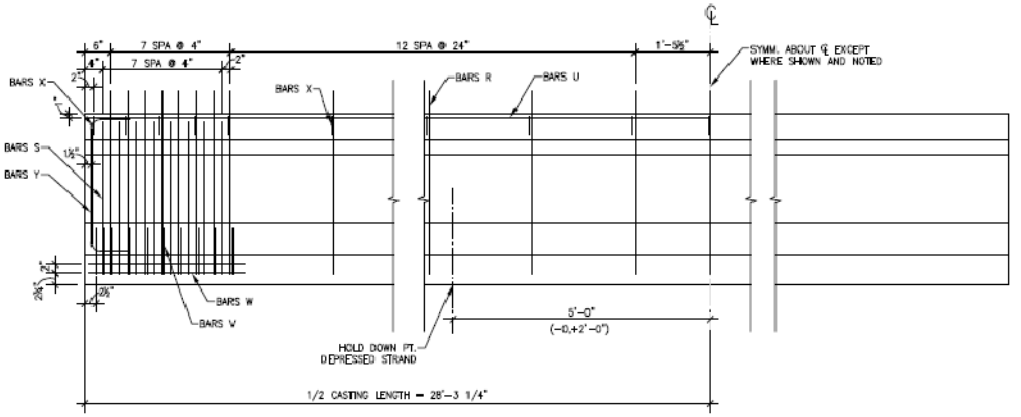

ELEVATION

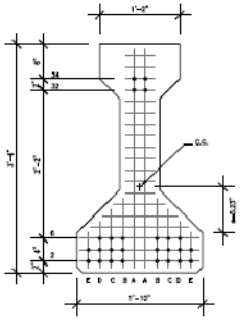

END SECTION

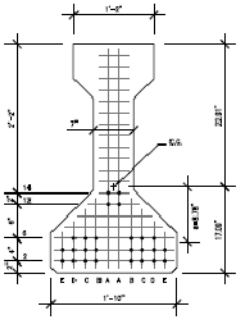

℄ SECTION

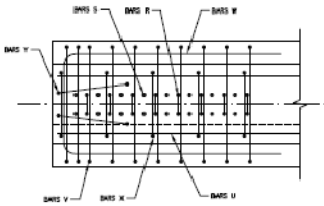

DETAIL A

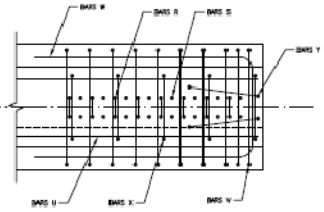

DETAIL B

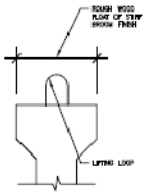

DETAIL "C"

REINFORCING BAR SCHEDULE								
BEAM MARK	NO. BEAMS REQ'D.	R #4	X #3	V #4	S #5	W #5	Y #5	U #5
C-65-1	6	41	35	40	32	4	4	2
	TOTALS	246	210	240	192	24	24	12

U-BAR LENGTH = 56'-3"

STRAND PATTERN	
NO. OF STRANDS	26-1/2"ø, 270K LOLAX @ 31.0 K/STR.
NO. STRAIGHT	22
NO. DEFLECTED	4 @ A28
RELEASE STRENGTH	4200 - 4400 PSI*
COARSE AGGREGATE	RIVER GRAVEL
CLASS OF CONCRETE	H

* Strength at release within this range is critical. See attached document detailing beam fabrication and cylinder testing.

STRAND PATTERN 26D4 @ A28 (TYPE C BEAM)					
FED RD. DIV. NO.	STATE	PROJECT NO.			HWY. NO.
NA	TEXAS	TxDOT PROJECT 5197			NA
STATE DISTRICT	COUNTY		CONTROL NO.	SECTION NO.	JOB NO.
AUSTIN	TRAVIS				
VALLEY PRESTRESSED			DATE		SHEET 3 OF 4
UNIVERSITY OF TEXAS - FSEL			FEB. '08		

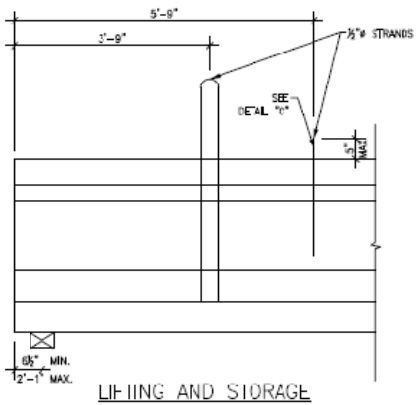

LIFTING AND STORAGE

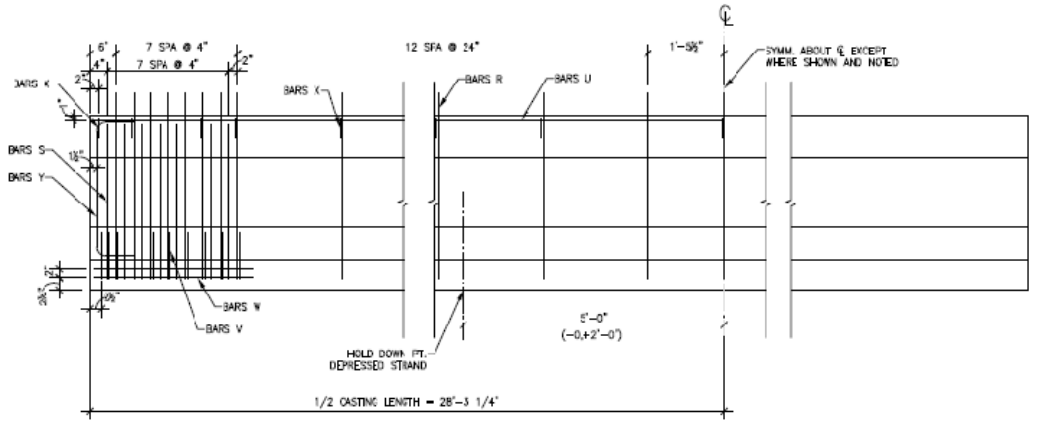

ELEVATION

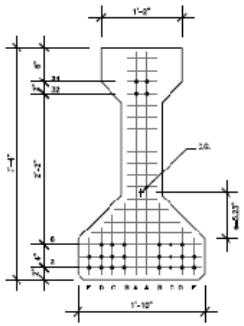

END SECTION

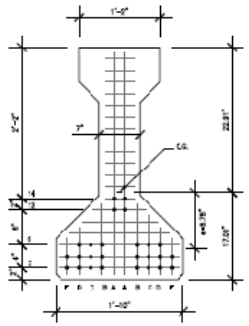

℄ SECTION

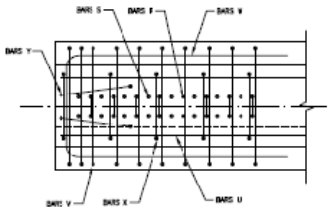

DETAIL A

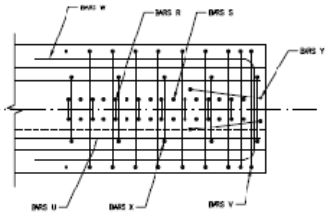

DETAIL B

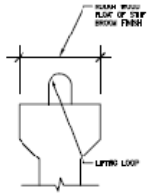

DETAIL "C"

REINFORCING BAR SCHEDULE								
BEAM MARK	NO. BEAMS REQ'D.	R #4	X #3	V #4	S #5	W #5	Y #6	U #5
C-60-1	3	4'	35	40	32	4	4	2
	TOTALS	123	105	120	96	12	12	6

U-BAR LENGTH = 56'-3"

STRAND PATTERN	
NO. OF STRANDS	26-1/2"ø, 270K LOIAX @ 31.0 K/STR.
NO. STRAIGHT	22
NO. DEFLECTED	4 @ A28
RELEASE STRENGTH	4600 – 4800 PSI*
COARSE AGGREGATE	RIVER GRAVEL
CLASS OF CONCRETE	H

* Strength at release within this range is critical. See attached document detailing seam fabrication and cylinder testing.

STRAND PATTERN 26D4 @ A28 (TYPE C BEAM)			
FED RD. DIV. NO.	STATE	PROJECT NO.	HWY. NO.
NA	TEXAS	TxDOT PROJECT 5197	NA
STATE DISTRICT	COUNTY	CONTROL NO.	SECTION NO. JOB NO.
AUSTIN	TRAVIS		
VALLEY PRESTRESSED		DATE	SHEET 4 OF 4
UNIVERSITY OF TEXAS – FSEL		FEB. '08	

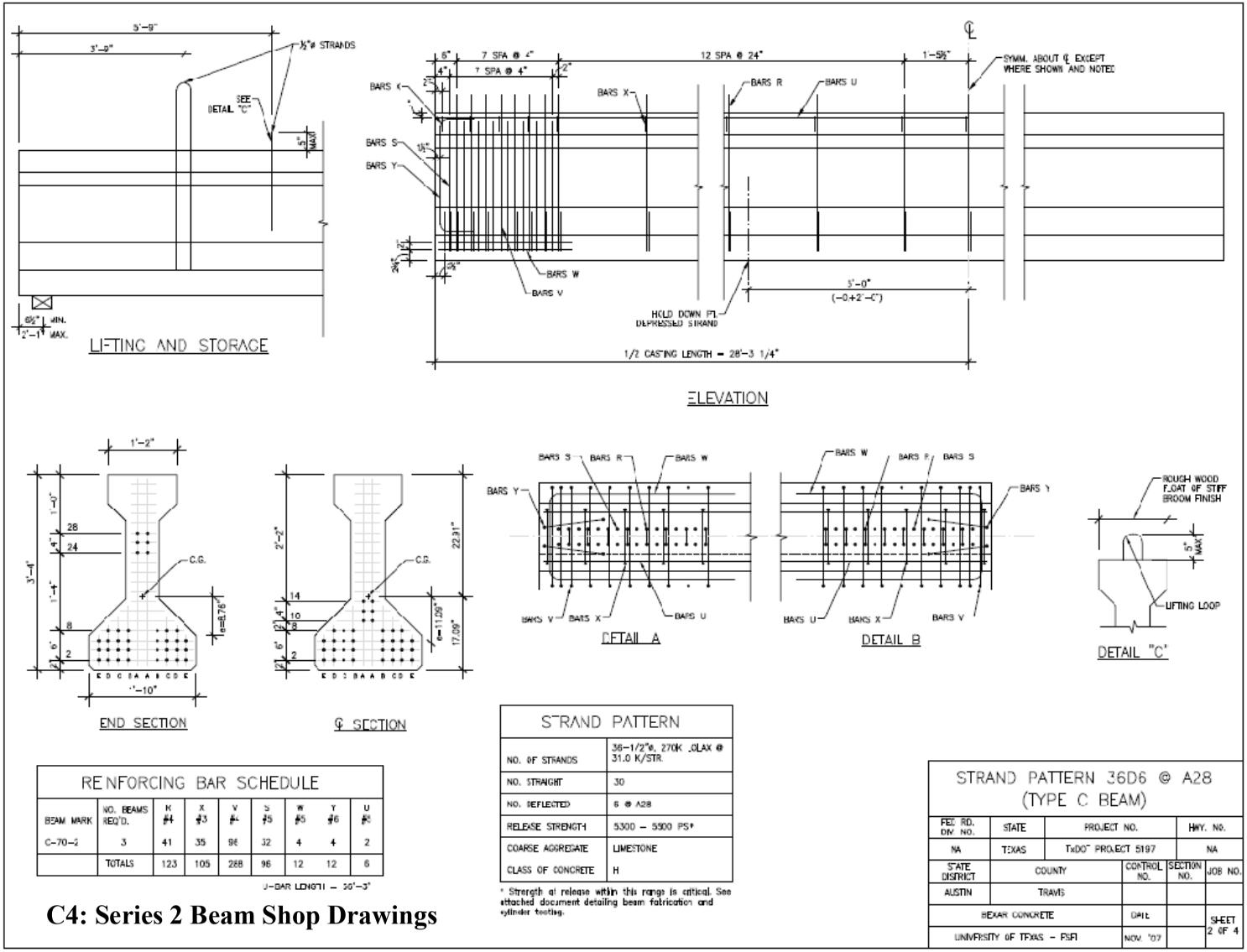

RENFORCING BAR SCHEDULE								
BEAM MARK	NO. BEAMS REQ'D.	K #4	X #3	V #4	S #5	W #5	Y #6	U #6
C-70-2	3	41	35	96	32	4	4	2
	TOTALS	123	105	288	96	12	12	6

J-BAR LENGTH = 30'-3"

STRAND PATTERN	
NO. OF STRANDS	36-1/2"ø, 270K .0LAX @ 31.0 K/STR.
NO. STRAIGHT	30
NO. DEFLECTED	6 @ A28
RELEASE STRENGTH	5300 – 5500 PSI*
COARSE AGGREGATE	LIMESTONE
CLASS OF CONCRETE	H

* Strength at release within this range is critical. See attached document detailing beam fabrication and cylinder testing.

STRAND PATTERN 36D6 @ A28 (TYPE C BEAM)				
FED RD. DIV. NO.	STATE	PROJECT NO.		HWY. NO.
NA	TEXAS	TxDOT PROJECT 5197		NA
STATE DISTRICT	COUNTY	CONTROL NO.	SECTION NO.	JOB NO.
AUSTIN	TRAVIS			
BEXAR CONCRETE		DATE		SHEET 2 OF 4
UNIVERSITY OF TEXAS – FSEL		NOV. '07		

C4: Series 2 Beam Shop Drawings

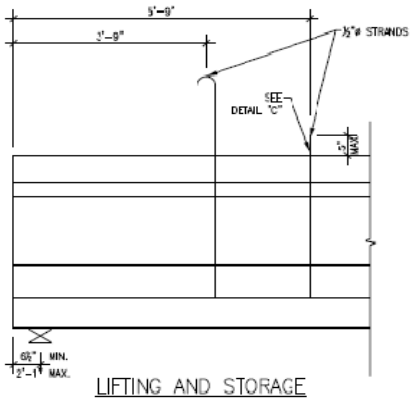

LIFTING AND STORAGE

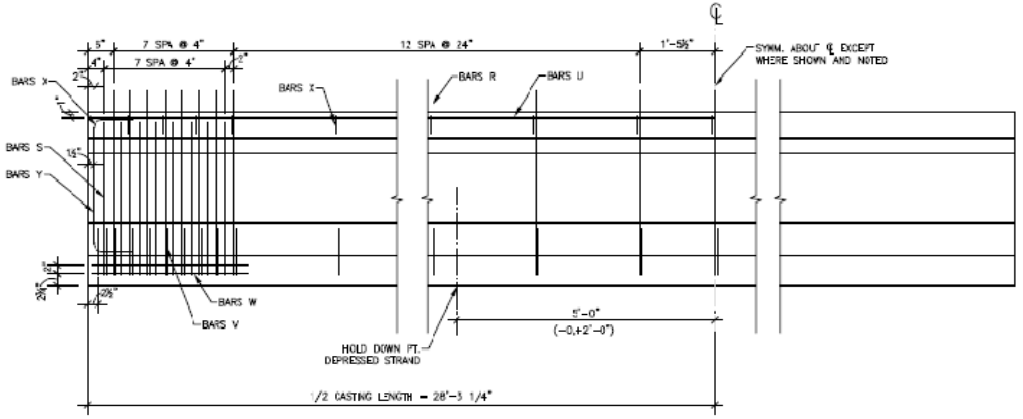

ELEVATION

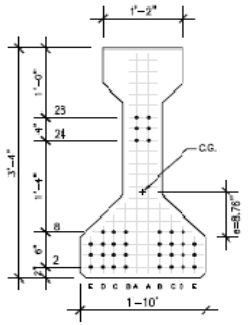

END SECTION

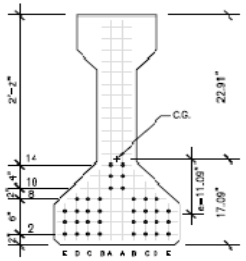

C SECTION

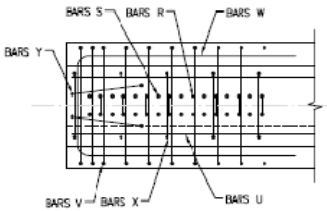

DETAIL A

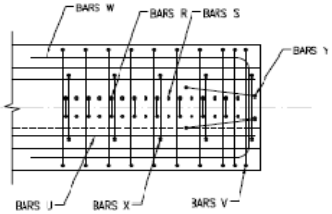

DETAIL B

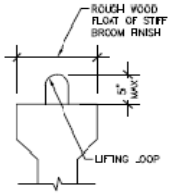

DETAIL "C"

REINFORCING BAR SCHEDULE								
BEAM MARK	NO. BEAMS REQ'D.	R #4	X #3	V #4	S #5	W #5	Y #6	U #5
C-65-2	6	41	35	96	32	4	4	2
	TOTALS	246	210	576	192	24	24	12

U-BAR LENGTH = 56'-3"

STRAND PATTERN	
NO. OF STRANDS	36-1/2"ø, 270k LoLax @ 31.2 K/STR.
NO. STRAIGHT	30
NO. DEFLECTED	6 @ A28
RELEASE STRENGTH*	5750 – 5950 PSI*
COARSE AGGREGATE	LIMESTONE
CLASS OF CONCRETE	H

* Strength at release within this range is critical. See attached document detailing beam fabrication and cylinder testing.

STRAND PATTERN 36D6 @ A28 (TYPE C BEAM)					
FED. RD. DIV. NO.	STATE	PROJECT NO.		HWY. NO.	
NA	TEXAS	TxDOT PROJECT 5197		NA	
STATE DISTRICT	COUNTY		CONTROL NO.	SECTION NO.	JOB NO.
AUSTIN	TRAVIS				
BEXAR CONCRETE			DATE		SHEET 3 OF 4
UNIVERSITY OF TEXAS - FSEL			NOV. '07		

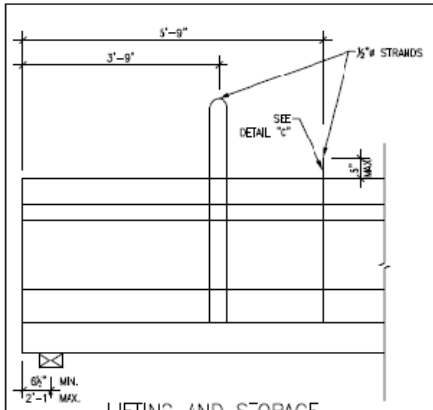

LIFTING AND STORAGE

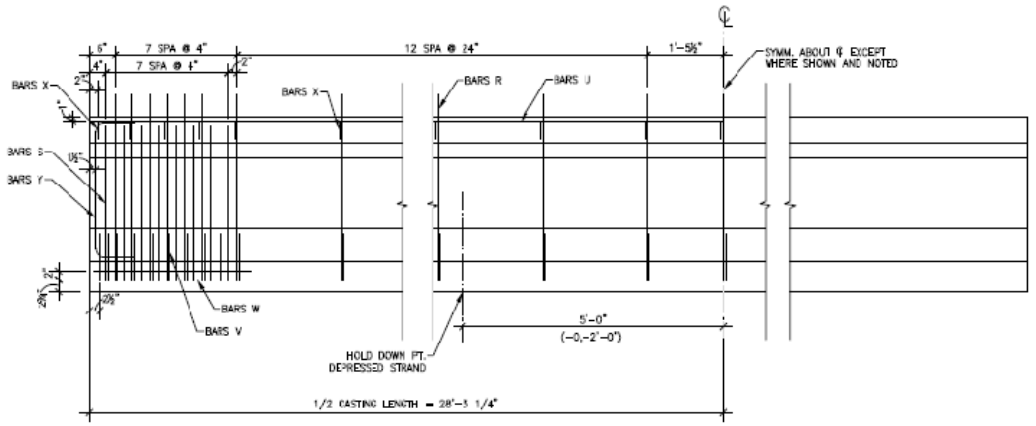

ELEVATION

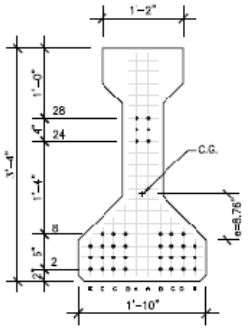

END SECTION

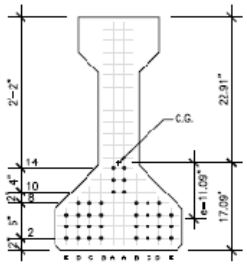

℄ SECTION

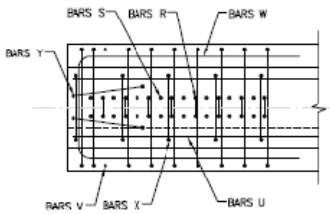

DETAIL A

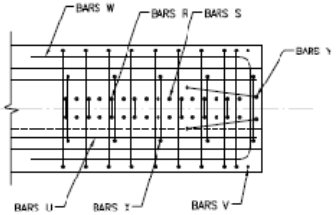

DETAIL B

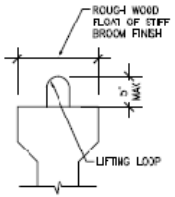

DETAIL "C"

REINFORCING BAR SCHEDULE								
BEAM MARK	NO. BEAMS REQ'D.	R #4	X #3	V #4	S #5	W #5	Y #6	U #5
C-60-2	3	41	35	96	32	4	4	2
	TOTALS	123	105	288	96	12	12	6

J-BAR LENGTH = 56'-3"

STRAND PATTERN	
NO. OF STRANDS	36-1/2"ø, 270K LOLAX @ 31.0 K/STK.
NO. STRAIGHT	30
NO. DEFLECTED	6 @ A28
RELEASE STRENGTH	6300 - 6500 PSI*
COARSE AGGREGATE	LIMESTONE
CLASS OF CONCRETE	H

* Strength at release within this range is critical. See attached document detailing beam fabrication and cylinder testing.

STRAND PATTERN 36D6 @ A28
(TYPE C BEAM)

FED. RD. DIV. NO.	STATE	PROJECT NO.		HWY. NO.	
NA	TEXAS	TxDOT PROJECT 5197		NA	
STATE DISTRICT	COUNTY		CONTROL NO.	SECTION NO.	JOB NO.
AUSTIN	TRAVIS				
DEXAR CONCRETE			DATE		SHEET 4 OF 4
UNIVERSITY OF TEXAS - FSEL			NOV. '07		

APPENDIX D

Compressive Strength Gain vs. Time Plots

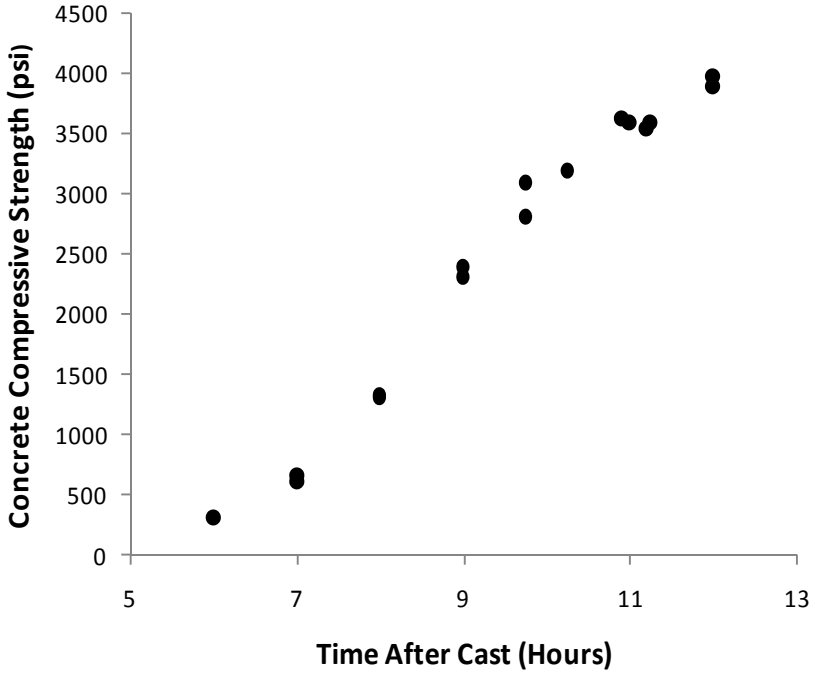

Figure D.1 Fabricator A – 0.70f'$_{ci}$ Target Cast

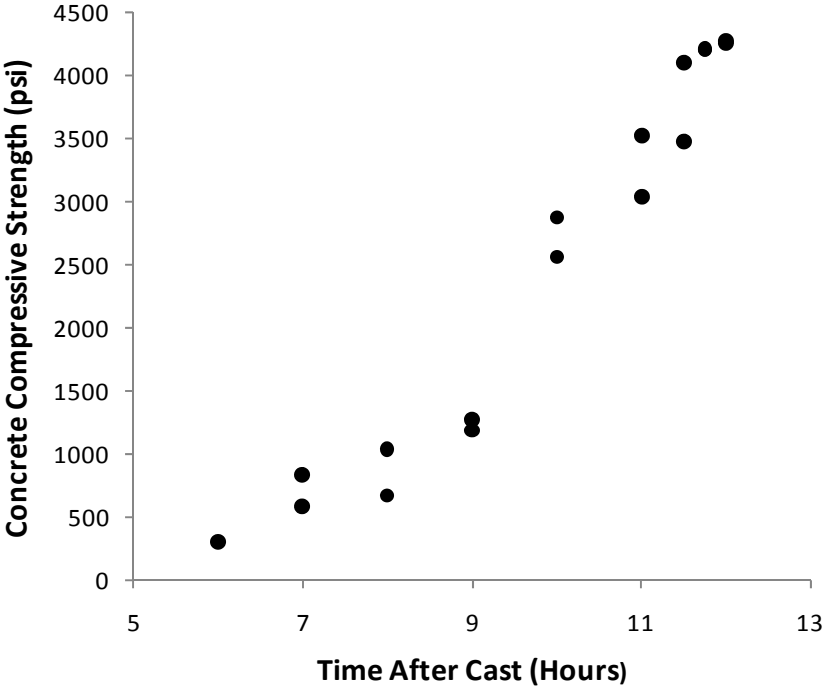

Figure D.2 Fabricator A – 0.65f'$_{ci}$ Target Cast

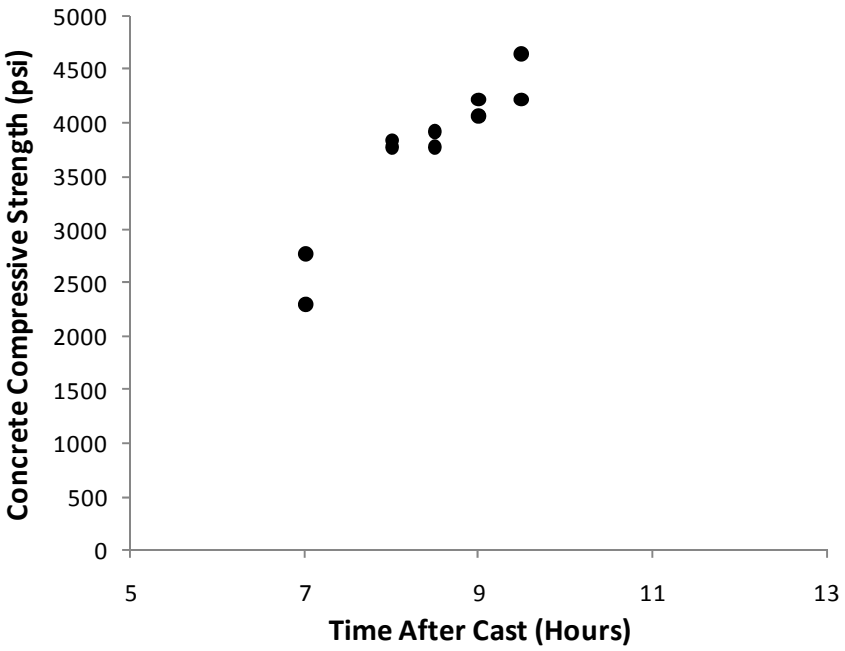

Figure D.3 Fabricator A – 0.60f'$_{ci}$ Target Cast

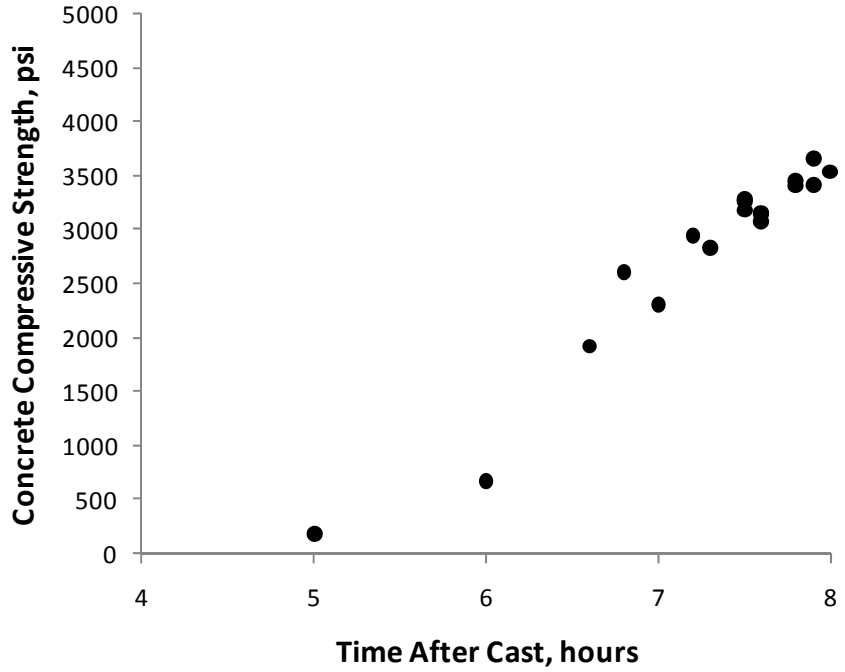

Figure D.4 Fabricator B – 0.70f'$_{ci}$ Target Cast

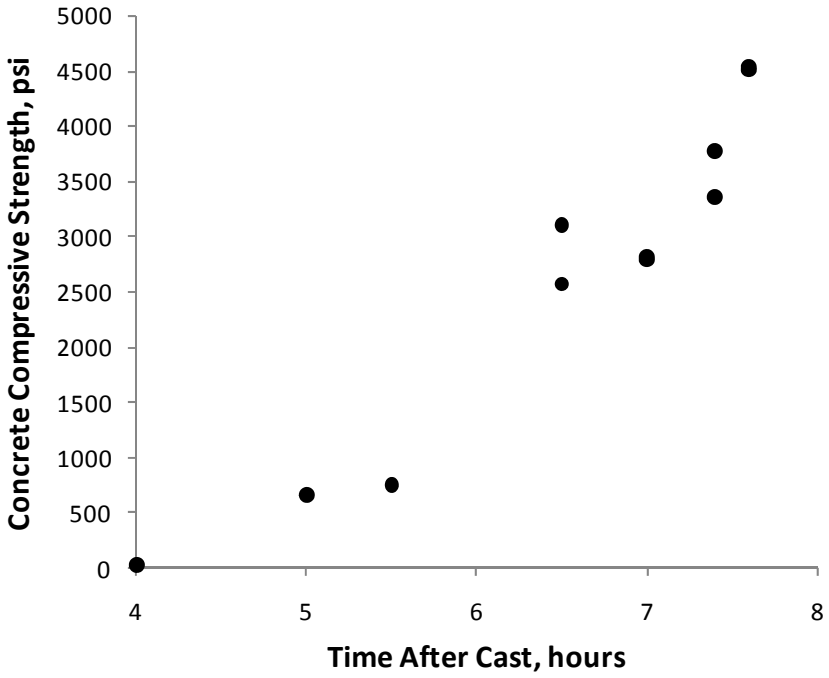

Figure D.5 Fabricator B – 0.60f'$_{ci}$ Target Cast

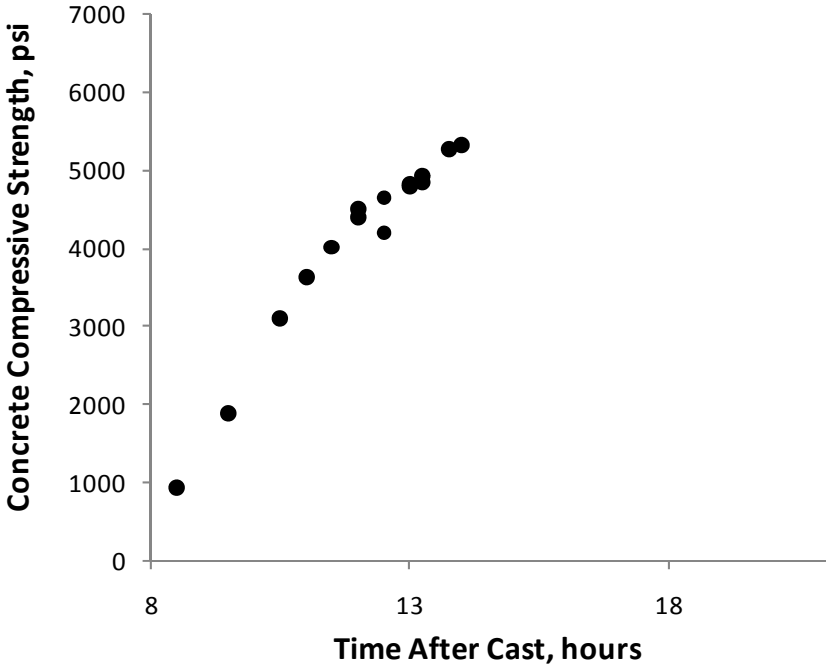

Figure D.6 Fabricator C – 0.70f'$_{ci}$ Target Cast

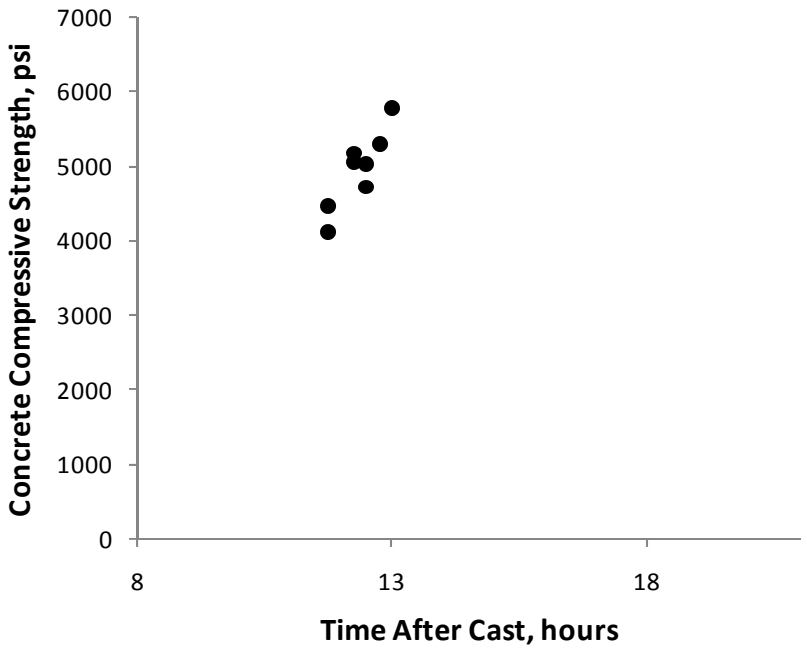

Figure D.7 Fabricator C – 0.65f'$_{ci}$ Target Cast

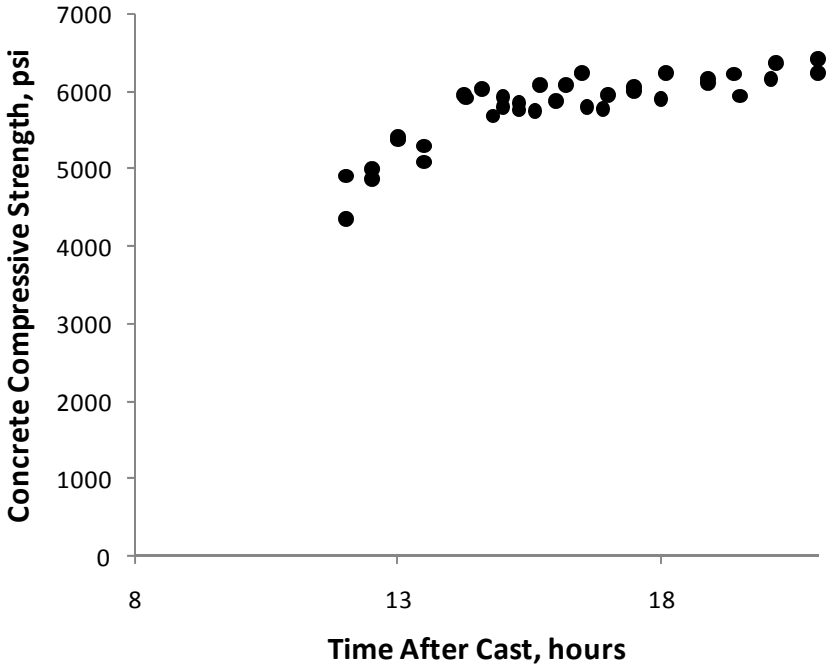

Figure D.8 Fabricator C – 0.60f'$_{ci}$ Target Cast

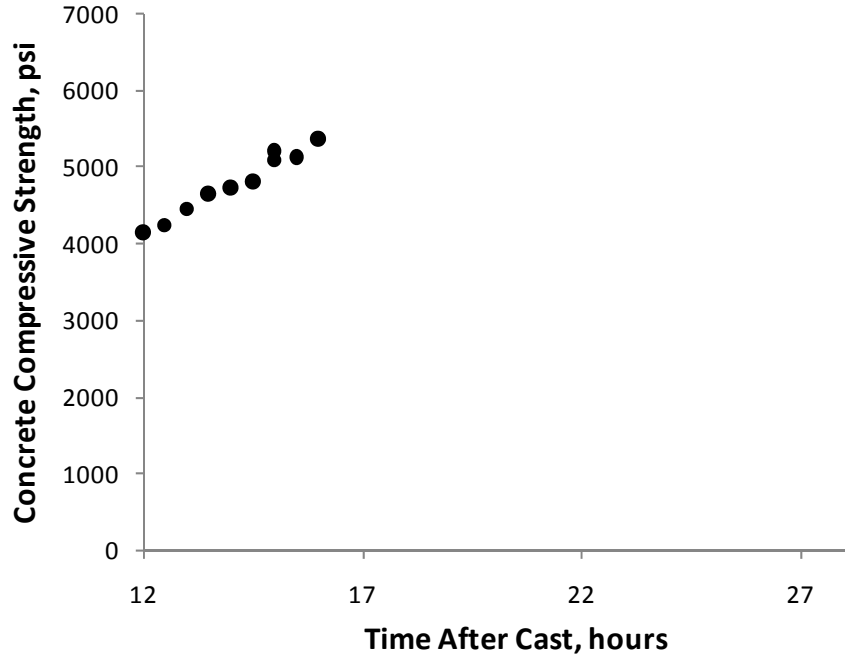

Figure D.9 Fabricator D – 0.70f'$_{ci}$ Target Cast

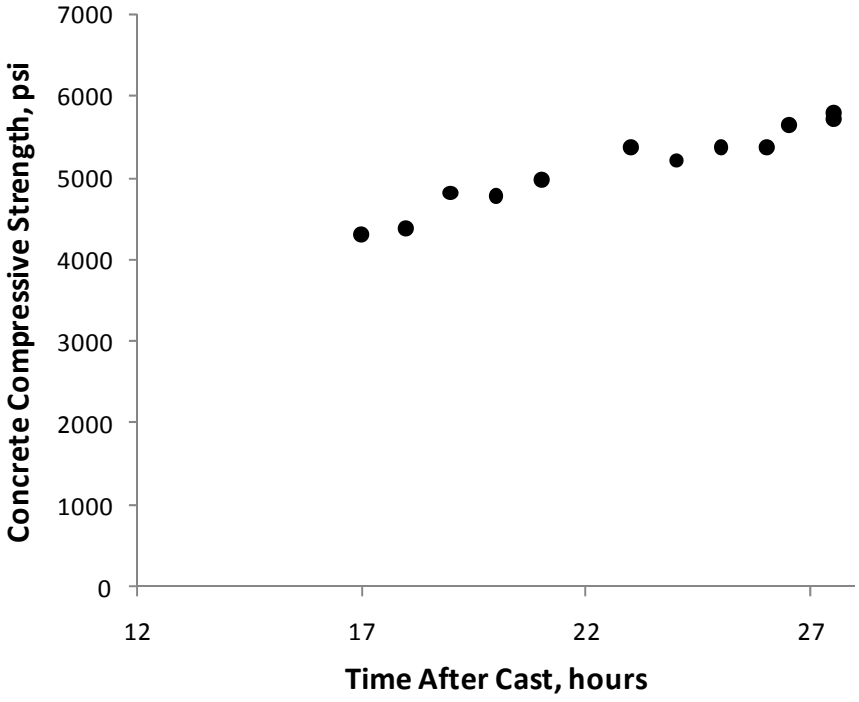

Figure D109 Fabricator D – 0.65f'$_{ci}$ Target Cast 1

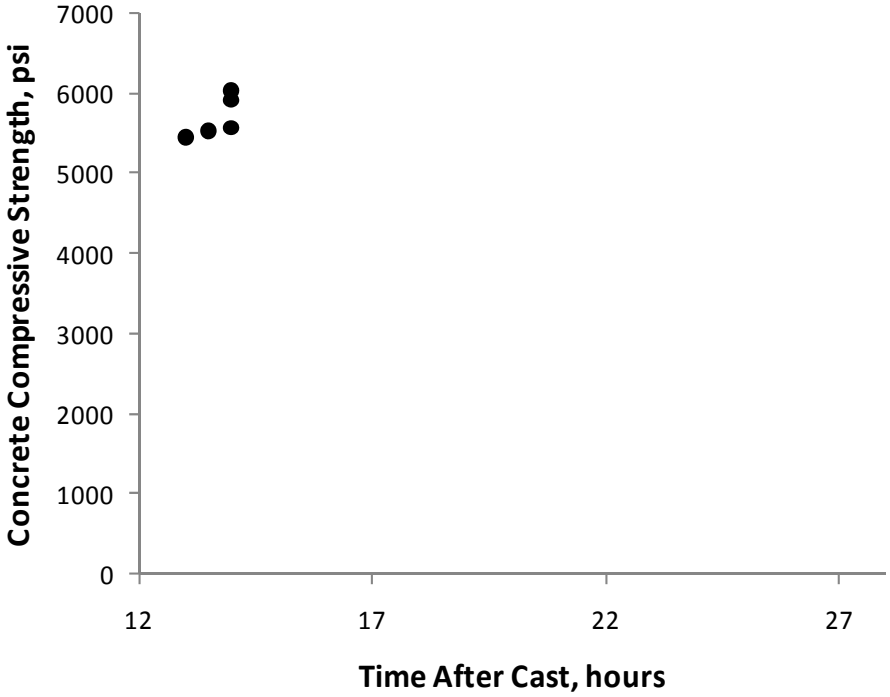

Figure D.11 Fabricator D – 0.65f'$_{ci}$ Target Cast 2

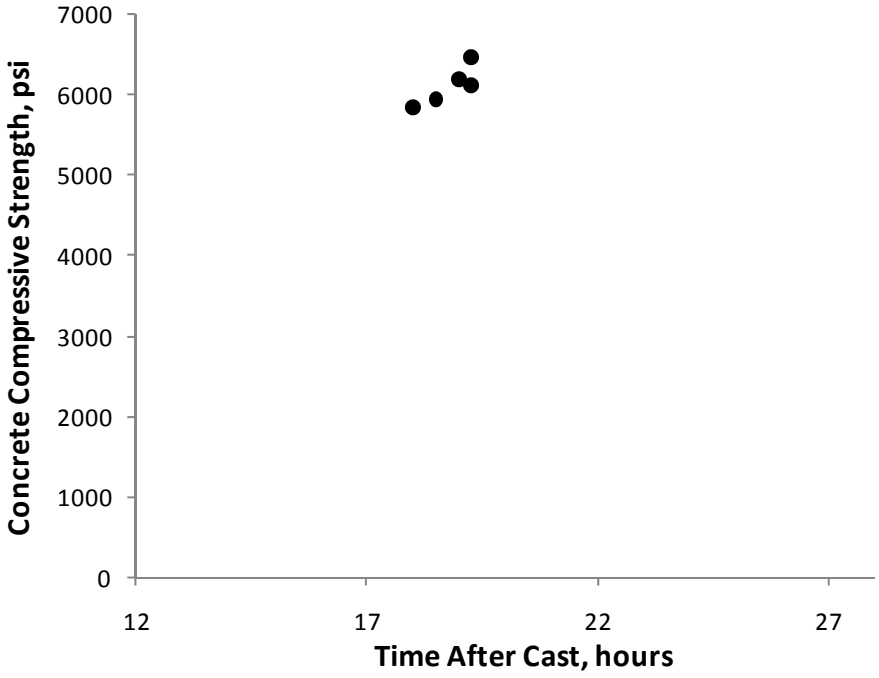

Figure D.12 Fabricator D – 0.60f'$_{ci}$ Target Cast

BIBLIOGRAPHY

1. AASHTO, *LRFD Bridge Design Specifications*, 4th Edition, American Association of State Highway and Transportation Officials, Washington D.C., 2007.

2. AASHTO, *LRFD Bridge Design Specifications*, 1st Edition, American Association of State Highway and Transportation Officials, Washington D.C., 1994

3. ACI Committee 318, *Building Code Requirements for Reinforced Concrete (ACI 318-63)*, American Concrete Institute, Detroit, MI, 1963.

4. ACI Committee 318, *Building Code Requirements for Reinforced Concrete (ACI 318-71)*, American Concrete Institute, Detroit, MI, 1971.

5. ACI Committee 318, *Building Code Requirements for Reinforced Concrete (ACI 318-08)*, American Concrete Institute, Farmington Hills, MI, 2008.

6. Alshegir, A., Ramirez, J. A., "Strut-Tie Approach in Pretensioned Deep Beams," ACI Structural Journal, Vol. 89, No. 3, May-June 1992, pp. 296-304.

7. Arthur, P.D., Bhatt, P., Duncan, W., "Experimental and Analytical Studies on the Shear Failure of Pretensioned I-Beams Under Distributed Loading," PCI Journal, V. 18, No. 1, January-February 1973, pp 50-67.

8. ASTM, Standard Test Method for Compressive Strength of Cylindrical Concrete Specimens (ASTM C39), American Society for Testing and Materials, Designation C 39/C 39 M, West Conshohocken, PA, 2005.

9. Avendaño, A. R., "Shear Strength and Behavior of Prestressed Concrete Beams," Master's Thesis, University of Texas at Austin, Austin, Texas, 2008.

10. Bennett, E. W., and Balasooriya, B.M.A., "Shear Strength of Prestressed Beams with Thin Webs Failing in Inclined Compression," ACI Journal, V. 68, No. 3, March 1971, pp. 204-212.

11. Birrcher, D. B., Bayrak, O., "Effects of Increasing the Allowable Compressive Stress at Release of Prestressed Concrete Girders," Center for Transportation Research, Technical Report 0-5197-1, University of Texas at Austin, Austin, Texas, January 2007.

12. Bruce, R. N., "An Experimental Study of the Action of Web Reinforcement in Prestressed Concrete Beams," PhD thesis, University of Illinois, Urbana, Illinois, September 1962.

13. Collins, M. P. and Mitchell, D., *Prestressed Concrete Structures*, Response Publications, Toronto and Montreal, Canada, 1997.

14. Durrani, A. J., and Robertson, I. N., "Shear Strength of Prestressed Concrete T-Beams with Welded Wire Fabric as Shear Reinforcement," PCI Journal, V. 32, No. 2, March-April 1987, pp. 46-61.

15. Elzanaty, A. H., Nilson, A. H., and Slate, F. O., "Shear Capacity of Prestressed Concrete Beams Using High-Strength Concrete," ACI Journal, V. 83, No. 3, May 1986, pp. 359-368.

16. Hartman, D. L., Breen, J. E., and Kreger, M.E., "Shear Capacity of High Strength Prestressed Concrete Girders," Research Report 381-2, Center of Transportation Research, University of Texas at Austin, Austin, Texas, January 1988.

17. Hawkins, N.M., Sozen, M. A., and Siess, C. P., "Strength and Behavior or Two-Span Continuous Prestressed Concrete Beams," Civil Engineering Studies, Structural Research Series, No. 225, University of Illinois, Urbana, Illinois, September 1961.

18. Hernandez, G., "Strength of Prestressed Concrete Beams with Web Reinforcement," Civil Engineering Studies, Structural Research Series, No. 153, University of Illinois, Urbana, Illinois, May 1958.

19. Kaufman, M. K., and Ramirez, J. A., "Re-Evaluation of Ultimate Shear Behavior of High Strength Concrete Prestressed I-Beams," ACI Structural Journal, V. 86, No. 4, July-August., 1989, pp. 376-382.

20. Laskar, A., Wang, J., Hsu, T.T.C., Mo Y. L., "Rational Shear Provisions for AASHTO-LRFD Specifications," Technical Report 0-4759-1, Texas Department of Transportation, Houston, Texas, January 2007.

21. Lin, T. Y., "Design of Prestressed Concrete Structures," New York, John Wiley and Sons, 1955.

22. Lyngberg, B. S., "Ultimate Shear Resistance of Partially Prestressed Reinforced Concrete I-Beams," Journal of the American Concrete Institute, Proceedings, V. 73, No. 4, April 1979, pp. 214-222.

23. Ma, Z., Tadros, M. K., and Basilla, M., "Shear Behavior of Pretensioned High-Strength Concrete I-Girders," ACI Journal, V. 97, No. 1, January-February 2000, pp. 185-192.

24. MacGregor, J. G., Sozen, M. A., and Siess, C. P., "Strength and Behavior of Prestressed Concrete Beams with Web Reinforcement," Civil Engineering Studies, Structural Research Series No. 201, University of Illinois, Urbana, Illinois, August 1960.

25. MacGregor, J. G., Sozen, M. A., and Siess, C. P., "Effect of Draped Reinforcement on behavior of Prestressed Concrete Beams," ACI Journal, V. 32, No. 6, December 1960, pp. 649-677.

26. Magnel, G., "Prestressed Concrete," New York, McGraw Hill, 1954

27. Maruyama, K. and Rizkalla, S., "Shear Design Consideration for Pretensioned Prestressed Beams," ACI Journal, Vol. 85, No. 5, September-October 1988, pp. 492-498.

28. Mattock, A. H., and Kaar, P. H., "Precast-Prestressed Concrete Bridges – 4: Shear Tests of Continuous Girders," Journal of the PCA Research Development Laboratories, Jan. 1961, pp. 19-47.

29. Morice, P. B., and Lewis, H. S., "The Ultimate Strength of Two-Span Continuous Prestressed Concrete Beams as Affected by Tendon Transformation and Un-Tensioned Steel," Second Congress of the Federation of Internationale de la Precontrainte, Amersterdam, 1955.

30. NCHRP Report 549, *Simplified Shear Design of Structural Concrete Members*, National Cooperative Highway Research Program, Washington D.C., 2005.

31. NCHRP Report 579, *Application of LRFD Bridge Design Specification to High-Strength Structural Concrete: Shear Provisions*, National Cooperative Highway Research Program, Washington D.C., 2005.

32. Rangan, B. V., "Web Crushing Strength of Reinforced and Prestressed Concrete Beams," ACI Journal, Vol 88., No. 1, January-February 1991, pp. 12-16.

33. Raymond, K.K., Bruce, R. N., and Roller, J. J., "Shear Behavior of HPC Bulb-Tee Girders," Special Publication, V. 228, June 2005, pp. 705-722.

34. Shahawy, M. A., and Batchelor, B., "Investigation of Prestressed Concrete Girders: Comparison Between AASHTO Specification and LRFD Code," PCI Journal, V. 41, No. 3, May-June 1996, pp. 48-62.

35. Sozen, M. A., Zwoyer, E. M., and Siess, C. P., "Shear Behavior of Full-Scale Prestressed Concrete for Highway Bridges, Part I: Strength in Shear of Beams Without Web Reinforcement," Bulletin No. 452, University of Illinois Engineering Experiment Station, April 1959.

36. Teoh, B. K., Mansur, M. A., and Wee, T. H., "Behavior of High-Strength Concrete I-Beams with Low Shear Reinforcement," ACI Journal, V. 99, No. 3, May-June 2002, pp. 299-307.

37. Texas Department of Transportation, *Standard Specifications for Construction and Maintenance of Highways, Streets, and Bridges*, 2004

38. Xuan, X., Rizkalla, S. and Maruyama, K., "Effectiveness of Welded Wire Fabric as Shear Reinforcement in Pretensioned Prestressed Concrete T-Beams," ACI Journal, Vol. 85, No. 4, July-August 1988, pp. 429-4366.

39. Zekaria, I., "Shear Failure of Two-Span Continuous Concrete Beams Without Web Reinforcement," Journal of the Prestressed Concrete Institute, V. 3, No. 1, June 1958.

40. Zhongguo, M., Tadros, M. K., and Baishya, M., "Shear Behavior of Pretensioned High-Strength Concrete Bridge I-Girders," ACI Journal, Vol. 97, No. S21, January-February 2000, pp. 185-192.

41. Zwoyer, E. M. and Siess, C. P., "Ultimate Strength of Simply Supported Prestressed Concrete Beams Without Web Reinforcement," ACI Journal, V. 26, No. 2, Oct. 1954, pp. 181-200.

42. http://texas.e-foreclosuresearch.com/